PNNL-28992 Rev. 0.0
RPT-SLAW-004 Rev. 0.0

Performance Metric for Cementitious Waste Form Inventory Release in the Integrated Disposal Facility

September 2019

R Matthew Asmussen
Yilin Fang
Guzel Tartakovsky
Xuehang Song
Joseph H. Westsik Jr.
Gary L. Smith

Prepared for the U.S. Department of Energy
under Contract DE-AC05-76RL01830

DISCLAIMER

This report was prepared as an account of work sponsored by an agency of the United States Government. Neither the United States Government nor any agency thereof, nor Battelle Memorial Institute, nor any of their employees, makes **any warranty, express or implied, or assumes any legal liability or responsibility for the accuracy, completeness, or usefulness of any information, apparatus, product, or process disclosed, or represents that its use would not infringe privately owned rights**. Reference herein to any specific commercial product, process, or service by trade name, trademark, manufacturer, or otherwise does not necessarily constitute or imply its endorsement, recommendation, or favoring by the United States Government or any agency thereof, or Battelle Memorial Institute. The views and opinions of authors expressed herein do not necessarily state or reflect those of the United States Government or any agency thereof.

PACIFIC NORTHWEST NATIONAL LABORATORY
operated by
BATTELLE
for the
UNITED STATES DEPARTMENT OF ENERGY
under Contract DE-AC05-76RL01830

Printed in the United States of America

Available to DOE and DOE contractors from the
Office of Scientific and Technical Information,
P.O. Box 62, Oak Ridge, TN 37831-0062;
ph: (865) 576-8401
fax: (865) 576-5728
email: reports@adonis.osti.gov

Available to the public from the National Technical Information Service
5301 Shawnee Rd., Alexandria, VA 22312
ph: (800) 553-NTIS (6847)
email: orders@ntis.gov <https://www.ntis.gov/about>
Online ordering: http://www.ntis.gov

PNNL-28992 Rev. 0.0
RPT-SLAW-004 Rev. 0.0

Performance Metric for Cementitious Waste Form Inventory Release in the Integrated Disposal Facility

September 2019

R Matthew Asmussen
Yilin Fang
Guzel Tartakovsky
Xuehang Song
Joseph H. Westsik Jr.
Gary L. Smith

Prepared for
the U.S. Department of Energy
under Contract DE-AC05-76RL01830

Pacific Northwest National Laboratory
Richland, Washington 99354

Executive Summary

This report describes work supporting Phase 1 of the 2018 U.S. Department of Energy Office of River Protection Grand Challenge award recipient "Cementitious Immobilization of Treated LAW and Ancillary Benefits to Risk Reduction in Cross Site Transfer." The purpose of Phase 1 was two-fold: 1) to establish a performance metric for grout leachability against which laboratory leach data (as observed diffusivities) can be assessed; and, 2) perform a comparison of historical test data against this metric. Historically, advancements in cementitious (grout) waste form performance have been made over the last 40 years, with a majority of the progress achieved within the past 8 years as part of the Washington River Protection *Solutions*, LLC testing program.

Grout was the original baseline immobilization plan for the double-shell tank waste at the Hanford Site until vitrification was selected in 1993. In a primary vitrification flowsheet at the Hanford Tank Waste Treatment and Immobilization Plant, grout is the baseline immobilization technology for secondary wastes, both liquids and solids, generated from vitrification activities. Recent reports from the Government Accountability Office, and an ongoing review by the National Academy of Sciences initiated by congress through the National Defense Authorization Act, have suggested that a grout immobilization pathway for the anticipated supplemental low-activity waste (SLAW) inventory can be beneficial to the Hanford mission lifecycle. Before any decision can be made on a SLAW technology for onsite disposal in the Hanford Integrated Disposal Facility (IDF), long-term prediction of its behavior is required through a performance assessment (PA).

To date, the disposal of low-activity waste (LAW) and SLAW inventories in grout waste forms have not been systematically included in PAs. However, in the past two decades improvements in the retention of contaminants have been observed in laboratory testing of grout waste forms.

The current effort is focused on determining whether these recent advancements in contaminant retention are sufficient to meet regulatory requirements for buried waste at the IDF. In addition, this work establishes a performance metric for four contaminants (Tc, I, NO_3^-, and Cr) in a SLAW inventory in the IDF that can serve as a measure to evaluate new laboratory results against the regulatory standard.

The performance metric is quantified as a retardation factor (R) based on the waste form retention capacity relative to a mobile (i.e., non-sorbing/non-reacting) species. The R value represents a minimum needed to maintain contaminant concentrations below the drinking water standard at points of compliance for the IDF. For comparison purposes, R can be converted to a corresponding laboratory observed diffusivity value (D_{obs}). The R performance metric was determined through an iterative set of simulations representing grout waste within the IDF and its variably saturated transport to groundwater. The outcome of this analysis is summarized below.

The major findings of this work were the calculation of the performance metrics and subsequent comparison of historical leach data against the metrics, as follows.

- **Performance Metrics:** The performance metric R values were established using grout properties based on the Cast Stone formulation for Tc, I, NO_3^-, and Cr. Each contaminant R value has a corresponding observed diffusivity value that can be used to screen laboratory observed diffusivity values measured to identify candidate grout formulations for further development and optimization. The specific metric values are given in Table S.1. The model simulations employed and fractional releases determined could be applied to define performance metrics for other waste form types (e.g., glass, steam reforming).

Table S.1. The distribution coefficient (K_d) used in the simulations, and the corresponding retardation factor (R) performance metric values; the associated fractional release rate from the simulated IDF; and, associated observed diffusivity (D_{obs}) calculated in this work.

Species	Simulation Waste Form K_d, mL/g	Performance Metric, R	Fractional Release Rate	Corresponding Observed Diffusivity (D_{obs})
Technetium	45	113	2.1×10^{-6} yr^{-1}	2×10^{-11} cm^2/s
Iodine	35	87	5.4×10^{-5} yr^{-1}	3×10^{-11} cm^2/s
Nitrate	0.5	2	1.1×10^{-5} yr^{-1}	2×10^{-9} cm^2/s.
Chromium	26	65	3.4×10^{-6} yr^{-1}	4×10^{-11} cm^2/s

Performance metrics allow for a rapid assessment of leach data and selection of optimized formulations for testing at larger scales and process scale-up.

Historical grout diffusivities were compared to the effective diffusivities identified in this study. A lower observed diffusivity corresponds to better retention of the contaminant in the waste form. The following conclusions were made from the comparisons.

- **Technetium:** Previous Tc diffusivities used in performance and risk calculations have been greater than the observed diffusivity established using the R performance metric. However, several Tc observed diffusivities were measured to be below the limit established by the performance metric, including LAW Cast Stone, getter containing systems, and hydrated-lime based formulations. Each of these waste forms is a candidate for optimizing the long-term retention of Tc, with due consideration of the impact that the redox condition within the IDF has on retention.
- **Iodine:** Analysis of historical iodine (as iodide) observed diffusivities showed that the R values used in performance assessment and risk calculations were greater than the performance metric. The one exception to this finding was for formulations containing Ag-based getters with getter loadings >5 wt% in the waste form, where reported observed diffusivity values were several orders of magnitude below the observed diffusivity limit established by the performance metric. This implies that the long-term stability of getter-containing materials should be further investigated.
- **Nitrate:** Of all nitrate leach data assessed, only a small number of tests (immobilized liquid secondary waste) measured an observed nitrate diffusivity below the limit established by the performance metric. Few attempts to improve nitrate retention in grout have been reported in the literature but may be possible using materials with a natural affinity for nitrate retention in grout waste forms.
- **Chromium:** All historical observed diffusivities for Cr were below the corresponding limit established by the performance metric value. The strong retention of Cr is likely due to the reducing capacity of waste forms and possible incorporation of Cr into grout mineral phases.

In summary, the performance metrics will allow rapid assessment of future grout leach data to select optimized formulations for maturation and eventual deployment to facilitate the Hanford mission. It should be noted that these simulations only consider the contribution from the SLAW inventory and not any contribution to the overall release rate from the primary LAW inventory. As a result, the R values that achieve the target concentrations would be an underestimation of the full LAW inventory release. The performance metric is not intended for use in regulatory decision-making.

Acknowledgments

The authors are grateful to David Swanberg, Ridha Mabrouki, Rodney Skeen, Elvie Brown, and Jason Vitali at Washington River Protection *Solutions*, LLC, Richland, Washington, for the project funding and programmatic guidance. We would like to thank Diana Bacon for guidance during project planning and Tom Brouns for support with the National Defense Authorization Act Performance Evaluation. We would also like to thank Guzel Tartakovsky for calculation reviews and Philip Meyer, Diana Bacon, and Vicky Freedman of PNNL, James Dyer and Corey Trivelpiece of SRNL, Pat Lee (Orano) and Rodney Skeen (WRPS) for their technical reviews. Kirstin Sockwell, Nathan Doi and Lorraine Seymour are thanked for assistance in literature reviews of historical grout data. Rose Perry of PNNL contributed the graphics. Pacific Northwest National Laboratory is a multi-program national laboratory operated by Battelle for the U.S. Department of Energy.

Acronyms and Abbreviations

BFS	blast furnace slag
DOE	U.S. Department of Energy
DWS	drinking water standard
eSTOMP	exascale Subsurface Transport Over Multiple Phases
EIS	environmental impact statement
EPA	U.S. Environmental Protection Agency
FA	fly ash
FFRDC	Federally Funded Research and Development Center
FY	fiscal year
GAO	U.S. Government Accountability Office
HLW	high-level waste
IDF	Integrated Disposal Facility
ILAW	immobilized low-activity waste
K_d	distribution coefficient
K_{sat}	saturated hydraulic conductivity
LAW	low-activity waste (Hanford)
LSW	liquid secondary waste
NAS	National Academy of Sciences
NDAA	National Defense Authorization Act
OPC	ordinary portland cement
ORP	Office of River Protection
PA	performance assessment
PE	performance evaluation
PNNL	Pacific Northwest National Laboratory
POC	point of compliance (a well 100 m down gradient from the IDF)
QA	quality assurance
R	retardation factor
RA	risk assessment
RCRA	Resource Conservation and Recovery Act of 1976
SLAW	supplemental low-activity waste
SRNL	Savannah River National Laboratory
SSW	solid secondary waste
TC&WM	Tank Closure & Waste Management
WRPS	Washington River Protection *Solutions*, LLC
WTP	Hanford Tank Waste Treatment and Immobilization Plant
WWFTP	WRPS Waste Form Testing Program

Contents

Executive Summary ii
Acknowledgments iv
Acronyms and Abbreviations v
Contents vi
1.0 Introduction 1.1
1.1 Grout Constituent Release Representation 1.2
1.2 Previous Hanford Performance Assessments 1.5
1.3 Objective 1.6
1.4 Report Organization 1.6
1.5 Quality Assurance 1.7
2.0 Model Development and Simulations 2.1
2.1 Integrated Disposal Facility 2.1
2.2 Simulation Description, Software, and Methodology 2.1
2.3 IDF Design and Properties 2.2
2.3.1 Surface Barrier and Infiltration Rate 2.3
2.3.2 Waste Form Package and Stacking 2.3
2.4 Waste Form Properties 2.5
2.5 eSTOMP Input Cards for the IDF Waste Form Simulation 2.5
2.5.1 Solution Control Card 2.5
2.5.2 Grid Card 2.5
2.5.3 Rock/Soil Zonation Card 2.6
2.5.4 Mechanical Properties, Hydraulic Properties, Saturation Function Card 2.6
2.5.5 Aqueous Relative Permeability Card. 2.6
2.5.6 Solute/Fluid Interaction Card 2.6
2.5.7 Solute/Porous Media Interaction Card 2.6
2.5.8 Initial Condition Card 2.6
2.5.9 Boundary Condition Card 2.6
2.6 Subsurface Properties 2.8
2.7 eSTOMP Input Cards for the IDF Subsurface Simulation 2.1
2.7.1 Solution Control Card 2.1
2.7.2 Grid Card 2.1
2.7.3 Rock/Soil Zonation Card 2.1
2.7.4 Mechanical Properties, Hydraulic Properties, Saturation Function Card 2.1
2.7.5 Aqueous Relative Permeability Card 2.1
2.7.6 Solute/Fluid Interaction Card 2.1
2.7.7 Solute/Porous Media Interaction Card 2.1
2.7.8 Initial Condition Card 2.2

2.7.9 Boundary Condition Card 2.2
2.7.10 Source Card 2.2
3.0 Results 3.3
3.1 Technetium (Tc-99) 3.3
3.2 Iodine 3.4
3.3 Nitrate 3.5
3.4 Chromium 3.6
3.5 Performance Metric 3.7
3.6 Time Dependent Release and Simulation Sensitivity Cases 3.8
3.6.1 Time Dependent Release 3.8
3.6.2 Simulation Sensitivity Cases 3.9
4.0 Review of Historical Data 4.1
4.1 Summary of the SLAW Program 4.1
4.2 Assessment of Previous Data 4.1
4.2.1 Technetium 4.1
4.2.2 Iodine 4.2
4.2.3 Nitrate 4.3
4.2.4 Chromium 4.4
4.2.5 Comparisons Between Species 4.5
4.3 Path Forward 4.6
4.4 Summary and Conclusion 4.8
5.0 References 5.1
Appendix A – Example Input Files for IDF Waste Form Simulation and IDF Subsurface Simulation A.1
Appendix B – Simulation Summary B.1
Appendix C – Historical Leach Data Summary C.1

Figures

Figure 2-1. Cross-section schematic of the Hanford IDF and subsurface (DOE 2017). 2.2

Figure 2-2. Schematic of the full waste form container stacking used in the simulations showing the waste containers (red, W1), low-density backfill (green, LD_BACKF) and high-density backfill (blue, HD_BACKF). 2.3

Figure 2-3. North-south cross-section of the IDF showing the location of the liner sump (from Figure 2-8 of DOE 2017) 2.8

Figure 2-4. Visualization of the simulated subsurface below the IDF and the location of the sumps where release of contaminants from the IDF occurs. 2.9

Figure 3-1. Visualization of the R factor (black) used in the simulations and the resulting concentration of Tc determined at the POC in pCi/L. The corresponding observed diffusivity that would be measured for a grout with a specific R factor is also shown (red). Dashed lines corresponding to the target concentrations relative to the DWS are also provided. 3.4

Figure 3-2. Visualization of the R factor (black) used in the simulations and the resulting concentration of I-129 determined at the POC in pCi/L. The corresponding observed diffusivity that would be measured for a grout with a specific R factor is also shown (red). Dashed lines corresponding to the target concentrations relative to the DWS are also provided. 3.5

Figure 3-3. Visualization of the R factor (black) used in the simulations and the resulting concentration of NO_3^- determined at the POC in mg/L. The corresponding observed diffusivity that would be measured for a grout with a specific R factor is also shown (red). Dashed lines corresponding to the target concentrations are also provided. 3.6

Figure 3-4. Visualization of the R factor (black) used in the simulations and the resulting concentration of Cr determined at the POC in mg/L. The corresponding observed diffusivity that would be measured for a grout with a specific R factor is also shown (red). Dashed lines corresponding to the target concentrations are also provided. 3.7

Figure 3-5. Example plots showing the time dependent concentrations determined at the point of compliance from the simulations for a) Tc, b) I, c) NO_3^- and Cr. 3.8

Figure 4-1. Comparison of previously reported observed diffusivity values measured for Tc in deionized water (blue), simulated porewater (red), and those used in previous PAs and RAs (orange) with the performance metric for Tc (green line). 4.2

Figure 4-2. Comparison of previously reported observed diffusivity values for iodine measured in deionized water (blue), simulated porewater (red), and those used in previous PAs and RAs (orange) with the performance metric for I (green line). 4.3

Figure 4-3. Comparison of previously reported observed diffusivity values for NO_3 measured in deionized water (blue), simulated porewater (red), and those used in previous PAs and RAs (orange) with the performance metric for NO_3^- (green line). 4.4

Figure 4-4. Comparison of previously reported observed diffusivity values for Cr measured in deionized water (blue), simulated porewater (red), and those used in previous PAs and RAs (orange) with the performance metric for Cr (green line). 4.5

Figure 4-5. Comparison between the observed diffusivity of Tc, I, NO_3^- and Na from the same sample in individual test sets. The dashed lines represent the corresponding observed diffusivity for each species from the performance metric. 4.6

Tables

Table 1-1. Waste form types included in previous Hanford site assessments. 1.6
Table 1-2. Summary of the drinking water standard targets used in this work..... 1.6
Table 2-1. Summary of the properties of the low- and high-density backfills used in the simulated IDF. 2.4
Table 2-2. Summary of properties for the cementitious waste forms used in the simulations. 2.7
Table 2-3. Total inventories used for the SLAW simulations. 2.8
Table 2-4. Summary of properties used to represent the subsurface below the IDF in the simulations. 2.10
Table 3-1. List of the performance metric R values and associated observed diffusivities. 3.7
Table 3-2. Comparison of the total inventory, calculated release rate and corresponding fractional release rate for the individual simulation for each contaminant used to determine the performance metric. 3.8
Table 3-3. Summary of sensitivity cases performed using I-129 as the base case. 3.9

1.0 Introduction

This report describes work supporting Phase 1 of the 2018 U.S. Department of Energy (DOE) Office of River Protection (ORP) Grand Challenge award recipient "Cementitious Immobilization of Treated LAW and Ancillary Benefits to Risk Reduction in Cross Site Transfer."

The Hanford Site, in Washington state, houses over 56 million gallons of legacy wastes generated during decades of reprocessing activities. This waste inventory will be split into high-level waste (HLW) and low-activity waste (LAW) fractions and vitrified to produce glass waste forms. The HLW glass waste forms will be disposed of at a federal repository. The immobilized LAW (ILAW) glass waste forms will be disposed of onsite at the Hanford Integrated Disposal Facility (IDF).

Current process models indicate that the current design of the Hanford Tank Waste Treatment and Immobilization Plant (WTP) LAW facility will not have the capacity to process the full LAW inventory. As a result, upward of 54 million gallons of retrieved (volume increased during retrievals) and treated Hanford LAW will require supplemental immobilization, according to Rev. 8 of the DOE-ORP System Plan (Tilanus et al. 2017). This supplemental inventory does not yet have a defined immobilization pathway. A need to consider other technologies for supplemental immobilization of LAW was recently highlighted in a U.S. Government Accountability Office (GAO) report (Trimble and Persons 2017) and a subsequent assessment of possible supplemental low-activity waste (SLAW) technologies by a Federally Funded Research and Development Center (FFRDC) team supporting a review by the National Academy of Sciences (NAS) initiated by the National Defense Authorization Act (NDAA). Both reports suggest that a grout immobilization pathway for SLAW will reduce the amount of secondary wastes generated and potentially lead to cost and schedule savings in the mission.

The long-term performance of any waste form inventory to be placed in the IDF needs to be assessed using computer models to comply with DOE Order 435.1, *Radioactive Waste Management*. The primary means for complying with this requirement is through performance assessments (PAs) and risk assessments (RAs) and these analyses have been carried out since the 1990s. The most recent version of the IDF PA is from 2017 (DOE, 2017). The 2017 IDF PA evaluated the baseline disposal scenario with a fully vitrified LAW inventory and grouted secondary waste streams; no consideration was given to supplemental technologies since vitrification is the only planned primary waste form. Two earlier analyses of alternate supplemental immobilization technologies have been performed: 1) the 2003 Supplemental LAW Risk Assessment (Mann 2003); and, 2) the 2012 Hanford Tank Closure and Waste Management (TC&WM) Environmental Impact Statement (EIS) (DOE 2012). Both studies used the best information available at the time.

As part of the NDAA review of SLAW immobilization technologies, a team of subject matter experts from the national laboratories performed a technology evaluation of the possible candidate SLAW technologies, which included a performance evaluation (PE) of the various supplemental waste forms in the IDF (see Appendix F, Bates et al. 2019). The PE used available laboratory data to represent the low-performing, high-performing, and projected best cases for each waste form type. The results showed that a grouted SLAW inventory would perform slightly better as a full system than a full glass system inventory or a fluidized bed steam reformer inventory. It should be noted that the PE assumed that performance is constant over time with no evolution of waste form properties and conditions.

As further developments are made to grout technologies and as new data on all waste form types are generated, there are no methods or metrics to assess laboratory data against projected long-term behavior without execution of a full PA or PE. This effort seeks to establish a performance metric for a supplemental grout inventory at the IDF to allow rapid assessment of laboratory leach performance data.

A performance metric will be defined for the four target contaminants/radionuclides listed below. Other radionuclide and chemical constituents will be present in LAW and are summarized in Table 3-25 and Table 3-26 of the 2017 IDF PA (DOE, 2017). The simulations carried out within can be adjusted to evaluate other contaminants in future efforts if required, although comparative leach test data for the other contaminants may be limited.

- **Technetium-99** (half-life 211,000 years) – primary radionuclide component of LAW that has high environmental mobility in its oxidized form (pertechnetate, $Tc(VII)O_4^-$) and is prevalent in Hanford wastes. Tc is a redox-sensitive element with several oxidation states, where Tc(IV) species (e.g., $Tc(IV)O_2$, Tc_2S_7) have low solubility and, in turn, far lower mobility compared to TcO_4^-.
- **Iodine** (I-129 half-life 15,700,000 years) – radionuclide contained in the LAW inventory that has high environmental mobility in either reduced (iodide, I^-) or oxidized (IO_3^-) states. Iodine retention can be achieved through precipitation as a low-solubility compound such as AgI (solubility product (K_{sp}) = 8×10^{-17}) or incorporation into a mineral phase.
- **Chromium** – a major Resource Conservation and Recovery Act (RCRA) metal component of LAW that is also redox sensitive (Peterson et al. 2018).
- **Nitrate** – large component of LAW and in-turn regulated by the Washington State Department of Ecology. Nitrate is considered a non-sorbing species within grout.
- In this report the drinking water standards established by the U.S. Environmental Protection Agency (EPA) are utilized as the testing limit.

1.1 Grout Constituent Release Representation

The release of constituents from a grout waste form is assumed to be a diffusive process, although other physical and chemical processes within the waste form may be involved (e.g., sorption, redox). Diffusion processes are represented through Fick's laws. Fick's first law of diffusion states that an aqueous species will migrate from a region of high concentration to a region of low concentration and is represented by Eq. (1.1). A larger diffusion coefficient, D, results in a larger flux in the system. It is known that individual species have different D values in water (e.g., D_{TcO4-} is 1.95×10^{-9} m^2/s and D_{Cs+} is 2.17×10^{-9} m^2/s per Sato et al. 1996). However, as a model simplification for the purpose of this work, all species are assumed to equally diffuse in water.

$$J = D\frac{d\varphi}{dx} \tag{1.1}$$

where:

J = diffusion flux, $mol/m^2 \cdot s$
D = diffusion coefficient, m^2/s
φ = concentration of species (in an ideal mixture), mol/m^3
x = distance, m

Fick's second law expands the description to include the changes in concentration of the diffusing species over time. It is represented by the partial differential, Eq. (1.2). In the second law, a larger D corresponds to a faster rate of diffusion in the system.

$$\frac{\partial\varphi}{\partial t} = D\frac{\partial^2\varphi}{\partial^2 x} \tag{1.2}$$

where:

φ = concentration of species (in an ideal mixture), mol/m^3
D = diffusion coefficient, m^2/s
x = distance, m
t = time

Fick's laws can be applied directly to simple systems and ideal mixtures. Grouts are porous materials and diffusive release is a complex diffusive process involving the interstitial pore network of the grout. The release pathway for contaminants is then directly affected by the overall porosity, the tortuosity of the porous network, and constrictivity of the pores themselves. Thus, the diffusion coefficient in water, D, from Fick's laws cannot be directly used to represent diffusion of a species from a grout. Instead, an intrinsic diffusion coefficient, D_i, is used, where D_i is represented in Eq. (1.3) as a modification to D from Fick's law based on the grout's properties (Serne et al. 2016b).

$$D_i = D\frac{\varepsilon\delta}{\tau^2} \tag{1.3}$$

where:
D_i = intrinsic diffusion coefficient, cm^2/s
D = diffusion coefficient, cm^2/s
ε = porosity
τ = tortuosity
δ = constrictivity

D_i may be possible to measure for an individual sample by: 1) quantifying the porosity, tortuosity, and constrictivity, which is a time- and cost-intensive effort; or, 2) dynamic leach testing to monitor a solute that does not react with the grout matrix. However, not all solutes in the system will be unreactive with the grout matrix, and thus not all solutes can be represented by D_i. Instead, dynamic leach tests in the laboratory are used to generate observed diffusivities, D_{obs}. D_{obs} is also known as an apparent diffusion coefficient, D_a; however, for the purpose of this report, only D_{obs} will be used to refer to laboratory leach data.

The laboratory measurement of D_{obs} can be made using several methods: EPA Method 1315 (EPA 2013), ANS/ANSI 16.1 (note that this method has recently been updated to serve as a 7-day screening test and not a long-term assessment) (ANS/ANSI 2019), and ASTM C1308-08(2017). Discrepancies in terminology and methodology between the tests are discussed in detail in Section 3.2 of Serne et al. 2016b. All tests follow a similar protocol, with monolithic samples placed into a bath of solution (termed leachant before sample addition and leachate afterward) at a high solution-volume-to-grout-surface-area ratio for a series of predetermined intervals. At the conclusion of the interval, the monolith is placed in a fresh solution and the previous leachate is analyzed to quantify the mass of each species released. Recent Hanford-focused testing has used EPA Method 1315, and the D_{obs} is determined from that method using Eq. (1.4). Eq. (1.4) is derived from a solution to Fick's second law and is described in detail elsewhere (deGroot et al. 1992; Kosson et al. 2002; EPA 2013).

$$D_{obs} = \pi\left[\frac{M_{t_i}}{2\rho C_0(\sqrt{t_i}-\sqrt{t_{i-1}})}\right]^2 \tag{1.4}$$

where:
D_{obs} = observed diffusivity of a specific constituent during the interval, m^2/s
M_{ti} = mass of constituent released during interval, mg/m^2
t_i = cumulative contact time at the end of the current interval, s
t_{i-1} = cumulative contact time at the end of the preceding interval, s
ρ = bulk density of dry sample, kg-dry/m^3

C_0 = initial concentration of constituent in dry sample, mg/kg-dry

D_{obs} calculated from Eq. (1.4) is for a specific interval. In previous work, D_{obs} values are reported as either the value from the final leach interval or as an average of the final intervals; an average of 28 to 63 days is common for EPA Method 1315 (Serne et al. 2016b). The form of Eq. (1.4) does not account for release from the top and bottom faces of a cylindrical monolith; however, this assumption of release only from the sides of the sample is only valid if < 20% of the initial inventory of the solute has been released (Kosson et al. 2002).

The mass of each constituent released, M_{ti}, is controlled by various processes (e.g., redox reactions, solid phase sorption, and chemical reactions involving separate species) within the waste form and can lead to different D_{obs} values being measured for different species in the same waste form. An example of this difference comes from a grout waste form with a reducing environment where the release of Na, which has no interaction with the waste form matrix itself, is compared with the release of Cr. Because Na is highly mobile, its measured D_{obs} should be the same as D_i and can be assigned as the maximum release rate. On the other hand, the reducing environment of the waste form will favor formation of insoluble Cr(III) species over soluble Cr(VI) species and the release rate will be much lower, in turn yielding a lower D_{obs}.

The ratio between D_{obs} for the reacting species and the non-sorbing/non-reacting species (D_i) can be represented as follows in Eq. (1.5):

$$D_{obs-X} = \frac{D_i}{R} \tag{1.5}$$

where:
D_{obs-X} = observed diffusivity of a specific constituent during the interval, m^2/s
D_i = intrinsic diffusion coefficient, cm^2/s
R = retardation factor, unitless

R, the retardation factor, represents the ability of a grout material to retain a specific constituent relative to a non-sorbing/non-reactive constituent in the same sample. The parameter is an empirical representation that reflects the cumulative effect of all retarding phenomena that occur over the duration of a leach test. R is commonly represented in two forms; using the total porosity and solid phase density as written in Eq. (1.6) (Bates et al. 2019; Flach et al. 2016), or using the bulk density as shown in Eq. (1.7) (Serne et al. 2016b).

$$R = \left[1 + \frac{(1-\varepsilon)\rho_s K_d}{S\varepsilon}\right] \tag{1.6}$$

where:
R = retardation factor, unitless
ε = porosity, volume fraction
ρ_s = solid-phase density, g/cm^3
K_d = species-specific distribution coefficient, cm^3/g
S = moisture content, volume fraction

$$R = \left[1 + \left(\frac{\rho_b}{\varepsilon}\right) K_d\right] \tag{1.7}$$

where:
R = retardation factor, unitless

ρ_b = bulk density of the dry sample, g/cm^3
K_d = species-specific distribution coefficient, cm^3/g
ε = porosity, volume fraction

The distribution coefficient (K_d) is commonly used in geochemistry to represent the linear, reversible equilibrium sorption of an aqueous constituent to a solid material. In the case of Eq. (1.4), where the constituent can be retained in the waste form through multiple processes, the K_d becomes an all-encompassing term to represent the portion of the constituent inventory that is not available for release. *R* for a specific constituent can be determined experimentally if the D_{obs} is known for a constituent and a D_{obs} is known for a non-sorbing/non-reacting constituent (or D_i) where K_d is near zero (e.g., Na). In reactive transport modeling of grout materials, the R value can be used to assign retention capability to the waste form through use of a K_d for the material. This is the process that was used to represent reducing conditions in a grouted secondary waste form in the 2017 IDF PA.

The performance metric for the four target constituents (Tc, I, Cr, NO_3^-) will be defined as an R value that will lead to a specific groundwater concentration at the point of compliance (POC, a well 100-m down gradient) for the IDF. The following steps will be used for the simulations:

1. A K_d will be assigned to the individual waste form container with the K_d varied for each simulation run. The K_d's were selected arbitrarily to give retention capability to the waste form in the simulations.
2. The individual waste form containers are placed as two rows stacked on top of one another and separated by low-density backfill; this arrangement is one lift. Within the IDF there will be four lifts extending from the bottom of the facility to the top. This set of four lifts makes up a single stack. The resulting release from an individual waste form stack will be calculated and then multiplied to represent the full inventory.
3. A fractional release at the bottom of the IDF will then be determined for the 10,000-year simulation time frame.
4. The fractional release will serve as a continuous source term for subsurface transport represented by a variable transport and flow model.
5. The maximum concentration of the species of interest will be assessed at the POC, as again, a well 100-m down gradient of the IDF.
6. Using Eq. (1.6) or (1.7), an R value will be calculated for each K_d input to the simulations.

The simulation will use a unit waste-form concentration and all transport parameters remain fixed for the simulation, with the K_d being varied. This R value can then be used in future work to determine if a laboratory D_{obs} will lead to a set concentration at the POC, without the need for a timely PA/PE exercise. This metric can be used to rapidly screen new grout test data and technologies.

It should be noted that these simulations only consider the contribution from the SLAW inventory and not any contribution to the overall release rate from the primary LAW inventory. As a result, the R values that achieve the target concentrations would be an underestimation of the full LAW inventory release.

1.2 Previous Hanford Performance Assessments

Grout waste forms have been included in previous PAs for disposal at Hanford, and a summary of the assessments are given in Table 1-1. The 1995 PA covered the original grout vault disposal system for double-shell tank waste (Kincaid et al. 1995). The next two ILAW PAs, performed in 1998 (Mann et al. 1998) and 2001 (Mann et al. 2001), only evaluated the primary glass waste form. The 2003 Risk

Assessment considered grouted secondary wastes and the Supplemental Immobilization Risk Assessment in 2003 included a grouted SLAW inventory (Mann 2003). The unreleased 2005 PA included grouted low-level and secondary wastes, but no SLAW grout (Pierce et al. 2004). In 2012, the Tank Closure and Waste Management Environmental Impact Statement (TC&WM EIS) compared alternative supplemental waste forms for LAW, including grout (DOE, 2012). The 2017 edition of the IDF PA evaluated grouted secondary waste stream, but only the primary glass waste form for LAW (DOE, 2017). Most recently, in 2019, the PE from the NDAA review of Hanford supplemental technologies included a grouted SLAW inventory. A full description of the various evaluations can be found in Appendix F of Bates et al. 2019.

Table 1-1. Waste form types included in previous Hanford site assessments.

Year	Assessment Type	LAW Glass	Secondary Waste Grout	LAW Grout
1995	Performance Assessment	-	-	×
1997	Performance Assessment	×	-	-
2001	Performance Assessment	×	-	-
2003	Risk Assessment	×	-	×
2005	Performance Assessment	×	×	-
2012	Environmental Impact Study	×	×	×
2017	Performance Assessment	×	×	-

1.3 Objective

The objective of this report is to define a quantitative performance metric (defined as an R, and corresponding laboratory D_{obs}) for an SLAW inventory of cementitious waste forms in the IDF that results in groundwater concentrations below the drinking water standard (DWS), which are listed in Table 1-2. The performance metric will set targets for D_{obs} in laboratory testing and serve as a basis to compare previously published grout leach test data for treated LAW and other grout waste forms. In addition, the simulations developed in this work can be used in future efforts to assess alternative SLAW technologies and inventories.

Table 1-2. Summary of the drinking water standard targets used in this work.

Contaminant	Drinking Water Standard	Reference
Technetium	900 pCi/L	EPA 2002a
Iodine	1 pCi/L	Bartholomay, 2013
Nitrate	10 mg/L as Nitrogen or 44.3 mg/L Nitrate	EPA 2002b
Chromium	0.1 mg/L	EPA 2002b

1.4 Report Organization

The sections that follow present the simulation approach and assessment of previously published data. Section 2.0 describes the model setup and simulation parameters. Simulation results and their interpretation are provided in Section 2.7. Section 4.0 uses the metric to interpret historical leach test data for different contaminants.

1.5 Quality Assurance

This work was funded by Washington River Protection *Solutions*, LLC (WRPS) under contract 36437-265, *Supplemental Immobilization of Hanford Low-Activity Waste.* The work was conducted as part of Pacific Northwest National Laboratory (PNNL) Project 72968, Supplemental Immobilization of Hanford LAW.

This work was performed in accordance with the WRPS Waste Form Testing Program (WWFTP) quality assurance (QA) program. The WWFTP QA program is based on the requirements of NQA-1-2008, *Quality Assurance Requirements for Nuclear Facility Applications*, and NQA-1a-2009, *Addenda to ASME NQA-1-2008 Quality Assurance Requirements for Nuclear Facility Applications*, graded on the approach presented in NQA-1-2008, Part IV, Subpart 4.2, "Guidance on Graded Application of Quality Assurance (QA) for Nuclear-Related Research and Development." The WWFTP QA program consists of the WWFTP Quality Assurance Plan (QA-WWFTP-001) and associated procedures that provide detailed instructions for implementing NQA-1 requirements for research and development work.

The WWFTP QA Program works in conjunction with PNNL's laboratory-level Quality Management Program, which is based upon the requirements as defined in the U.S. Department of Energy (DOE) Order 414.1D, *Quality Assurance,* and 10 CFR 830, *Nuclear Safety Management*, Subpart A, "Quality Assurance Requirements." Performance of this work and preparation of this report were assigned the technology level "Applied Research". All staff members contributing to the work have technical expertise in the subject matter and received QA training before performing quality-affecting work. The "Applied Research" technology level provides adequate controls to ensure that the activities were performed correctly and that all client QA expectations were addressed in performing the work.

2.0 Model Development and Simulations

2.1 Integrated Disposal Facility

The IDF is located in the 200 East Area of the Central Plateau at Hanford, southwest of the WTP (Krupka et al. 2004). The current design of the IDF includes two cells (300,000-m^3 capacity) that were constructed in 2006 (Bates et al. 2019). The IDF will be covered with a RCRA barrier to limit intrusion of water and prevent inadvertent intrusion from plant and animal life. Waste packages will be surrounded by the original backfill excavated from the site and a liner and a leak detection system will provide secondary containment and water management after closure (DOE 2017). The center of the IDF is elevated to provide a slope to prevent mixing of leachates from the individual cells of the IDF. Contaminant releases from the IDF are anticipated to be primarily from the sumps. The slope will direct leachate toward sumps in each cell.

The bottom of the IDF sits ≈ 300 ft above an unconfined aquifer and the vadose zone is a mix of sand and gravel, corresponding to the Hanford and Ringold formations. The Hanford formation consists of pebble-to-cobble gravel with fine-to-coarse-grained sand and small amounts of clay and silt. The Ringold Formation, underlying the Hanford formation, is made of partially-cemented fluvial gravel sediments.

A full description of the IDF and its geological setting can be found in Section 2 of the 2017 IDF PA (DOE 2017).

2.2 Simulation Description, Software, and Methodology

The simulations were performed using the scalable version of the Subsurface Transport Over Multiple Phases (STOMP) simulator (White et al. 2012), known as exascale STOMP or eSTOMP. eSTOMP is managed as safety software and complies with NQA-1 QA standards (Freedman et al. 2016). eSTOMP has also been used to simulate the Field Lysimeter Test Facility experiment (Bacon et al. 2018) and for the NDAA PE (Bates et al., 2019). The 2017 IDF PA used the serial STOMP (original version), and other simulators including GOLDSIM® and The Geochemist's Workbench (DOE 2017). A comparison between the results of STOMP vs. eSTOMP is given in Figure F7 of the NDAA PE (Bates et al. 2019).

The simulations were designed in parallel with the NDAA PE to ensure consistency between the two individual efforts. The base case for this simulation was the release of Tc from the NDAA PE to determine flux out of the disposal facility and into the vadose zone. To estimate groundwater concentrations at a downstream compliance point in the NDAA PE, a linear correlation calculation was performed based on simulations executed for the 2017 IDF PA (Bates et al. 2019). In the present work, flow and solute transport through the vadose zone and into the groundwater are explicitly represented as a 3D variably saturated flow and transport model to determine the groundwater concentrations.

The following steps were carried out to calculate the fractional release rate from an inventory of cementitious waste forms. The wastes represent a SLAW volume within the IDF that would result in concentrations equal to 100%, 10%, and 1% of the drinking water standards for I, Tc, NO_3^-, and Cr at the compliance point (water well 100 m downgradient from the IDF boundary). All simulations used a constant SLAW inventory and volume.

A two-step simulation approach was executed. In the first step, the simulation domain represented a stack of waste form boxes in the IDF (see Section 2.3). A uniform distribution of each contaminant was assumed, with a total mass or radioactivity of 1 kg or 1 Ci, respectively. The waste forms were also

assumed to have uniform hydraulic properties. A full description of the waste form properties is given in Section 2.4.

A range of K_d values were applied to the waste forms in the simulations to generate a retardation effect on constituent release as described in Eqs. (1.6) and (1.7). The resulting release was used to identify the impact of K_d on contaminant flux (as a constant release rate) from the facility. The concentrations of the contaminants being released at the bottom of the IDF after 10,000 years were transformed from a unit concentration in the waste forms by adjusting to account for the entire SLAW inventory of the constituent.

In the second step, a domain representing the vadose zone and groundwater beneath the facility was used to assign a constant contaminant release rate assuming a uniform spatial distribution to the west and east sump under the IDF. In this second step, 3D variably saturated flow and transport simulations predicted contaminant concentrations 100 meters downgradient of the facility at the POC based on the simulated release rates. The simulation domain was identical to the one used in the 2017 IDF PA (DOE 2017). A description of subsurface properties is provided in Section 2.6.

The above steps were iterated by changing the waste form K_d until each target POC concentration (1×, 0.1 × and 0.01 × times the DWS) was achieved.

2.3 IDF Design and Properties

A cross-sectional view of the conceptual IDF is shown in Figure 2-1. The simulations were designed to replicate the IDF with the properties/scenarios described below. The IDF design consists of an engineered surface barrier, four lifts of waste forms (containing two layers of B-25 boxes) surrounded by backfill, and an engineered liner system at the bottom.

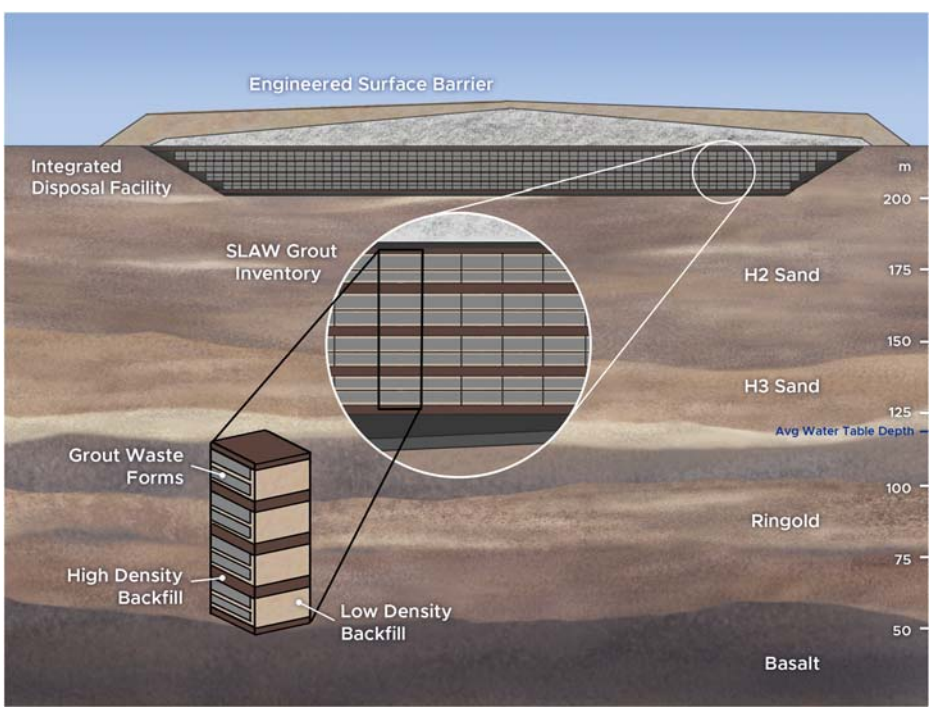

Figure 2-1. Cross-section schematic of the Hanford IDF and subsurface (DOE 2017).

2.3.1 Surface Barrier and Infiltration Rate

The infiltration rate through the engineered surface barrier was assumed to be 3.5 mm/yr throughout the simulation. Two sensitivity cases were considered with alternate infiltration rates of 1.7 and 5.1 mm/yr. The 2012 TC&WM EIS (DOE 2012), 2017 IDF PA, and NDAA PE assumed a 500-year lifecycle for the surface barrier before failure.

2.3.2 Waste Form Package and Stacking

As shown in Figure 2-1, the IDF cells will be filled in four lifts of waste form containers. In the current plan for the IDF, each lift will contain two layers of waste form containers, for a total of eight waste form containers high in the four lifts. The 2017 IDF PA simulated one lift (two containers high) to allow for computational efficiency with the serial STMOP simulator. Both this work and the NDAA PE simulated the full four lift stack with each lift stack containing two waste packages.

The grout waste package was assumed to be a B-25 steel container (46” W × 72” L × 47” H, 2.5-m^3 volume), identical to the NDAA PE. The steel container was not represented in the simulation.

Each layer of waste form containers will be surrounded by a low-density backfill previously excavated from the IDF site, whereas each lift will be surrounded by a high-density backfill as shown in Figure 2.2. The size of the backfill regions were chosen to be consistent with the 2017 IDF PA and NDAA PE. The dimensional representation of the full stack used in the simulations is shown in Figure 2-2. The full list of properties used to represent the IDF backfill is given in Table 2-1.

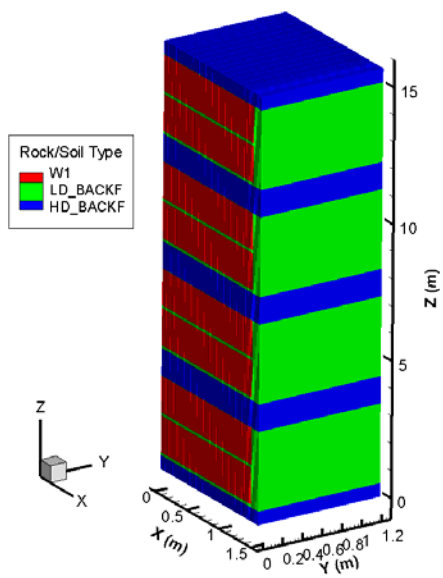

Figure 2-2. Schematic of the full waste form container stacking used in the simulations showing the waste containers (red, W1), low-density backfill (green, LD_BACKF) and high-density backfill (blue, HD_BACKF).

Table 2-1. Summary of the properties of the low- and high-density backfills used in the simulated IDF.

Backfill Information	Low-Density Backfill	High-Density Backfill	Reference	Reasoning
Particle Density (g/cm^3)	2.710	2.710	Table 4.7 by Meyer et al. 2004	Consistency with 2017 IDF PA and NDAA PE
Saturated Hydraulic Conductivity (cm/s)	1.86E-02	4.91E-03	Table 4.7 by Meyer et al. 2004	Consistency with 2017 IDF PA and NDAA PE
van Genuchten, α (1/cm)	5.70E-02	6.50E-02	Table 4.7 by Meyer et al. 2004	Consistency with 2017 IDF PA and NDAA PE
Van Genuchten , n (unitless)	2.8	1.7	Table 4.7 by Meyer et al. 2004	Consistency with 2017 IDF PA and NDAA PE
Porosity	0.37	0.35	Table 4.7 by Meyer et al. 2004	Consistency with 2017 IDF PA and NDAA PE
Residual Saturation (%)	8.1	8.6	2017 IDF PA Run File	Consistency with 2017 IDF PA and NDAA PE
Longitudinal Dispersivity (m)	0	0	Section 5.1 by Meyer et al. 2004, Section 2.7 by Bacon et al. 2018	Consistency with 2017 IDF PA and NDAA PE
Transverse Dispersivity (m)	0	0	Section 2.7 by Bacon et al. 2018	Consistency with 2017 IDF PA and NDAA PE
Initial Concentrations in Backfill Pore Water	0	0	See Reasoning	Section 2.18 in PNNL-27394 (Bacon et al. 2018) suggests a starting concentration of Tc/I in the backfill of 1E-10 mol/L; this was replaced with zero.
Intrinsic Diffusion Coefficient, D_i (cm^2/s)	2.60E-09	2.60E-09	2017 IDF PA Run File (DOE 2017)	Consistency with 2017 IDF PA and NDAA PE
Initial Saturation	0.09	0.2	Pg 4-113 by DOE 2017	Consistency with 2017 IDF PA and NDAA PE

2.4 Waste Form Properties

The simulations were performed to represent a SLAW inventory of grout waste forms in the IDF. As grout is currently only a possible candidate for SLAW, baseline grout waste form properties are not yet defined. Cast Stone, a dry mixture of 47 wt% ground, granulated blast furnace slag (BFS), 45 wt% Class F fly ash (FA), and 8 wt% type II ordinary portland cement (OPC), is recognized as the baseline formulation to immobilize Hanford liquid wastes based on a down-selection effort to initially identify an SLAW technology in 2005 (Lockrem 2005; mixture DF2 in the test). The Cast Stone formulation for LAW is very similar to the saltstone formulation used for low-level, liquid salt waste at the Savannah River Site. Where appropriate, the known properties of Cast Stone were used in the simulation, but when a parameter has not yet been determined for LAW (e.g., saturated hydraulic conductivity), data for either a Cast Stone waste form from liquid secondary waste or saltstone were used. A summary of the grout waste form properties used in the simulations is given in Table 2-2.

The inventory of Tc, I, Cr, and NO_3^- distributed throughout the waste packages was based on the Integrated Flowsheet data supporting System Plan Rev. 8 (Tilanus et al. 2017; Base Case) and is consistent with the NDAA PE. The System Plan Rev. 8 inventory is slightly lower than the inventory used in the 2017 IDF PA; however, the split factors captured in the System Plan inventory are different. The best basis inventory feed vector inventory is similar in both the NDAA PE and 2017 IDF PA. The inventory used for each constituent is given in Table 2-3. The number of waste packages was calculated by dividing the volume of grout by the volume of a B-25 box.

2.5 eSTOMP Input Cards for the IDF Waste Form Simulation

The eSTOMP input cards are described below. If not explicitly stated, the input cards for the IDF simulation are the same as those used in simulations executed for the 2017 IDF PA. For the facility release simulations, a four-stack B-25 container model was executed and the run file can be found in Appendix A. For the vadose zone and groundwater simulation scenarios, inputs were the same as in the 2017 IDF PA but were modified to represent various contaminant release scenarios.

It should be noted that these simulations only consider the contribution from the SLAW inventory and not any contribution from the primary waste form inventory.

2.5.1 Solution Control Card

The time-dependent information is specified in the Solution Control Card. Simulations were executed for a total simulation time of 10,000 years. The maximum time step was set at 500 years, chosen to be as large as possible while allowing the simulations to reach completion without convergence failure.

2.5.2 Grid Card

For the IDF waste form simulation, the grid extends from the two-lift B-25 container model used in the 2017 IDF PA to the four-lift B-25 container model (Bates et al. 2019). Each lift held two stacks of waste forms with 0.13 m of low-density backfill packed between the containers and 1 m of high-density backfill along with 0.12 m of low-density backfill between each lift. A quarter of the IDF stack is simulated, with a length of 1.025 m, width of 0.695 m, and height of 14.52 m. A total waste footprint of 49,795 m^2 was represented and split into 498 grid cells distributed as 11 full rows in IDF cell 1 and 2 (374 grid cells), 3 full rows (102 grid cells) and 2 partial rows in cell 3 and 4. A full description is given in Section 2.3.

2.5.3 Rock/Soil Zonation Card

The two-stack model for the waste packages used in the 2017 IDF PA (DOE, 2017) was extended to represent the full vertical IDF space of four stacks.

2.5.4 Mechanical Properties, Hydraulic Properties, Saturation Function Card

The mechanical, hydraulic, and saturation properties were all selected to be consistent with the representation in the 2017 IDF PA. Mechanical properties were defined for four material types: high-density backfill, low-density backfill, and the IDF structure. The steel overpack surrounding the waste forms was not included. The hydraulic conductivities were assigned from the data packages for the 2017 IDF PA (DOE 2017). The saturation function parameters were assigned as defined in the 2017 IDF PA (DOE 2017). A full description of the properties is given in Table 2-1 and Table 2-2 .

2.5.5 Aqueous Relative Permeability Card.

The Mualem (1976) relative permeability function was assumed for all materials. This is the same assumption used in the 2017 IDF PA and NDAA PE efforts. eSTOMP used the water mode to allow the gas phase to be infinitely mobile compared to the aqueous phase. No interphase mass transfer was considered in these simulations.

2.5.6 Solute/Fluid Interaction Card

An intrinsic diffusion coefficient, D_i, equal to 2.6×10^{-9} cm^2/s was selected to represent a non-reacting/non-sorbing solute; this value is then adjusted by an R factor that is implemented as a K_d in the simulation. In the IDF backfill and the subsurface below the IDF, the diffusion coefficient was set to 2.5×10^{-5} cm^2/s, which is the same as used in previous IDF simulations.

Full details are in Section 2.4 for the waste form and Section 2.6 for the subsurface.

2.5.7 Solute/Porous Media Interaction Card

A longitudinal dispersivity of 0.0 meters and transverse dispersivity of 0.0 meters were used for the IDF waste form simulation.

2.5.8 Initial Condition Card

A unit mass (1 kg) or unit radioactivity (1 Ci) of each species of interest was distributed evenly between the IDF forms. Initial flow fields from each material type are the same as in the 2017 IDF PA (DOE, 2017) and NDAA PE (Bates et al, 2019).

2.5.9 Boundary Condition Card

The upper boundary condition is a constant water flux rate of 3.5 mm/yr which corresponds to the water intrusion rate in the IDF simulations once the protective cap is lost. The rest of the boundary conditions are the same as previously used in IDF simulations and the NDAA PE.

Table 2-2. Summary of properties for the cementitious waste forms used in the simulations.

Property	Value	Resource	Reasoning
Particle Density (g/cm^3)	2.82 (LSW Grout, Test ID 11)	Table 3.4 by Cantrell et al. 2016	Value chosen from Table 3.4, Test ID 11, as this mixture is similar to the standard Hanford formulation for Cast Stone, a mix of OPC/FA/BFS.
Saturated Hydraulic Conductivity (cm/s)	1.54E-9 (LSW Grout, Test ID 11)	Table 3.4 by Cantrell et al. 2016	Value chosen from Table 3.4, Test ID 11, as this mixture is similar to the standard Hanford formulation for Cast Stone, a mix of OPC/FA/BFS.
van Genuchten α (1/cm)	6.03E-6	Table 3.6 by Cantrell et al. 2016	Because saltstone is a low-activity cementitious waste form, this value best represents a Hanford LAW waste form.
van Genuchten, n (unitless)	1.649	Table 3.6 by Cantrell et al. 2016	Because saltstone is a low-activity cementitious waste form, this value best represents a Hanford LAW waste form.
Porosity	55.7%	Table 3.5 by Cantrell et al. 2016	Chosen value is an average for a set of LAW Cast Stone samples at a high waste loading (0.6).
Initial Saturation	0.9	Table 9.2, “Hanford Sand,” by Flach et al. 2016	This value was selected because a mortar is most like a waste form based on its physical properties.

Table 2-3. Total inventories used for the SLAW simulations.

Species	Inventory	Source
Technetium	11,593 Ci	Table F-9 by Bates et al. (2019)
Iodine	10.5 Ci	Table F-9 by Bates et al. (2019)
Chromium	7.98×10^{8} g	Table 6.7, Column 45, in RPP-RPT-27991, Rev. 2 (Anderson et al. 2017)
Nitrate	2.54×10^{10} g	Table 6.7, Column 45, in RPP-RPT-27991, Rev. 2 (Anderson et al. 2017)
Grout Volume	320,489 m^3	Table 5-8 in ORP-11242, Rev. 8 (converted from gallons) (Tilanus et al. 2017)
Number of Packages	139,599	Calculated
Waste Footprint	49,795 m^2	Calculated

2.6 Subsurface Properties

Following release from the waste stacks, the migrating species were modeled to be released from the IDF via the sump in the liner located at the bottom of the IDF. A cross-section, north-south view of the IDF is shown in Figure 2-3, where the liner sump is located at the bottom of the facility.

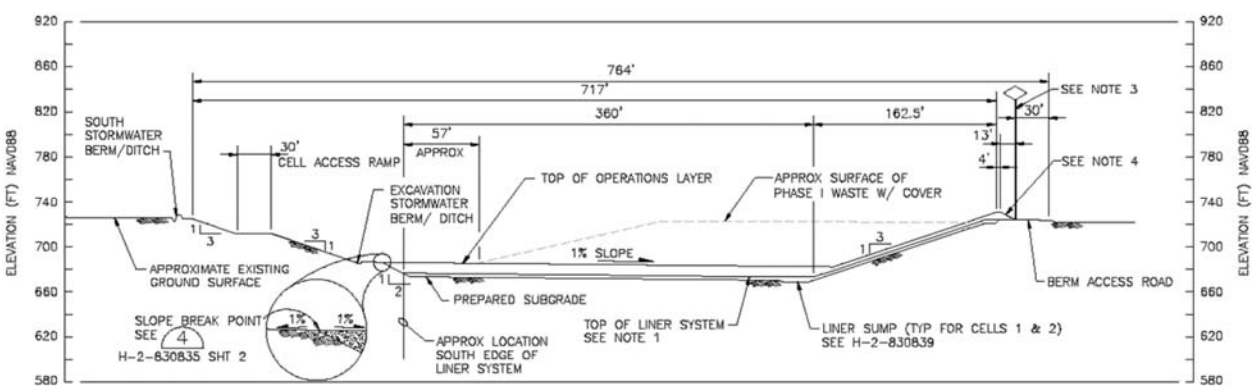

Figure 2-3. North-south cross-section of the IDF showing the location of the liner sump (from Figure 2-8 of DOE 2017)

The fractional release from the IDF to the vadose zone occurred at the sump location. Released contaminants are then transported through the vadose zone to the water table and migrate with the groundwater. A visual of the sump locations above the simulated subsurface layers is shown in Figure 2-4. Contaminant transport in the vadose zone and aquifer were simulated using eSTOMP to describe 3D variable saturated flow and transport. The properties used to represent the subsurface were the same as those used in the 2017 IDF PA and are listed in Table 2-4. The source of the values are explained in detail in Rockhold et al. 2015. Within the subsurface, iodine was the only species to be assigned a K_d (equal to 0.1) in the Hanford Sand layer. The K_d values for all other species were set equal to zero.

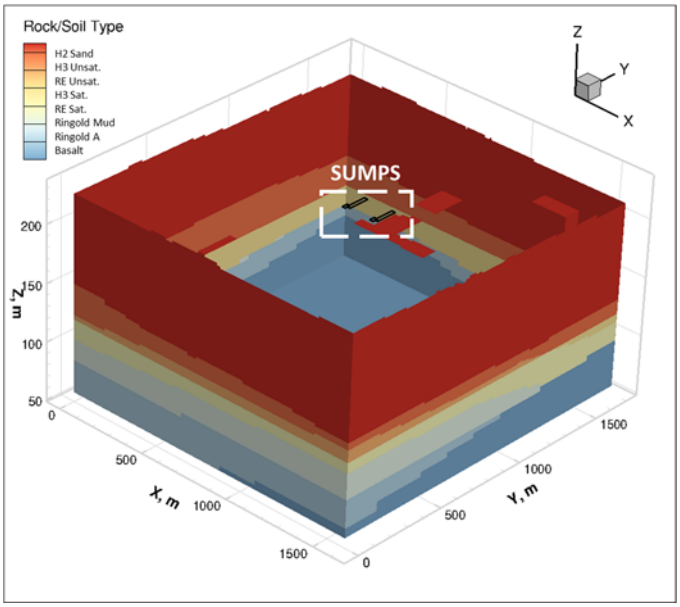

Figure 2-4. Visualization of the simulated subsurface below the IDF and the location of the sumps where release of contaminants from the IDF occurred in the simulations.

Table 2-4. Summary of properties used to represent the subsurface below the IDF in the simulations.

Subsurface Information (Layer Type)	Basalt	Ringold A Gravel	Ringold Lower Mud	Hanford Gravel (saturated)	Ringold E Gravel (saturated)	Hanford Gravel (unsaturated)	Ringold E Gravel (unsaturated)	Hanford Sand
Particle Density (g/cm^3)	2.65	2.4189	2.4189	2.75	2.4189	2.6634	2.6634	2.776
Vertical Saturated Hydraulic Conductivity (cm/s)	1.00E-05	0.48	8.00E-04	1200	0.5	7.71E-03	7.71E-03	6.16E-03
Horizontal Saturated Hydraulic Conductivity (cm/s)	1.00E-04	4.8	8.00E-03	17000	5.0	4.671E-02	4.671E-02	6.196E-03
van Genuchten, α (1/cm)	0.08859	0.08859	0.08859	0.08859	0.08859	0.08859	0.08859	0.06419
van Genuchten n (unitless)	1.271	1.271	1.271	1.271	1.271	1.271	1.271	1.698
Porosity	0.05	0.0905	0.0905	0.2	0.0905	0.174	0.174	0.384
Residual Saturation (%)	2.18E-02	2.18E-02	2.18E-02	2.18E-02	2.18E-02	2.18E-02	2.18E-02	7.55E-02
Longitudinal Dispersivity (m)	1	1	1	1	1	0.2	0.2	0.25
Transverse Dispersivity (m)	0.01	0.01	0.01	0.01	0.01	0.02	0.02	0.025
Initial Concentrations in Pore Water	0	0	0	0	0	0	0	0
Intrinsic Diffusion Coefficient, D_i (cm^2/s)	2.50E-05	2.50E-05	2.50E-05	2.50E-05	2.50E-05	2.50E-05	2.50E-05	2.50E-05
Pore-scale Parameter for Modified Mualem Relative Perm Model in X Direction	0.637	0.637	0.637	0.637	0.637	0.637	0.637	-0.683
Pore-scale Parameter for Modified Mualem Relative Perm Model in Y Direction	0.637	0.637	0.637	0.637	0.637	0.637	0.637	-0.683
Pore-scale Parameter for Modified Mualem Relative Perm Model in Z Direction	-0.225	-0.225	-0.225	-0.225	-0.225	-0.225	-0.225	0.375

2.7 eSTOMP Input Cards for the IDF Subsurface Simulation

If not explicitly stated, the simulation input cards for the subsurface flow and transport below the IDF were designed to be the same as for simulations executed for the 2017 IDF PA but were changed to represent various contaminant release scenarios.

2.7.1 Solution Control Card

The time-dependent information is specified in the Solution Control Card. Simulations were executed for a total simulation time of 10,000 years. The maximum time step was set at 1 year, chosen to be as large as possible, while allowing the simulations to complete without convergence failure. A restart file generated using initial conditions from historical simulations of the IDF subsurface was used.

2.7.2 Grid Card

The grid is the same as used in previous IDF subsurface simulations.

2.7.3 Rock/Soil Zonation Card

A total of 8 rock types were defined as zones to be consistent with the previous IDF subsurface simulations. The rock properties are given in Table 2-4.

2.7.4 Mechanical Properties, Hydraulic Properties, Saturation Function Card

The mechanical, hydraulic, and saturation properties were all selected to be consistent with the representation in the 2017 IDF PA. Mechanical properties, hydraulic properties, and saturation functions were defined for 8 material types (Table 2-4). They were assigned to be consistent with the 2017 IDF PA (DOE 2017, Rockhold et al. 2015).

2.7.5 Aqueous Relative Permeability Card

The modified Mualem relative permeability function was assumed for all materials (Mualem 1976). This is the same assumption used for the 2017 IDF PA. eSTOMP employed the water mode to allow the gas phase to be infinitely mobile relative to the aqueous phase. No interphase mass transfer was considered in these simulations.

2.7.6 Solute/Fluid Interaction Card

An intrinsic diffusion coefficient, D_i, equal to 2.5×10^{-5} cm^2/s was selected to represent a non-reacting/non-sorbing solute, the same as used in previous IDF simulations.

2.7.7 Solute/Porous Media Interaction Card

A longitudinal dispersivity of 1.0 m and transverse dispersivity of 0.01 m were assumed for Basalt, Ringold A Gravel, Ringold Lower Mud, saturated Hanford Gravel, and saturated Ringold E Gravel. A longitudinal dispersivity of 20.0 cm and transverse dispersivity of 2.0 cm were assumed for unsaturated Hanford Gravel, unsaturated Ringold E Gravel, and 25.0 cm and 2.5 cm for the Hanford Sand.

2.7.8 Initial Condition Card

The flow field was initialized from a restart file generated using initial conditions from historical simulations of the IDF subsurface. Initially, no solutes were present in the subsurface.

2.7.9 Boundary Condition Card

An infiltration from a background rate of 3.5 mm/yr was used during the full simulation. The rest of the boundary conditions are the same as previously used in IDF simulations.

2.7.10 Source Card

Contaminant releases from the IDF leachate were uniformly allocated to the west and east sumps under the IDF facility. The release rates were calculated for each contaminant based on the total IDF leachate over the 10,000 years.

3.0 Results

This section summarizes the simulation results for the study described in this report. The plots presented show the corresponding R (retardation factor) needed to maintain concentrations below the DWS at a well 100 meters downgradient of the IDF after 10,000 years. The plots also show the corresponding observed diffusivity, D_{obs} value, that would be measured in a laboratory sample with an identical R factor using Eq. (1.6). The D_i assumed for a non-reacting/non-sorbing species for the R calculation was 2×10^{-9} cm^2/s. Detailed simulation results are presented in Appendix B.

3.1 Technetium (Tc-99)

Tc-99 is present in Hanford wastes as a fission product from used nuclear fuel. Upon dissolution, the Tc is released from the fuel as anionic pertechnetate (TcO_4^-), which is highly soluble and thus leads to its presence in the wastes (Serne et al. 2016a). Tc will comprise most of the radioactive component in the treated LAW inventory.

The DWS established by the EPA for Tc-99 is 900 pCi/L based on a 4-mrem/yr beta exposure limit (EPA 2002a). A 900 pCi/L concentration at the POC was the initial target for the simulations. Subsequent simulations assumed one-tenth (90 pCi/L) and one-hundredth (9 pCi/L) of the DWS target. Results of the simulations are shown in Figure 3-1.

To meet the 900-pCi/L target for Tc, an R factor of 113 would be required, which corresponds to an observed diffusivity of 2×10^{-11} cm^2/s in laboratory testing. To achieve 90 pCi/L, an R factor of 1,285 was determined, which corresponds to an observed diffusivity of 2×10^{-12} cm^2/s. Finally, to achieve 9 pCi/L, an R factor of 13,093 would be required, which corresponds to an observed diffusivity equal to 2×10^{-13} cm^2/s.

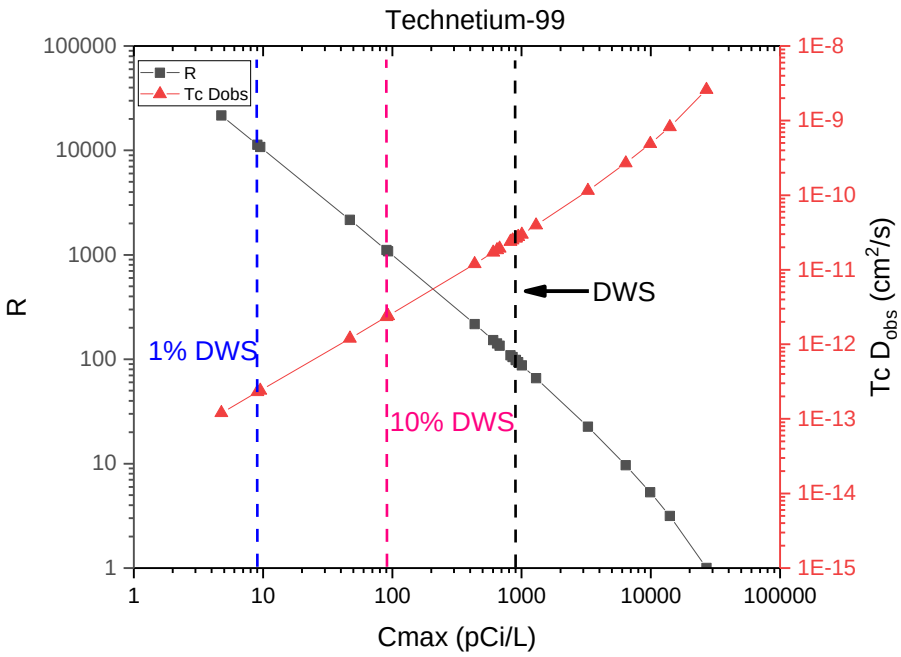

Figure 3-1. Visualization of the R factor (black) used in the simulations and the resulting concentration of Tc determined at the POC in pCi/L. The corresponding observed diffusivity that would be measured for a grout with a specific R factor is also shown (red). Dashed lines corresponding to the target concentrations relative to the DWS are also provided.

3.2 Iodine

I-129 is present in Hanford wastes and is also a fission product from used nuclear fuel. In fuel dissolution, iodine is released as $I_{2(g)}$; however, in an aqueous environment, the $I_{2(g)}$ will hydrolyze to form a soluble iodine species, such as iodide or iodate (Riley et al. 2016). The primary iodine form in the Hanford waste is assumed to be iodide; however, further understanding of the speciation is required.

The DWS established by the EPA for I-129 is 1 pCi/L based on a 4-mrem/yr exposure limit, although it has been proposed to increase the DWS to 21 pCi/L (Bartholomay 2013). A concentration of 1 pCi/L at the POC was set as the initial target for the simulations. Subsequent simulations assumed one-tenth (0.1 pCi/L) and one-hundredth (0.01 pCi/L) of the DWS target as well as the proposed 21 pCi/L DWS. Results of the simulations are shown in Figure 3-2.

To meet the 1-pCi/L target for I-129, an R factor of 87 would be required, corresponding to an observed diffusivity of 3×10^{-11} cm^2/s. To achieve 0.1 pCi/L, an R factor of 624 was determined, which corresponds to an observed diffusivity of 4×10^{-12} cm^2/s. Finally, to achieve 0.01 pCi/L, an R factor of 10,801 would be required, which would equal an observed diffusivity of 2×10^{-13} cm^2/s.

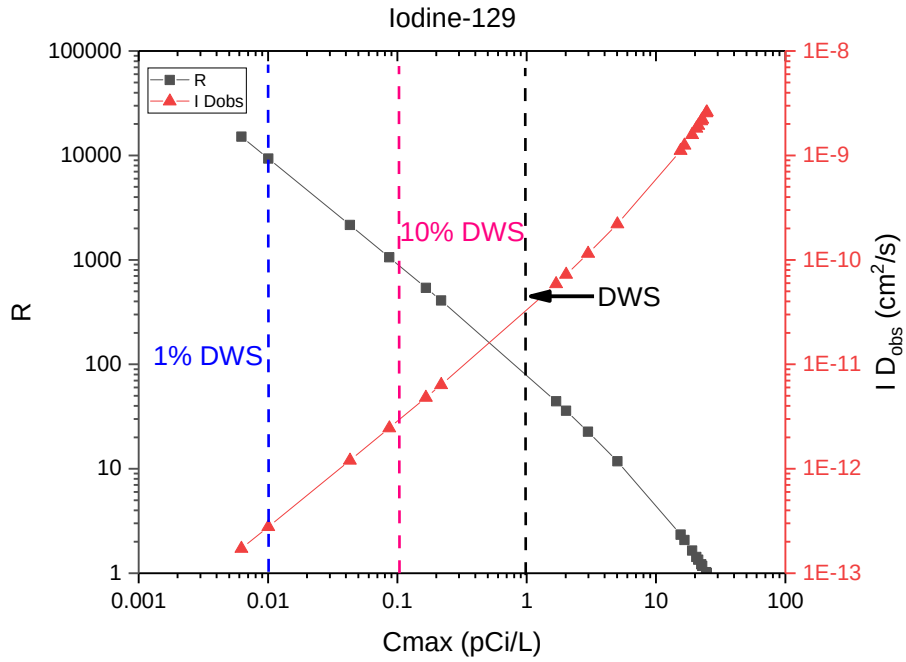

Figure 3-2. Visualization of the R factor (black) used in the simulations and the resulting concentration of I-129 determined at the POC in pCi/L. The corresponding observed diffusivity that would be measured for a grout with a specific R factor is also shown (red). Dashed lines corresponding to the target concentrations relative to the DWS are also provided.

3.3 Nitrate

The nitrate (NO_3^-) inventory present in Hanford wastes originates from various steps in the multiple reprocessing flowsheets used, but primarily from dissolution in nitric acid (Peterson et al. 2018). An inventory of NO_2 is also present in the wastes but was not included in the assessment due to complexities with NO_2 transformation in the subsurface (Szecsody et al. 2017).

The DWS established by the EPA for NO_3^- is 10 mg/L as total nitrogen (EPA 2002b), this equals 44.3 mg/L of NO_3^-. This concentration at the POC was set as the initial target of the simulations. Subsequent simulations assumed one-tenth (4.4 mg/L) and one-hundredth (0.4 mg/L) of the DWS target. Results of the simulations are shown in Figure 3-3.

To meet the 44-mg/L target for NO_3^-, an R factor of 2 would be required, corresponding to an observed diffusivity of 2×10^{-9} cm^2/s. To achieve 4.4 mg/L, an R factor of 45 is needed and corresponds to an observed diffusivity of 6×10^{-11} cm^2/s. Finally, to achieve 0.44 mg/L, an R factor of 550 would be required, which would equal an observed diffusivity of 4×10^{-12} cm^2/s.

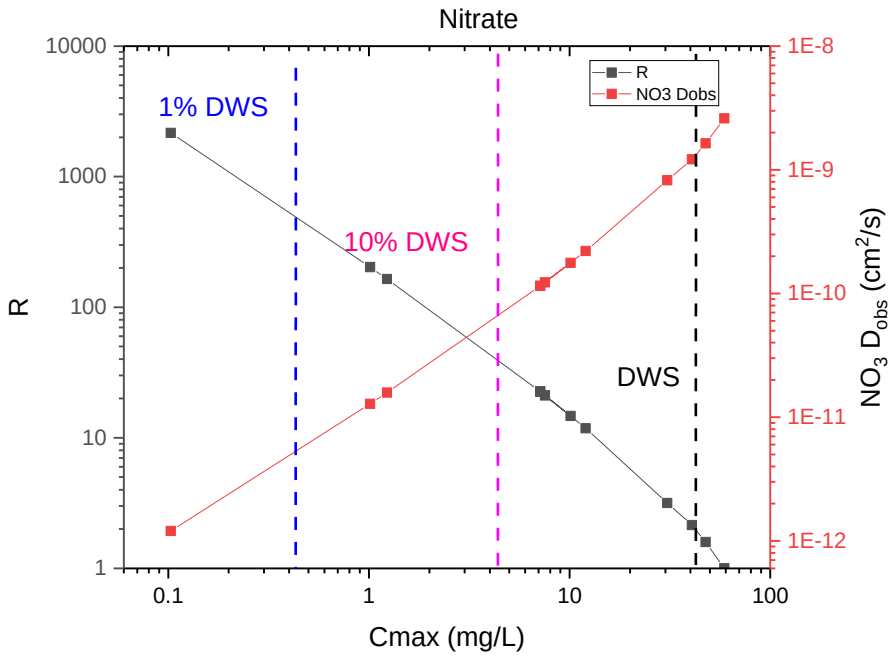

Figure 3-3. Visualization of the R factor (black) used in the simulations and the resulting concentration of NO_3^- determined at the POC in mg/L. The corresponding observed diffusivity that would be measured for a grout with a specific R factor is also shown (red). Dashed lines corresponding to the target concentrations are also provided.

3.4 Chromium

The Cr inventory present in Hanford wastes originates from various flowsheets as a redox buffer or as a corrosion product (Peterson et al. 2018).

The DWS established by the EPA for Cr is 0.1 mg/L (EPA 2002b). This concentration at the POC was set as the initial target for the simulations. Subsequent simulations assumed one-tenth (0.01 mg/L) and one-hundredth (0.001 mg/L) of the DWS target. Results of the simulations are shown in Figure 3-4.

The 0.1 mg/L target for Cr was observed with an R factor of 65, corresponding to an observed diffusivity of 4×10^{-11} cm^2/s. To achieve 0.01 mg/L, an R factor of 773 is needed and corresponds to an observed diffusivity of 3×10^{-12} cm^2/s. Finally, to achieve 0.001 mg/L, an R factor of 7000 would be required, which would equal an observed diffusivity of 3×10^{-13} cm^2/s.

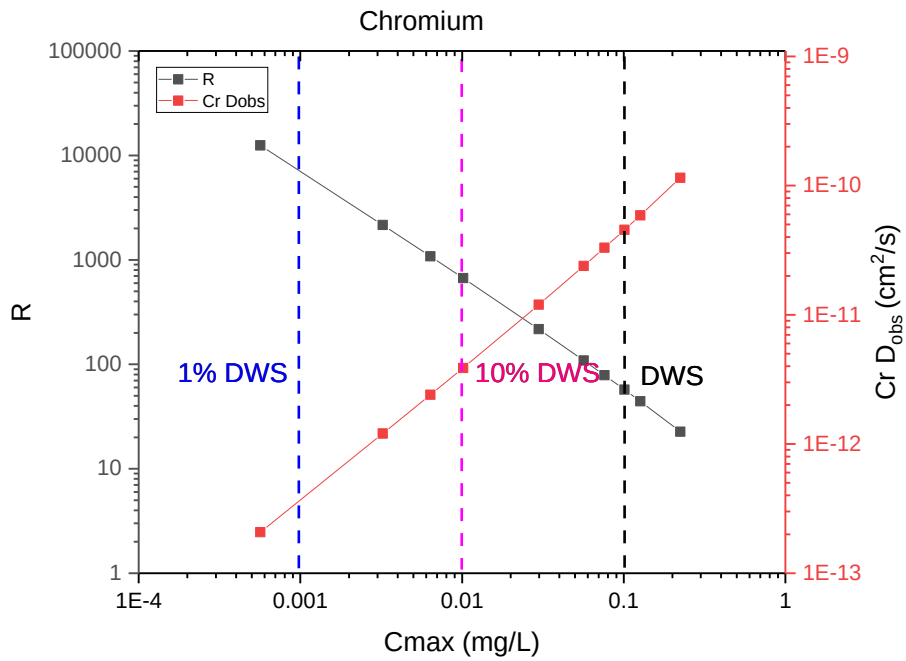

Figure 3-4. Visualization of the R factor (black) used in the simulations and the resulting concentration of Cr determined at the POC in mg/L. The corresponding observed diffusivity that would be measured for a grout with a specific R factor is also shown (red). Dashed lines corresponding to the target concentrations are also provided.

3.5 Performance Metric

The performance metric R retardation values and corresponding observed diffusivities are listed in Table 3-1. The R values were determined assuming a porosity of 0.557, solid density of 2.82 g/cm^3, saturation of 90%, and non-sorbing/non-reacting species intrinsic diffusivity, D_i, of 2.6×10^{-9} cm^2/s. The R values necessary to achieve groundwater concentrations below the DWS are dependent on the total SLAW contaminant inventory, described in Table 2-3. The R value would change accordingly due to alterations to any of the above variables. However, the fractional releases listed in Section 3.6.1 represent releases needed to achieve concentrations below the DWS regardless of inventory. To account for waste form properties, the R value can be adjusted to specific systems using Eq. (1.4). The performance metrics should be used for rapid assessment of laboratory leach test data (observed diffusivities) in testing programs focused on improving the retention in grout waste forms. They are not to be used for regulatory decision-making related to waste form disposal.

Table 3-1. List of the performance metric R values and associated observed diffusivities.

Species	Simulation Waste Form K_d, mL/g	Performance Metric, R	Corresponding Observed Diffusivity
Technetium	45	113	2×10^{-11} cm^2/s
Iodine	35	87	3×10^{-11} cm^2/s
Nitrate	0.5	2	2×10^{-9} cm^2/s.
Chromium	26	65	4×10^{-11} cm^2/s

3.6 Time Dependent Release and Simulation Sensitivity Cases

3.6.1 Time Dependent Release

During the simulations the resulting concentrations projected at the point of compliance were monitored over time. An example of the time dependent release is shown in Figure 3-5. Similar trends were observed for Tc, NO_3^- and Cr with the maximum concentration being reached at ≈ 3000 years, while iodine reached its maximum at ≈5500 years.

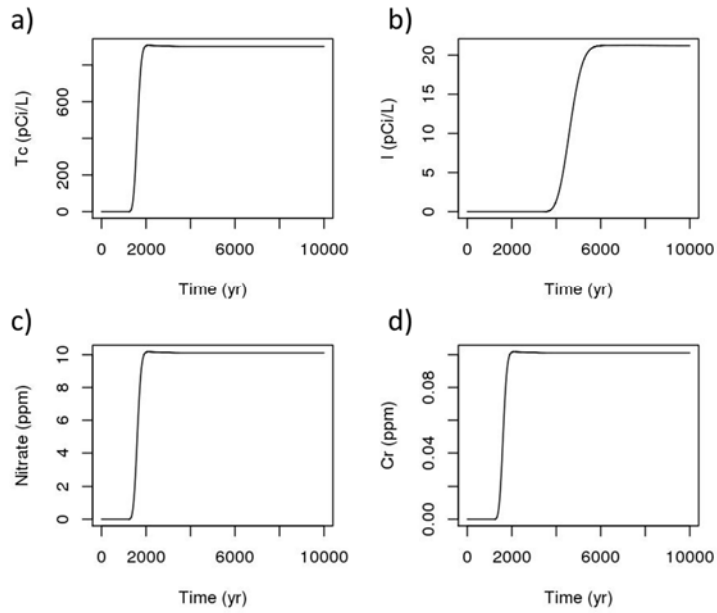

Figure 3-5. Example plots showing the time dependent concentrations determined at the point of compliance from the simulations for a) Tc, b) I, c) NO_3^- and d) Cr.

The simulations controlled release to the vadose zone through a fractional release from the bottom of the IDF. Table 3-2 lists the fractional release rate measured for test case that established the performance metric using the corresponding SLAW inventory of each of the four species evaluated in this work.

Table 3-2. Comparison of the total inventory, calculated release rate and corresponding fractional release rate for the individual simulation for each contaminant used to determine the performance metric.

Species	Inventory	Release Rate	Fractional Release Rate
Technetium	11,593 Ci	0.0242 Ci/yr	2.1×10^{-6} yr^{-1}
Iodine	10.5 Ci	0.000565 Ci/yr	5.4×10^{-5} yr^{-1}
Nitrate	2.54×10^{10} g	272,514 g/yr	1.1×10^{-5} yr^{-1}
Chromium	7.98×10^{8} g	2724 g/yr	3.4×10^{-6} yr^{-1}

3.6.2 Simulation Sensitivity Cases

Several sensitivity-case eSTOMP simulation runs were performed for the I-129 system to determine the potential influence of other grout properties on retention. The I-129 base case assumed a K_d value of 0.16 (providing a concentration of 21.21 pCi/L), porosity of 55.7%, and saturation of 90%. Additional base-case parameters, including a description of how each parameter was individually varied, are given in Table 3-3. The results were benchmarked against the calculated concentration of I-129 at the POC. The most significant impacts were as follows: 1) the saturated hydraulic conductivity, when increased by four orders of magnitude (from 1.5×10^{-9} cm/s to 1×10^{-5} cm/s), increased the I-129 POC concentration by 96%; and, 2) a decrease in infiltration rate to 1.7 mm/yr led to a 33% decrease in the I-129 POC concentration. All other sensitivity cases resulted in a minimal change to the I-129 POC concentration, which agrees well with observations made based on similar sensitivity analyses in the 2017 IDF PA (DOE 2017).

Table 3-3. Summary of sensitivity cases performed using I-129 as the base case.

Property	Base Case Value	Sensitivity Case Value	POC Concentration (pCi/L)
Base Case	-	-	21.21
Porosity	0.557	0.4	20.95
		0.2	19.27
van Genuchten, α (1/cm)	1.0008×10^{-5}	1.01×10^{-5}	21.21
van Genuchten, *n*	1.6271	2.4	21.23
Saturated Hydraulic Conductivity, K_{sat}	1.5×10^{-9}	3.9×10^{-8}	30.19
		1×10^{-5}	39.49
Infiltration Rate (mm/yr)	3.5	1.7	14.29
		5.2	22.54
Backfill Diffusivity (cm^2/s)	2×10^{-9}	2×10^{-8} (change tortuosity to 10)	25.11

4.0 Review of Historical Data

This section compares previously obtained laboratory leach data against performance metrics for the four species of interest: Tc (Section 4.2.1), I (Section 4.2.2), NO_3^- (Section 4.2.3), and Cr (Section 4.2.4).

4.1 Summary of the SLAW Program

Testing to identify a SLAW immobilization technology began in 2003 with evaluation of possible technologies to support the 2003 RA for SLAW (Mann 2003). Grout was included in this effort, with work being performed by CH2M Hill to identify baseline formulations (Lockrem 2005).

In fiscal year (FY) 2012, WRPS began a Supplemental Immobilization of Hanford Low-Activity Waste (SLAW) program with PNNL and Savannah River National Laboratory (SRNL) to obtain additional information on cementitious waste forms (using the Cast Stone baseline) for LAW and to further mature the technology for application at Hanford. PNNL prepared a detailed testing program description to address technology needs identified in the Cast Stone technology development plan. Four chemical simulants of LAW streams were defined and developed for use in developing the Cast Stone formulations for LAW. In FY13, PNNL and SRNL teamed to conduct a Cast Stone formulation screening matrix to evaluate the performance of the Cast Stone formulation for properties including waste composition, waste concentration as defined by sodium molarity, fly ash (FA) and blast furnace slag (BFS) sources, and water-to-dry-mix ratios. The study culminated at the end of FY13 in a detailed technical report on the impact of the formulation parameters on the processing and final waste form properties (Westsik et al. 2013). In October 2013, an engineering-scale demonstration of the preparation of Cast Stone was conducted in a pilot-scale facility at SRNL.

Work continued in FY14 and FY15 and included refining the Cast Stone formulation through additional testing of formulation enhancements, characterizing the Cast Stone product from the engineering-scale demonstration, preparing and characterizing Cast Stone with actual radioactive waste using an adjusted Tank 50 sample from SRNL, and obtaining performance data on a cementitious waste form to support the IDF PA (Asmussen et al. 2016a,b; Serne et al. 2016b; Crawford et al. 2017). No further direct work in support of SLAW was performed after 2016 until the performance metric work summarized in this report.

4.2 Assessment of Previous Data

In the following figures a comparison is made between historical leach test data and the observed diffusivities corresponding to the performance metrics for the individual contaminants. In the plots the green line represents the maximum observed diffusivity to meet the drinking water regulations, orange triangles in the plots represent values used in previous PAs or RAs, blue dots represent data collected in deionized water and red squares represent data collected in simulated Hanford vadose zone pore water. The Hanford vadose zone pore water was formulated to simulate the groundwater expected to contact the waste forms within the IDF (Serne et al. 2016b). The associated references for the data presented can be found in Appendix C.

4.2.1 Technetium

Because Tc is the largest contributor to the projected LAW radionuclide inventory at Hanford, several testing programs have targeted Tc retention in waste forms (both glass and grout) destined for onsite disposal in the IDF. Several studies have quantified Tc release from a variety of waste forms for both primary and secondary wastes. Figure 4-1 displays the observed diffusivities for Tc in monolithic

cementitious waste forms and the year reported. The green line represents the maximum observed diffusivity to meet theoretical drinking water regulations (2×10^{-11} cm^2/s) corresponding to the performance metric.

Since 1990, there has been a general decrease in laboratory-observed diffusivities for Tc. All values used in previous PAs and RAs, marked in orange in Figure 4-1, are above the observed diffusivity corresponding to the performance metric.

Within the experimental data sets shown, there are examples where the observed diffusivities fall below the performance metric line. These formulations use various mechanisms for Tc retention and include subsets of the baseline LAW Cast Stone screening work (Westsik et al. 2013; Serne et al. 2016b), getter additions (e.g., tin apatite, KMS-2) (Duncan et al. 2009; Asmussen et al. 2016a), alternate materials (e.g., geopolymers for liquid secondary wastes) (Pierce et al. 2010), and the lowest values to date in a hydrated lime-based liquid secondary formulation giving high amounts of ettringite (Um et al. 2016; Saslow et al. 2017). Two of these test sets were evaluated for LAW while the others are from separate targeted waste streams that may be extended to LAW.

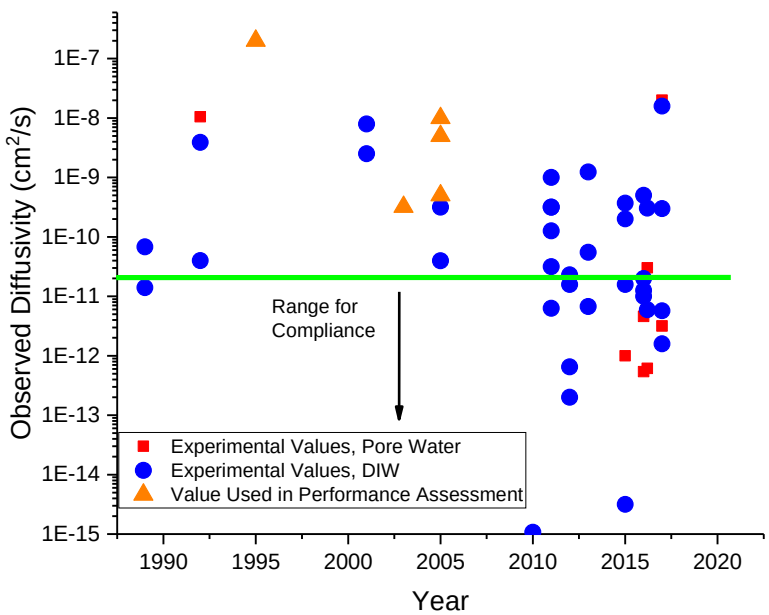

Figure 4-1. Comparison of previously reported observed diffusivity values measured for Tc in deionized water (blue), simulated porewater (red), and those used in previous PAs and RAs (orange) with the performance metric for Tc (green line).

4.2.2 Iodine

Iodine species, primarily as iodide, have commonly been reported to be leached from grout waste forms at the same rate as non-reacting/non-sorbing species, such as Na. Figure 4-2 highlights this behavior, showing a summary of observed diffusivities for iodine measured to date. Most of the data fall between 1×10^{-8} cm^2/s and 1×10^{-9} cm^2/s, which is above the observed diffusivity of 3×10^{-11} cm^2/s corresponding to the performance metric. Six datasets have observed diffusivities below the observed diffusivity corresponding to the performance metric. Three used Ag-zeolite/mordenite as I-getters at 5 wt% loading

or higher in waste forms fabricated from generic secondary waste simulant (Lockrem 2005), an EMF caustic scrubber secondary waste (Saslow et al. 2017), and an adjusted Savannah River Site Tank 50 sample to resemble Hanford LAW (Crawford et al. 2017). The fourth data set is from leach testing of an evaporated off-gas condensate sample immobilized as Cast Stone (Saslow et al. 2019), the fifth is an original grout vault screening sample (Serne et al. 1989), and the sixth was a concrete sample spiked with iodine (Mattigod et al. 2001).

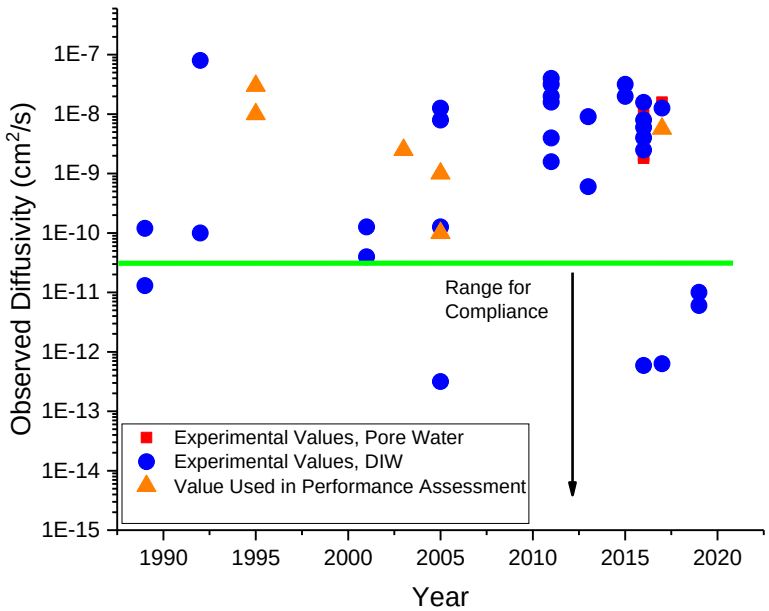

Figure 4-2. Comparison of previously reported observed diffusivity values for iodine measured in deionized water (blue), simulated porewater (red), and those used in previous PAs and RAs (orange) with the performance metric for I (green line).

4.2.3 Nitrate

NO_3^- is a non-reacting/non-sorbing constituent in cementitious materials that has no known interaction within cementitious matrices. A summary of the observed diffusivities available for NO_3^- is shown in Figure 4-3. Nearly all reported values are > 2×10^{-9} cm^2 /s, and thus larger than the observed diffusivity corresponding to the performance metric. The only data sets that measured an observed diffusivity below the corresponding to the limits defined by the performance metric, were from liquid secondary waste simulant immobilization (Saslow et al. 2017, Um et al. 2015). In these sample sets a higher D_{obs} for Na was measured compared to NO_3^-. The common assumption is both Na and NO_3^- are highly mobile species and would migrate out of a grout waste form at similar rates. This difference in Na and NO_3^- D_{obs} suggests that the waste form properties may be providing some level of NO_3^- retention.

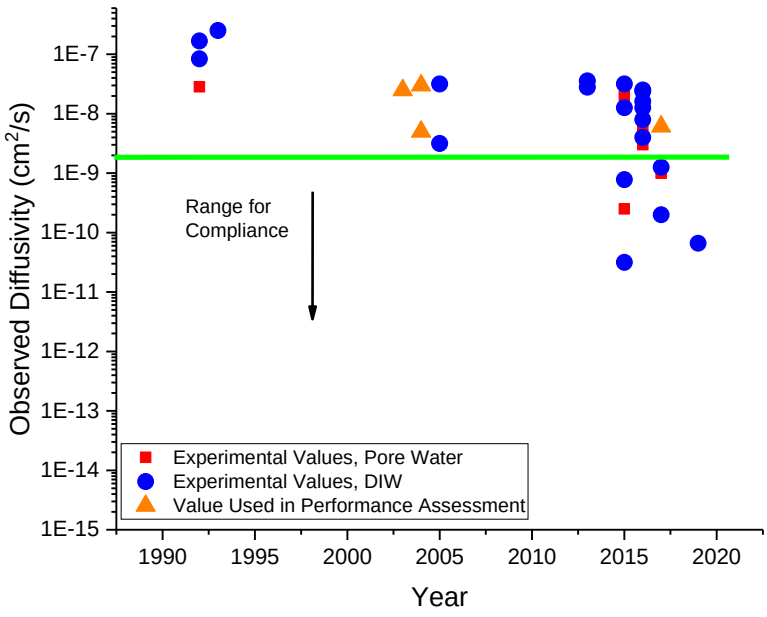

Figure 4-3. Comparison of previously reported observed diffusivity values for NO_3^- measured in deionized water (blue), simulated porewater (red), and those used in previous PAs and RAs (orange) with the performance metric for NO_3^- (green line).

4.2.4 Chromium

Throughout the historical leach testing of Cr-containing waste forms, very low Cr release rates have been observed in BFS-containing systems. A reducing environment is highly favorable for Cr retention (Langton 1988) and there is evidence in the literature of Cr(VI) anionic species incorporating into the minerals of hardening cement paste (Park et al. 2006). The low leachability of Cr is evident in Figure 4-4 which shows measured observed diffusivities for Cr versus time. All reported observed diffusivities for Cr but one fall below the observed diffusivity corresponding to the performance metric. The only exception is the estimated value for secondary waste used in the 2005 PA. This trend indicates that current grout formulations are suitable for Cr retention.

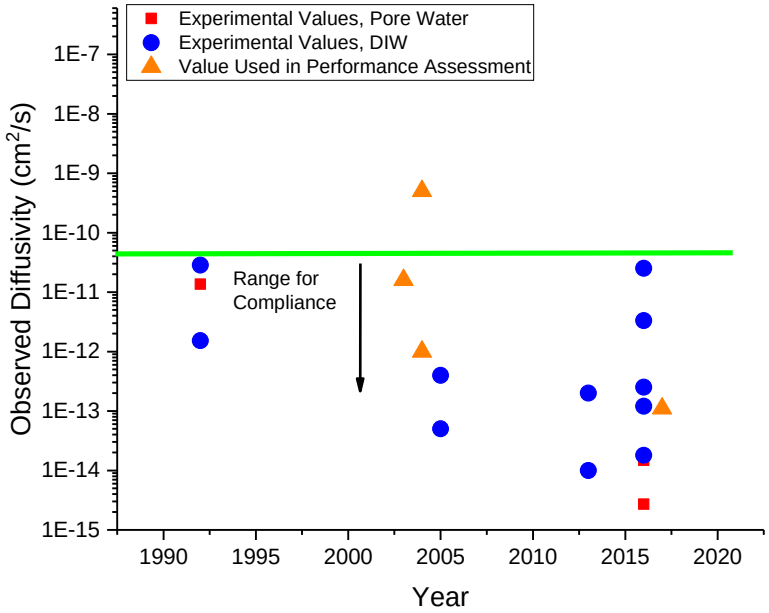

Figure 4-4. Comparison of previously reported observed diffusivity values for Cr measured in deionized water (blue), simulated porewater (red), and those used in previous PAs and RAs (orange) with the performance metric for Cr (green line).

4.2.5 Comparisons Between Species

For the example datasets above, several systems evaluated measured observed diffusivities for more than contaminant/radionuclide. A comparison of Tc, NO_3^- and I behavior for select datasets where more than one contaminant observed diffusivity was available is given in Figure 4-5. The observed diffusivity for Na is also presented where available. This comparison highlights that while some formulations provide sufficient retention for one contaminant, the formulation may not have adequate retention for another. Also, there is variation for which species the observed diffusivity would be considered the D_i in the individual test sets.

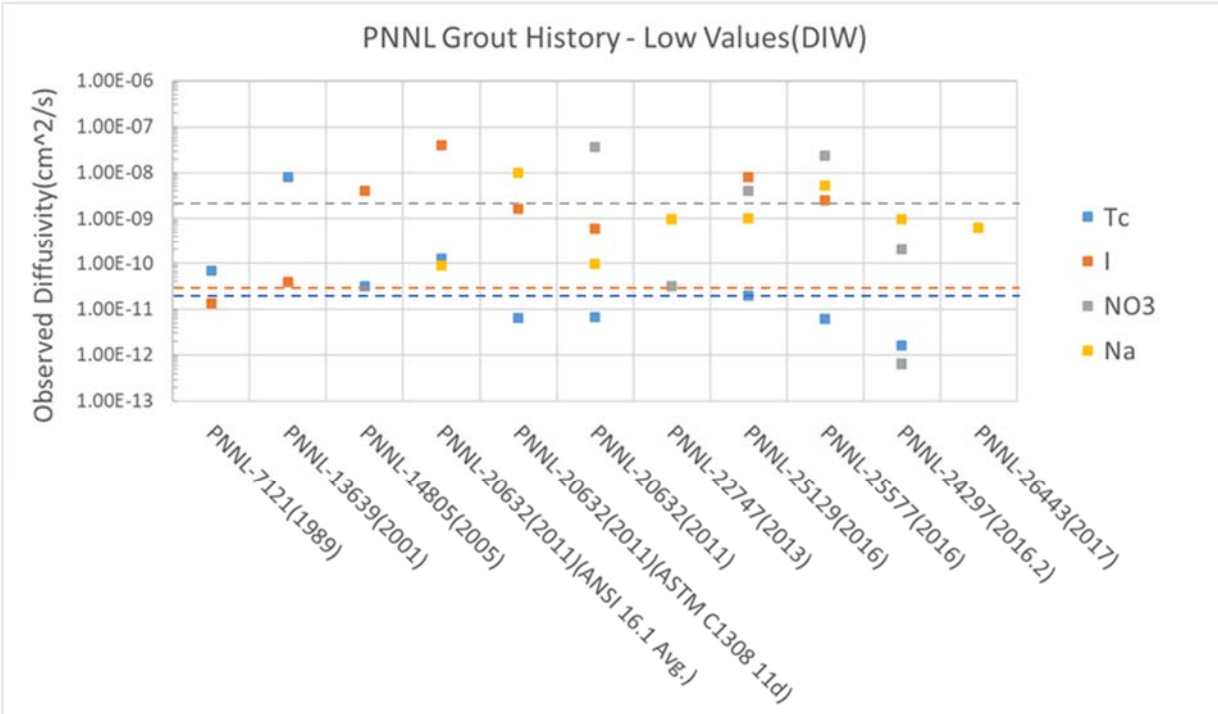

Figure 4-5. Comparison between the observed diffusivity of Tc, I, NO_3^- and Na from the same sample in individual test sets. The dashed lines represent the corresponding observed diffusivity for each species from the performance metric.

4.3 Path Forward

The approach of comparing previously reported observed diffusivities for Tc, I, NO_3^-, and Cr to the corresponding observed diffusivities calculated from the performance metric R (retardation factor) values should not be used in making regulatory decisions. Instead, the performance metric approach can serve as a screening tool for laboratory data and provide programmatic guidance in future years. The performance metric provides an indication of improvements needed to assess LAW grout as a viable waste form for disposal at the IDF. The metric also provides an indication of grout formulations/systems that are candidates for further scale-up/optimization/development. The following is a summary of the authors' opinion on promising areas to advance the feasibility of LAW grout.

- **Long-Term Reoxidation**: For redox-active Tc and Cr, comparing leachability against the performance metrics identified viable formulations (in all cases for Cr). Both species benefit from overall reducing conditions within the waste form. However, little is known about the re-oxidation rate (i.e., loss of reducing conditions) caused by infiltrating oxygen and water in the Hanford subsurface. This information would be highly valuable in assessing how long the processes contributing to the favorable leach behavior observed in the laboratory will endure in the field.

  This information can be gathered using both modeling and experimental approaches. The rate of oxygen ingress through a waste form package can be coupled with a kinetic reaction to simulate consumption of the reducing capacity. This calculation was performed previously in support of the Savannah River Site PA (Kaplan et al. 2005) and showed that the large saltstone vaults will retain their reducing capacity over 10,000 years. Experimental measurement of a re-oxidation rate has been attempted through a quick-leach approach and synchrotron technologies. Currently, an ongoing lysimeter experiment at the Hanford IDF Test Platform (previously recovered Hanford Field

Lysimeter Test Facility) will provide crucial data on re-oxidation rates of slag-containing waste forms exposed to actual Hanford subsurface conditions (Bacon et al. 2018).

- **Long-Term Getter Stability:** The most commonly suggested approach for reducing contaminant release from grout waste forms is the addition of getters. The performance metric assessment highlighted that getter additions are a viable approach for lowering laboratory diffusivities for Tc and I. However, the long-term stability of the getter complexes within waste forms are unknown. For Tc, the getters primarily function through redox reactions, essentially supplying additional reducing capacity to the local Tc environment. Similar modeling/experimental approaches to those described for re-oxidation above can be used. If an increase in overall reducing capacity is required within the waste form, a simple getter (e.g., iron) may be used.

  For I, the successful systems are three formulations containing Ag-getters. The long-term solubility resistance of the AgI product may be determined through simulations based on the solubility of AgI in grout porewater environments. There is evidence of cases where Ag-getters added in small doses did not improve I-retention; however, all three formulations in this study that exceed the performance metric level contained > 5 wt% of the Ag-getter. There is clear room for optimization of the solubility-controlled I getters.

- **Nitrate Retention:** To date, no formulation or method has targeted improving NO_3^- retention. Only samples from immobilization of liquid secondary waste measured an observed diffusivity below the limit corresponding to the performance metric level. Three avenues to address NO_3^- release are possible: 1) identification of a NO_3^--sorbing material/getter; 2) NO_3^- destruction/removal; and, 3) subsurface control. The most practical solution would be identification of a NO_3^--getter because activated carbons and other materials have shown proficiency in NO_3^- capture from aqueous environments.

- **Unsaturated Behavior:** The datasets evaluated against the performance metric were based on tests conducted under accelerated, saturated leaching conditions, as is required for the experimental timeframes available. These data are then modeled under unsaturated conditions. Previous reports have suggested that the unsaturated leach behavior may be several orders of magnitude lower than for saturated conditions, best summarized in Section 5.4 of Serne et al. (2016b). Unsaturated leach data would be valuable for validating models and refining conservatism. The lysimeter experiment at the IDF Test Platform will provide a long-term measurement of unsaturated release (Bacon et al. 2018), while shorter-term laboratory tests are possible using hanging columns (Serne et al. 2016b) or centrifuge techniques (Heller 1999).

- **Mineral Interaction with Other Contaminants:** The lowest observed diffusivity for Tc to date was a high-sulfate secondary waste simulant with a hydrated lime-based formulation (Um et al. 2016). This blend produces a waste form with high ettringite content, and evidence exists that ettringite can incorporate species such as Tc and Cr. If immobilized in a mineral phase, the duration and susceptibility of the release mechanism needs to be known and modeled accurately.

For the sensitivity cases in this work, where parameters were varied individually, the chemical/physical processes related to contaminant retention within the waste form (i.e., K_d values used in the simulations) have the largest impact on release in the Hanford subsurface environment. The other physical and hydraulic properties considered in the sensitivity study, on the other hand, had a smaller impact on contaminant retention. However, if coupled accordingly (e.g., decreased porosity with adjusted van Genuchten parameters), a benefit may be realized.

4.4 Summary and Conclusion

The simulations presented in this report define performance metrics for grout waste form release for SLAW inventory in the IDF. The performance metric is defined as a unitless retardation factor (R) that represents the ratio of the diffusivity of a non-sorbing/non-reacting species, D_i, and the observed diffusivity of a species of interest, D_{obs}. The analysis does not consider the physical state (monolithic, fractured), chemical state (reduced, oxidized), or age of the waste form in the IDF. The metric only defines a minimum performance in terms of leachability regardless of the physical condition of the waste form. The observed diffusivity corresponding to each performance metric R retardation value is to be used for rapid assessment of laboratory leach test data targeting improved grout performance.

Performance metrics to rapidly assess laboratory leach data have been established for Tc, Cr, I, and NO_3^-. These metrics are defined as a retardation factor (R) for the waste form irrespective of physiochemical properties. A corresponding laboratory-observed diffusivity for the metric R factors exists and can be used to compare laboratory data to identify promising grout technologies. Based on an assessment of current grout leachability data to date, candidate formulations have been identified along with areas requiring further technology development. The performance metric simulations can be expanded to assess varying inventories and waste form types in the IDF.

It should be noted that these simulations only consider the contribution from the SLAW inventory and not any contribution to the overall release rate from the primary LAW inventory. As a result, the R values that achieve the target concentrations would be an underestimation of the full LAW inventory release. The performance metric is not intended for use in regulatory decision-making.

5.0 References

10 CFR 830, Subpart A. 2011. "Quality Assurance Requirements." Code of Federal Regulations, U.S. Department of Energy, Washington, D.C.

Anderson KA, MD Britton, JM Colby, LH Cree, MF Fountain, DW Nelson, VC Nguyen, and ME Stone. 2017. *One System River Protection Project Integrated Flowsheet*. RPP-RPT-57991, Rev. 2, Washington River Protection Solutions, LLC, Richland, WA.

ANS/ANSI. 2019. *Measurement of the Leachability of Solidified Low-Level Radioactive Wastes by a Short-Term Test Procedure*. ANSI/ANS-16.1-2019, American National Standards Institute, La Grange Park, IL.

ASME NQA-1-2008. *Quality Assurance Requirements for Nuclear Facility Applications*. American Society of Mechanical Engineers, New York, NY.

ASME NQA-1a-2009. *Addenda to ASME NQA-1-2008 Quality Assurance Requirements for Nuclear Facility Applications.* American Society of Mechanical Engineers, New York, NY.

Asmussen RM, CI Pearce, AJ Lawter, JJ Neeway, BW Miller, BD Lee, N Washton, JR Stephenson, RE Clayton, ME Bowden, EC Buck, E Cordova, BD Williams, and N Qafoku. 2016a. *Getter Incorporation into Cast Stone and Solid State Characterizations*. PNNL-25577, Pacific Northwest National Laboratory. Richland, WA.

Asmussen RM, CI Pearce, KE Parker, BW Miller, BD Lee, EC Buck, N Washton, ME Bowden, AR Lawter, E Cordova, and J Serne. 2016b. *Solid State Characterizations of Long Term Leached Cast Stone Monoliths*. PNNL-25578, Pacific Northwest National Laboratory, Richland, WA.

ASTM C1308-08(2017), Standard Test Method for Accelerated Leach Test for Diffusive Releases from Solidified Waste and a Computer Program to Model Diffusive, Fractional Leaching from Cylindrical Waste Forms, ASTM International, West Conshohocken, PA, 2017, www.astm.org

Bacon DH, PD Meyer, JJ Neeway, Y Fang, RM Asmussen, and CE Strickland. 2018. *Field-Scale Lysimeter Studies of Low-Activity Waste Form Degradation*. PNNL-27394, Pacific Northwest National Laboratory, Richland, WA.

Bartholomay RC. 2013. I*odine-129 in the Eastern Snake River Plain Aquifer at and near the Idaho National Laboratory, Idaho, 2010-12*. DOE/ID-22225, U.S. Geological Survey, Idaho Falls, ID.

Bates WF, ME Stone, TM Brouns, CA Langton, RT Jubin, AD Cozzi, NR Soelberg, GD Guthrie, and JR Cochran. 2019. *Report of Analysis of Approaches to Supplemental Treatment of Low-Activity Waste at the Hanford Nuclear Reservation*. SRNL-RP-2018-00687, Savannah River National Laboratory, Aiken, SC.

Cantrell KJ, JH Westsik, RJ Serne, W Um, and AD Cozzi. 2016. *Secondary Waste Cementitious Waste Form Data Package for the Integrated Disposal Facility Performance Assessment.* PNNL-25194, Pacific Northwest National Laboratory, Richland, WA.

Crawford C, A Cozzi, K Hill, and A Ramsey. 2017. *Analysis of Hanford Cast Stone Supplemental LAW using Composition Adjusted SRS Tank 50 Salt Solution*. SRNL-STI-2017-00619, Savannah River Site, Aiken, SC.

deGroot GJ and HAvd Sloot. 1992. *Determination of Leaching Characteristics of Waste Materials Leading to Environmental Product Certification. Stabilization and Solidification of Hazardous, Radioactive, and Mixed Wastes*. TM Gilliam and CC Wiles (eds.). 2nd Volume, STP1123:149-170, American Society for Testing and Materials, Philadelphia, PA.

DOE Order 414.1D. 2011. *Quality Assurance*. Approved 4/25/2011. U.S. Department of Energy, Washington, D.C.

DOE Order 435.1. 1999. *Radioactive Waste Management*. Approved 7/09/1999. U.S. Department of Energy, Washington, D.C.

DOE. 2012. *Final Tank Closure and Waste Management Environmental Impact Statement for the Hanford Site, Richland, Washington*. DOE/EIS-0391, U.S. Department of Energy, Office of River Protection, Richland, WA.

DOE. 2017. *Performance Assessment for the Integrated Disposal Facility, Hanford Site*. RPP-RPT-59958, Rev. A, Washington River Protection Solutions, LLC, Richland, WA.

Duncan JB, GA Cooke, and LL Lockrem. 2009. *Assessment of Technetium Leachability in Cement Stabilized Basin 43 Groundwater Brine*. RPP-RPT-39195, Washington River Protection Solutions, Richland, WA.

EPA. 2002a. *EPA Facts About Technetium-99*. U.S. Environmental Protection Agency, Washington, D.C.

EPA. 2002b. "National primary drinking water regulations: Long Term 1 Enhanced Surface Water Treatment Rule. Final rule." *Federal Register* 67(9):1811. U.S. Environmental Protection Agency, Washington, D.C.

EPA. 2013. *Mass Transfer Rates of Constituents in Monolithic or Compacted Granulated Materials Using a Semi-Dynamic Tank Leaching Procedure*. EPA SW-846, Method 1315, U.S. Environmental Protection Agency, Washington, D.C.

Flach GP, DI Kaplan, RL Nichols, RR Seitz, and RJ Serne. 2016. *Solid Secondary Waste Data Package Supporting Hanford Integrated Disposal Facility Performance Assessment*. SRNL-STI-2016-00175, Rev. 0, Savannah River National Laboratory, Aiken, SC.

Freedman VL, DH Bacon, and Y Fang. 2016. *Integrated Disposal Facility FY 2016: ILAW Verification and Validation of the eSTOMP Simulator*. PNNL-25185, Pacific Northwest National Laboratory, Richland, WA.

Heller P. 1999. *Measurement of Unsaturated Hydraulic Conductivity and Water Potential in Mineral Samples and Concrete Cores*. UFA-99-07, UFA Ventures, Richland, WA.

Kaplan DI. 2005. *Estimated Duration of the Subsurface Reducing Environment Produced by the Z-Area Saltstone Disposal Facility*. WSC-RP-2003-00362, Westinghouse Savannah River Company. Aiken, SC.

Kincaid C, J Voogd, J Shade, JH Westsik Jr., G Whyatt, M Freshley, MG Piepho, K Blanchard, K Rhoads, and B Lauzon. 1995. *Performance Assessment of Grouted Double Shell Tank Waste Disposal at Hanford*. WHC-SD-WM-EE-004, Rev. 1, Westinghouse Hanford Company, Richland, WA.

Kosson DS, HAvd Sloot, F Sanchez, and AC Garrabrants. 2002. "An Integrated Framework for Evaluating Leaching in Waste Management and Utilization of Secondary Materials." *Environmental Engineering Science* 19(3):159-204.

Krupka KK, RJ Serne, and DI Kaplan. 2004. *Geochemical Data Package for the 2005 Hanford Integrated Disposal Facility Performance Assessment*. PNNL-13037, Rev. 2, Pacific Northwest National Laboratory, Richland, WA.

Langton CA. 1988. "Slag Based Saltstone Formulations." *Materials Research Society Symposium Proceedings* 112:61-70.

Lockrem LL. 2005. *Hanford Containerized Cast Stone Facility Task 1-Process Testing and Development Final Report*. RPP-RPT-26742, Rev. 0, CH2M Hill, Richland, WA.

Mann F. 2003. *Risk Assessment Supporting the Decision on the Initial Selection of Supplemental ILAW Technologies*. RPP-RPT-17675, CH2M Hill, Richland, WA.

Mann FM, RJ Puigh, PD Rittmann, NW Kline, J Voogd, Y Chen, C Eiholzer, C Kincaid, BP McGrail, AH Lu, G Williamson, N Brown, and L LaMont. 1998. *Hanford Immobilized Low-Activity Tank Waste Performance Assessment*. DOE/RL-97-69, U.S. Department of Energy, Richland Operations Office, Richland, WA.

Mann FM, RJ Puigh, S Finfrock, EJ Freeman, R Khaleel, DH Bacon, MP Bergeron, BP McGrail, SK Wurstner, K Burgard, WR Root, and P LaMont. 2001. *Hanford Immobilized Low-Activity Tank Waste Performance Assessment: 2001 Version*. DOE/ORP-2000-24, Rev. 0, U.S. Department of Energy, Office of River Protection, Richland, WA.

Meyer PD, P Saripalli, and VL Freedman. 2004. *Near-Field Hydrology Data Package for the Integrated Disposal Facility 2005 Performance Assessment*. PNNL-14700, Pacific Northwest National Laboratory, Richland, WA.

Mualem Y. 1976. "A new model for predicting the hydraulic conductivity of unsaturated porous media." *Water Resources Research* 12(3):513-522.

Park J-Y, W-H Kang, and I Hwang. 2006. "Hexavalent chromium uptake and release in cement pastes." *Environmental Engineering Science* 23(1):133-140.

Peterson RA, EC Buck, J Chun, RC Daniel, DL Herting, ES Ilton, GJ Lumetta, and SB Clark. 2018. "Review of the Scientific Understanding of Radioactive Waste at the U.S. DOE Hanford Site." *Environmental Science & Technology* 52(2):381-396.

Pierce EM, BP McGrail, EA Rodriguez, HT Schaef, KP Saripalli, RJ Serne, PF Martin, SR Baum, KJ Geizler, LR Reed, and WJ Shaw. 2004. *Waste Form Release Data Package for the 2005 Integrated Disposal Facility Performance Assessment*. PNNL-14805, Pacific Northwest National Laboratory, Richland, WA.

Pierce EM, W Um, K Cantrell, M Valenta, J Westsik Jr, R Serne, and K Parker. 2010. *Secondary Waste Form Screening Test Results–Cast Stone and Alkali Alumino-Silicate Geopolymer*. PNNL-19505, Pacific Northwest National Laboratory, Richland, WA.

Riley BJ, JD Vienna, DM Strachan, JS McCloy, and JL Jerden. 2016. "Materials and processes for the effective capture and immobilization of radioiodine: A review." *Journal of Nuclear Materials* 470:307-326.

Rockhold ML, ZF Zhang, PD Meyer, and JN Thomle. 2015. *Physical, Hydraulic and Transport Properties of Sediments and Engineered Materials Associated with Hanford Immobilized Low-Activity Waste*. PNNL-23711, Pacific Northwest National Laboratory, Richland, WA.

Saslow SA, W Um, RL Russel, G Wang, RM Asmussen, and R Sahajpal. 2017. *Updated Liquid Secondary Waste Grout Formulation and Preliminary Waste Form Qualification*. PNNL-26443; RPT-SWCS-009, Rev. 0, Pacific Northwest National Laboratory, Richland, WA.

Saslow SA, M Snyder, BD Williams, RM Asmussen, S Baum, IL Leavy, and T Varga. 2019. *Leach Testing of Laboratory-Scale Melter Evaporator Condensate Cementitious Waste Forms*. PNNL-28917; RPT-SWCS-013, Rev. 0, Pacific Northwest National Laboratory, Richland, WA

Sato H, M Yui, and H Yoshikawa. 1996. "Ionic Diffusion Coefficients of Cs+, Pb2+, Sm3+, Ni2+, SeO- and TcO4-, in Free Water Determined from Conductivity Measurements." *Journal of Nuclear Science and Technology* 33(12):950-955.

Serne R, R Lokken, and L Criscenti. 1992. "Characterization of grouted low-level waste to support performance assessment." *Waste Management* 12(2-3):271-287.

Serne RJ, DC Lanigan, JH Westsik, BD Williams, HB Jung, and G Wang. 2016b. *Extended Leach Testing of Simulated LAW Cast Stone Monoliths*. PNNL-24297, Rev 1, Pacific Northwest National Laboratory, Richland, WA.

Serne RJ, JV Crum, BJ Riley, and TG Levitskaia. 2016a. *Options for the Separation and Immobilization of Technetium*. PNNL-25834, Pacific Northwest National Laboratory, Richland, WA.

Szecsody JE, BD Lee, AR Lawter, N Qafoku, CT Resch, SR Baum, II Leavy, and VL Freedman. 2017. *Effect of Co-Contaminants Uranium and Nitrate on Iodine Remediation*. PNNL-26955, Pacific Northwest National Laboratory, Richland, WA.

Tilanus SN, LM Bergmann, RO Lokken, AJ Schubick, EB West, RT Jasper, SL Orcutt, TM Holh, AN Praga, MN Wells, KW Burnett, CS Smalley, JK Bernards, SD Reaksecker, and TL Waldo. 2017. *River Protection Project System Plan*. ORP-11242, Rev. 8, Washington River Protection Solutions, LLC, Richland, WA.

Trimble DC and TM Persons. 2017. *Nuclear Waste: Opportunities Exist to Reduce Risks and Costs by Evaluating Different Waste Treatment Approaches at Hanford*. GAO-17-306, U.S. Government Accountability Office, Washington, D.C.

Um W, BD Williams, MM Valenta Snyder, and G Wang. 2016. *Liquid Secondary Waste Grout Formulation and Waste Form Qualification*. PNNL-25129, Rev. 1, Pacific Northwest National Laboratory, Richland, WA.

Westsik JH, GF Piepel, MJ Lindberg, PG Heasler, TM Mercier, RL Russell, A Cozzi, WE Daniel, RE Eibling, EK Hansen, MM Reigel, and DJ Swanberg. 2013. *Supplemental Immobilization of Hanford Low-Activity Waste: Cast Stone Screening Tests*. PNNL-22747; SRNL-STI-2013-00465, Pacific Northwest National Laboratory, Richland, WA.

White MD, DH Bacon, BP McGrail, DJ Watson, SK White, and Z Zhang. 2012. *STOMP Subsurface Transport Over Multiple Phases: STOMP-CO2 and STOMP-CO2e Guide: Version 1.0*. PNNL-21268, Pacific Northwest National Laboratory, Richland, WA.

Appendix A – Example Input Files for IDF Waste Form Simulation and IDF Subsurface Simulation

Input file for IDF waste form simulation

```
#-------------------------------------------------------~Simulation Title
Card
#-------------------------------------------------------
1,
input: LSW07_HL_ACM1_I129_PU5_v7(refined3)= ETF-LSW-HL-Based-grout
properties Deff and Kd in SRNL-00685, PNNL-23711, NQA1,
Barret Nicolas,modifield by Xuehang Song (PNNL) with Eight B25-container
and unit inventory 02/07/2019
,
3,
Mesh: Two B25-containers,
Nearfield_IDF_grid_B25_10cmEncaps_refined3.mView,
Water mode (STOMP-W),
Parameters: Solidification, Oxidizing conditions (ACM1), Long term
Infiltration 3.5mm/yr, LSW07_B25_model_properties_v4.xlsx,
#-------------------------------------------------------
~Solution Control Card
#-------------------------------------------------------
normal w/petsc,1.0E-12,1.0E-25,
Water w/Transport,
1,
0,s,10000,yr,1,s,500,yr,1.25,8,1.e-6,
99999,
0,
#-------------------------------------------------------
~Grid Card
#-------------------------------------------------------
Cartesian,
24,19,312,
0.0,m,0.055,m,0.115,m,0.175,m,0.235,m,0.335,m,0.435,m,0.535,m,0.635,m,0.73
5,m,\
0.775,m,0.815,m,0.835,m,0.855,m,0.875,m,0.895,m,0.905,m,0.915,m,0.925,m,0.
935,m,\
0.945,m,0.965,m,0.985,m,1.005,m,1.025,m,
0.0,m,0.055,m,0.105,m,0.205,m,0.305,m,0.405,m,0.445,m,0.485,m,0.525,m,0.54
5,m,\
0.565,m,0.575,m,0.585,m,0.595,m,0.605,m,0.615,m,0.635,m,0.655,m,0.675,m,0.
695,m,
0.0,m,0.1,m,0.2,m,0.3,m,0.36,m,0.42,m,0.46,m,0.5,m,0.54,m,0.56,m,\
0.58,m,0.59,m,0.6,m,0.61,m,0.62,m,0.63,m,0.64,m,0.66,m,0.68,m,0.72,m,\
0.76,m,0.86,m,0.96,m,1.06,m,1.16,m,1.26,m,1.36,m,1.46,m,1.56,m,1.605,m,\
1.65,m,1.71,m,1.74,m,1.77,m,1.79,m,1.8,m,1.81,m,1.82,m,1.83,m,1.84,m,\
1.87,m,1.9,m,1.91,m,1.92,m,1.93,m,1.94,m,1.95,m,1.96,m,1.98,m,2.0,m,\
2.04,m,2.08,m,2.18,m,2.28,m,2.38,m,2.48,m,2.58,m,2.68,m,2.78,m,2.88,m,\
2.925,m,2.97,m,3.03,m,3.06,m,3.09,m,3.11,m,3.12,m,3.13,m,3.14,m,3.15,m,\
3.16,m,3.18,m,3.2,m,3.24,m,3.28,m,3.33,m,3.43,m,3.53,m,3.63,m,3.73,m,\
3.83,m,3.93,m,3.99,m,4.05,m,4.09,m,4.13,m,4.17,m,4.19,m,4.21,m,4.22,m,\
4.23,m,4.24,m,4.25,m,4.26,m,4.27,m,4.29,m,4.31,m,4.35,m,4.39,m,4.49,m,\
```

```
4.59,m,4.69,m,4.79,m,4.89,m,4.99,m,5.09,m,5.19,m,5.235,m,5.28,m,5.34,m,\
5.37,m,5.4,m,5.42,m,5.43,m,5.44,m,5.45,m,5.46,m,5.47,m,5.5,m,5.53,m,\
5.54,m,5.55,m,5.56,m,5.57,m,5.58,m,5.59,m,5.61,m,5.63,m,5.67,m,5.71,m,\
5.81,m,5.91,m,6.01,m,6.11,m,6.21,m,6.31,m,6.41,m,6.51,m,6.555,m,6.6,m,\
6.66,m,6.69,m,6.72,m,6.74,m,6.75,m,6.76,m,6.77,m,6.78,m,6.79,m,6.81,m,\
6.83,m,6.87,m,6.91,m,6.96,m,7.06,m,7.16,m,7.26,m,7.36,m,7.46,m,7.56,m,\
7.62,m,7.68,m,7.72,m,7.76,m,7.8,m,7.82,m,7.84,m,7.85,m,7.86,m,7.87,m,\
7.88,m,7.89,m,7.9,m,7.92,m,7.94,m,7.98,m,8.02,m,8.12,m,8.22,m,8.32,m,\
8.42,m,8.52,m,8.62,m,8.72,m,8.82,m,8.865,m,8.91,m,8.97,m,9.0,m,9.03,m,\
9.05,m,9.06,m,9.07,m,9.08,m,9.09,m,9.1,m,9.13,m,9.16,m,9.17,m,9.18,m,\
9.19,m,9.2,m,9.21,m,9.22,m,9.24,m,9.26,m,9.3,m,9.34,m,9.44,m,9.54,m,\
9.64,m,9.74,m,9.84,m,9.94,m,10.04,m,10.14,m,10.185,m,10.23,m,10.29,m,10.32
,m,\
10.35,m,10.37,m,10.38,m,10.39,m,10.4,m,10.41,m,10.42,m,10.44,m,10.46,m,10.
5,m,\
10.54,m,10.59,m,10.69,m,10.79,m,10.89,m,10.99,m,11.09,m,11.19,m,11.25,m,11
.31,m,\
11.35,m,11.39,m,11.43,m,11.45,m,11.47,m,11.48,m,11.49,m,11.5,m,11.51,m,11.
52,m,\
11.53,m,11.55,m,11.57,m,11.61,m,11.65,m,11.75,m,11.85,m,11.95,m,12.05,m,12
.15,m,\
12.25,m,12.35,m,12.45,m,12.495,m,12.54,m,12.6,m,12.63,m,12.66,m,12.68,m,12
.69,m,\
12.7,m,12.71,m,12.72,m,12.73,m,12.76,m,12.79,m,12.8,m,12.81,m,12.82,m,12.8
3,m,\
12.84,m,12.85,m,12.87,m,12.89,m,12.93,m,12.97,m,13.07,m,13.17,m,13.27,m,13
.37,m,\
13.47,m,13.57,m,13.67,m,13.77,m,13.815,m,13.86,m,13.92,m,13.95,m,13.98,m,1
4.0,m,\
14.01,m,14.02,m,14.03,m,14.04,m,14.05,m,14.07,m,14.09,m,14.13,m,14.17,m,14
.22,m,\
14.32,m,14.42,m,14.52,m,
-------------------------------------------------------
~Rock/Soil Zonation Card
#-------------------------------------------------------
formatted zonation
file,../../template/rock_B25_hd_ld_backf_10e_refi3_8container.zon,
HD_BACKF,
LD_BACKF,
W1,
W2,
#-------------------------------------------------------
~Mechanical Properties Card
#-------------------------------------------------------
HD_BACKF,2.710,g/cm^3,0.35,0.35,,,Constant       ,1,
LD_BACKF,2.710,g/cm^3,0.37,0.37,,,Constant       ,1,
W1,2.820,g/cm^3,0.557,0.557,,,Constant       ,1,
W2,2.820,g/cm^3,0.557,0.557,,,Constant       ,1,
#-------------------------------------------------------
~Hydraulic Properties Card
#-------------------------------------------------------
HD_BACKF,4.91e-03,hc cm/s,4.91e-03,hc cm/s,4.91e-03,hc cm/s,
LD_BACKF,1.86e-02,hc cm/s,1.86e-02,hc cm/s,1.86e-02,hc cm/s,
W1,1.54E-09,hc cm/s,1.54E-09,hc cm/s,1.54E-09,hc cm/s,
```

```
W2,1.54E-09,hc cm/s,1.54E-09,hc cm/s,1.54E-09,hc cm/s,
#-------------------------------------------------------
~Saturation Function Card
#-------------------------------------------------------
#Residual saturation and not teta R
HD_BACKF,van Genuchten,6.50e-02,1/cm,1.7,0.086,,
LD_BACKF,van Genuchten,5.70e-02,1/cm,2.8,0.081,,
W1,van Genuchten,6.03E-06,1/cm,1.649,0.108,,
W2,van Genuchten,6.03E-06,1/cm,1.649,0.108,,
#-------------------------------------------------------
~Aqueous Relative Permeability Card
#-------------------------------------------------------
HD_BACKF,Mualem,,
LD_BACKF,Mualem,,
W1,Mualem,,
W2,Mualem,,
#-------------------------------------------------------
~Initial Conditions Card
#-------------------------------------------------------
Gas Pressure, Aqueous saturation,
43,
Gas Pressure      ,  1.0135e+5     ,Pa,,,,,,,1,24,1,19,1,312,
Aqueous Saturation,0.2091,,0.0,1/m,0.0,1/m,0.0,1/m,1,24,1,19,1,7,
Aqueous Saturation,0.2091,,0.0,1/m,0.0,1/m,0.0,1/m,1,24,1,19,68,85,
Aqueous Saturation,0.2091,,0.0,1/m,0.0,1/m,0.0,1/m,1,24,1,19,146,163,
Aqueous Saturation,0.2091,,0.0,1/m,0.0,1/m,0.0,1/m,1,24,1,19,224,241,
Aqueous Saturation,0.2091,,0.0,1/m,0.0,1/m,0.0,1/m,1,24,1,19,302,312,
Aqueous Saturation,0.0878,,0.0,1/m,0.0,1/m,0.0,1/m,1,24,1,19,8,67,
Aqueous Saturation,0.0878,,0.0,1/m,0.0,1/m,0.0,1/m,1,24,1,19,86,145,
Aqueous Saturation,0.0878,,0.0,1/m,0.0,1/m,0.0,1/m,1,24,1,19,164,223,
Aqueous Saturation,0.0878,,0.0,1/m,0.0,1/m,0.0,1/m,1,24,1,19,242,301,
Aqueous Saturation,0.9,,0.0,1/m,0.0,1/m,0.0,1/m,1,17,1,12,15,36,
Aqueous Saturation,0.9,,0.0,1/m,0.0,1/m,0.0,1/m,1,17,1,12,46,67,
Aqueous Saturation,0.9,,0.0,1/m,0.0,1/m,0.0,1/m,1,17,1,12,93,114,
Aqueous Saturation,0.9,,0.0,1/m,0.0,1/m,0.0,1/m,1,17,1,12,124,145,
Aqueous Saturation,0.9,,0.0,1/m,0.0,1/m,0.0,1/m,1,17,1,12,171,192,
Aqueous Saturation,0.9,,0.0,1/m,0.0,1/m,0.0,1/m,1,17,1,12,202,223,
Aqueous Saturation,0.9,,0.0,1/m,0.0,1/m,0.0,1/m,1,17,1,12,249,270,
Aqueous Saturation,0.9,,0.0,1/m,0.0,1/m,0.0,1/m,1,17,1,12,280,301,
Aqueous Saturation,0.9,,0.0,1/m,0.0,1/m,0.0,1/m,1,11,1,7,20,31,
Aqueous Saturation,0.9,,0.0,1/m,0.0,1/m,0.0,1/m,1,11,1,7,51,62,
Aqueous Saturation,0.9,,0.0,1/m,0.0,1/m,0.0,1/m,1,11,1,7,98,109,
Aqueous Saturation,0.9,,0.0,1/m,0.0,1/m,0.0,1/m,1,11,1,7,129,140,
Aqueous Saturation,0.9,,0.0,1/m,0.0,1/m,0.0,1/m,1,11,1,7,176,187,
Aqueous Saturation,0.9,,0.0,1/m,0.0,1/m,0.0,1/m,1,11,1,7,207,218,
Aqueous Saturation,0.9,,0.0,1/m,0.0,1/m,0.0,1/m,1,11,1,7,254,265,
Aqueous Saturation,0.9,,0.0,1/m,0.0,1/m,0.0,1/m,1,11,1,7,285,296,
Solute,generic,0,1/m^3,,,,,,1,24,1,19,1,312,
Solute,generic,0.1962396,1/m^3,,,,,,1,17,1,12,15,36,
Solute,generic,0.1962396,1/m^3,,,,,,1,17,1,12,46,67,
Solute,generic,0.1962396,1/m^3,,,,,,1,17,1,12,93,114,
Solute,generic,0.1962396,1/m^3,,,,,,1,17,1,12,124,145,
Solute,generic,0.1962396,1/m^3,,,,,,1,17,1,12,171,192,
Solute,generic,0.1962396,1/m^3,,,,,,1,17,1,12,202,223,
```

```
Solute,generic,0.1962396,1/m^3,,,,,,1,17,1,12,249,270,
Solute,generic,0.1962396,1/m^3,,,,,,1,17,1,12,280,301,
Solute,generic,0.1962396,1/m^3,,,,,,1,11,1,7,20,31,
Solute,generic,0.1962396,1/m^3,,,,,,1,11,1,7,51,62,
Solute,generic,0.1962396,1/m^3,,,,,,1,11,1,7,98,109,
Solute,generic,0.1962396,1/m^3,,,,,,1,11,1,7,129,140,
Solute,generic,0.1962396,1/m^3,,,,,,1,11,1,7,176,187,
Solute,generic,0.1962396,1/m^3,,,,,,1,11,1,7,207,218,
Solute,generic,0.1962396,1/m^3,,,,,,1,11,1,7,254,265,
Solute,generic,0.1962396,1/m^3,,,,,,1,11,1,7,285,296,
#-------------------------------------------------------
~Boundary Conditions Card
#-------------------------------------------------------
2,
top,Neumann,zero flux,
1,24,1,19,312,312,2,
0,yr,-3.5,mm/yr,,,
#100,yr,0.0,mm/yr,,,
#100,yr,-0.5,mm/yr,,,
#500,yr,-0.5,mm/yr,,,
#500,yr,-3.5,mm/yr,,,
10000,yr,-3.5,mm/yr,,,
bottom,Dirichlet,Outflow,
1,24,1,19,1,1,1,
0,d,7.5E+4,Pa,,,

#-------------------------------------------------------
~Solute/Fluid Interactions Card
#-------------------------------------------------------
1,
generic,constant,2.6E-09,cm^2/s,continuous,1.57E+07,yr,,,
0,
#-------------------------------------------------------
~Solute/Porous Media Interactions Card
#-------------------------------------------------------
HD_BACKF,0.0,cm, 0.,cm,
generic, 0.0E+00,mL/g,
LD_BACKF,0.0,cm, 0.,cm,
generic, 0.0E+00,mL/g,
W1,0.0,cm, 0.,cm,
generic, 45.1,mL/g,
W2,0.0,cm, 0.,cm,
generic, 45.1,mL/g,
#-------------------------------------------------------
~Output Options Card
#-------------------------------------------------------
2,
#bottom center
1,1,1,
15,11,16,
1,1,yr,m,6,6,6,
6,
aqueous saturation,,
aqueous pressure,Pa,
```

```
znc aqueous volumetric flux,mm/yr,
Solute Aqueous Concentration,generic,1/m^3,
Solute volumetric Concentration,generic,1/m^3,
solute integrated mass,generic,,
16,
0,s,
1,yr,
10,yr,
50,yr,
100,yr,
500,yr,
1000,yr,
1500,yr,
2000,yr,
4000,yr,
5000,yr,
6000,yr,
7000,yr,
8000,yr,
9000,yr,
10000,yr,
13,
Final restart,,
rock/soil type,,
diffusive porosity,,
aqueous relative permeability,,
aqueous saturation,,
aqueous pressure,Pa,
gas pressure,Pa,
xnc aqueous volumetric flux,mm/yr,
ync aqueous volumetric flux,mm/yr,
znc aqueous volumetric flux,mm/yr,
Solute Aqueous Concentration,generic,1/m^3,
Solute Volumetric Concentration,generic,1/m^3,
aqueous courant,,

#-------------------------------------------------------
~Surface Card
#-------------------------------------------------------
2,
Aqueous Volumetric Flux,m^3/year,m^3,bottom,1,24,1,19,1,1,
Solute Flux, generic, 1/year,,bottom,1,24,1,19,1,1,
```

Input File for IDF Subsurface Simulation

```
~Simulation Title Card
1,
Modified from IDF PA VZSZ Distributed Infiltration Case for Tc-99 Release
from 3 Major Waste Streams in Phase I and II Cells,
Arun Wahi,
6,
Distributed infiltration case based on background rate of 3.5 mm/y with
IDF closed after Phase I and II construction
Vzp00 vadose zone properties for low anisotropy case using TCT model
Gwp15 saturated zone properties are Kh(H3) 17,000 m/d, Kh(Re) 5 m/d,
gradient 2e-5 to E, alphaL 1 m, alphaT 0.01 m, n(H3) 0.2, n(Re) 0.0905
SZ boundary conditions applied with pressures prescribed E and W and each
node N and S via seepage face option
VZSZ model configuration using upper 9 m of saturated zone with water
table 119.5 m NAVD88, vadose zone inactive above base of excavation, and
reduced horizontal domain
TVD Solver


~Solution Control Card
Restart file, ../../gw_spinup/restart.3484,
Water w/ Transport TVD Courant,1.0,
1,
0.0, yr, 10000.0, yr, 1.0E-09, yr, 1.0E+00, yr, 1.25, 8, 1.0E-06,
100000,
1,
Aqueous Relative Permeability, Upwind,


~Grid Card
Cartesian,
# number of cells in x-, y-, and z-dimensions (i,j,k indices)
# several layers from top and bottom will be inactive
60,70,86,
# spacing in x-dimension for i-indices proceeding east from origin easting
in meters Washington State Plane South NAD83 HARN
# Origin "lower left" is 573612.194 m, 134305.39 m, 56.5 m
0.0,m,1@188.33,m,1@125.56,m,1@83.71,m,1@55.81,m,1@37.21,m,1@24.81,m,3@22.5
0,m,1@15,m,40@10,m,1@15,m,2@22.5,m,1@23.749,m,1@24.81,m,1@37.21,m,1@55.81,
m,1@83.71,m,1@125.56,m,1@188.33,m,
# spacing in y-dimension for j-indices proceeding north from origin
northing in meters Washington State Plane South NAD83 HARN
0.0,m,1@188.33,m,1@125.56,m,1@83.71,m,1@55.81,m,1@37.21,m,1@24.81,m,1@18.8
45,m,2@22.50,m,1@15,m,50@10,m,1@15,m,2@22.50,m,1@18.845,m,1@24.81,m,1@37.2
1,m,1@55.81,m,1@83.71,m,1@125.56,m,1@188.33,m,
# spacing in z-dimension for k-indices proceeding upward from origin
elevation in meters on NAVD88
56.5,m,11@4,m,6@2,m,6@1,m,4@0.5,m,4@1,m,1@1.5,m,39@2,m,15@1.667,m,


~Inactive Nodes Card
7,
```

```
# Inactive below upper 9 m of saturated zone (below layer 17)
1,60,1,70,1,16,
# Reduce domain by 2 rows on the west based on prior testing
1,2,1,70,17,86,
# Reduce domain by 3 rows on the south based on prior testing
3,60,1,3,17,86,
# Reduce domain by 1 row on the north based on prior testing
3,60,70,70,17,86,
# Inactive above base of Phase I excavation at 204 m NAVD88 (above layer
71)
3,60,43,69,72,86,
# Inactive above base of Phase II excavation at 205.667 m NAVD88 (above
layer 72)
3,60,29,42,73,86,
# Inactive above base of Phase III excavation at 207.334 m NAVD88 (above
layer 73)
3,60,4,28,74,86,


~Rock/Soil Zonation Card
zonation file
unformatted,../../template/idf_pa_3d_geology_entire_model.zon,
#
#  Zones designated cell by cell in external file looping through i, then
j, then k.
#  List order below establishes zone numbering for external file:
#
#  Inactive nodes are 0 by default (see inactive nodes card);
#  Zone 1 = Basalt;
#  Zone 2 = Ringold A gravel (ra);
#  Zone 3 = Ringold Lower Mud (rlm);
#  Zone 4 = Ringold E gravel (saturated) (re_sat);
#  Zone 5 = H3 gravel (saturated) (h3_sat);
#  Zone 6 = Ringold E gravel (unsaturated) (re_unsat);
#  Zone 7 = H3 gravel (unsaturated) (h3_unsat);
#  Zone 8 = H2 sand (h2).
#
basalt,
ra,
rlm,
re_sat,
h3_sat,
re_unsat,
h3_unsat,
h2,


~Mechanical Properties Card
# lower saturated zone material types are not used (inactive)
basalt,    2.650,   g/cm^3,  0.050,    0.050,,,    millington and quirk,
ra,        2.4189,  g/cm^3,  0.09050,  0.09050,,,  millington and quirk,
rlm,       2.4189,  g/cm^3,  0.09050,  0.09050,,,  millington and quirk,
# upper saturated zone material types (active)
```

```
# using CPGWM 6.3.3 specific yield for porosities with bulk density of 2.2
g/cm3
h3_sat,    2.750,   g/cm^3,  0.200,    0.200,,,    millington and quirk,
re_sat,    2.4189,  g/cm^3,  0.09050,  0.09050,,,  millington and quirk,
# vadose zone material types (active)
# using measured porosities and bulk densities for sand sequence and
gravel sequence from MPR
h3_unsat,  2.6634,  g/cm^3,  0.1740,   0.1740,,,   millington and quirk,
re_unsat,  2.6634,  g/cm^3,  0.1740,   0.1740,,,   millington and quirk,
h2,        2.7760,  g/cm^3,  0.3840,   0.3840,,,   millington and quirk,


~Hydraulic Properties Card
# lower saturated zone material types are not used (inactive)
# Kh and Kv from CPGWM 6.3.3 for Ringold
basalt,    1.0E-04,   hc m/d,   1.0E-04,   hc m/d,   1.0E-05,   hc m/d,
ra,        4.80,      hc m/d,   4.80,      hc m/d,   0.480,     hc m/d,
rlm,       8.0E-03,   hc m/d,   8.0E-03,   hc m/d,   8.0E-04,   hc m/d,
# upper saturated zone material types (active)
# using CPGWM 6.3.3 Kh and Kv
h3_sat,    17000,     hc m/d,   17000,     hc m/d,   1200,      hc m/d,
re_sat,    5.0,       hc m/d,   5.0,       hc m/d,   0.50,      hc m/d,
# vadose zone material types (active) low anisotropy case (P=1 x & y,
P=1/3 z)
# using fit values for sand sequence and gravel sequence from MPR
h3_unsat,  4.671E-2,  hc cm/s,  4.671E-2,  hc cm/s,  7.714E-3,  hc cm/s,
re_unsat,  4.671E-2,  hc cm/s,  4.671E-2,  hc cm/s,  7.714E-3,  hc cm/s,
h2,        6.196E-3,  hc cm/s,  6.196E-3,  hc cm/s,  6.157E-3,  hc cm/s,


~Saturation Function Card
# saturated zone curves not invoked since boundary conditions prescribe
head
# input same parameters as unsaturated gravels without adjusting residual
saturation
basalt,    Nonhysteretic van Genuchten,  0.088590,1/cm,  1.2710,
2.18390E-02,,
ra,        Nonhysteretic van Genuchten,  0.088590,1/cm,  1.2710,
2.18390E-02,,
rlm,       Nonhysteretic van Genuchten,  0.088590,1/cm,  1.2710,
2.18390E-02,,
h3_sat,    Nonhysteretic van Genuchten,  0.088590,1/cm,  1.2710,
2.18390E-02,,
re_sat,    Nonhysteretic van Genuchten,  0.088590,1/cm,  1.2710,
2.18390E-02,,
# vadose zone material types (active) low anisotropy case (P=1 x & y,
P=1/3 z)
# using fit values for sand sequence and gravel sequence from MPR
h3_unsat,  Nonhysteretic van Genuchten,  0.088590,1/cm,  1.2710,
2.18390E-02,,
re_unsat,  Nonhysteretic van Genuchten,  0.088590,1/cm,  1.2710,
2.18390E-02,,
h2,        Nonhysteretic van Genuchten,  0.064190,1/cm,  1.6980,
7.55210E-02,,
```

```
~x-Aqueous Relative Permeability Card
# saturated zone curves not invoked since boundary conditions prescribe
head
# input same parameters as unsaturated gravels
basalt,    Modified Mualem,,  0.637,
ra,        Modified Mualem,,  0.637,
rlm,       Modified Mualem,,  0.637,
h3_sat,    Modified Mualem,,  0.637,
re_sat,    Modified Mualem,,  0.637,
# vadose zone material types (active) low anisotropy case (P=1 x & y,
P=1/3 z)
# using fit values for sand sequence and gravel sequence from MPR
h3_unsat,  Modified Mualem,,  0.637,
re_unsat,  Modified Mualem,,  0.637,
h2,        Modified Mualem,, -0.683,


~y-Aqueous Relative Permeability Card
# saturated zone curves not invoked since boundary conditions prescribe
head
# input same parameters as unsaturated gravels
basalt,    Modified Mualem,,  0.637,
ra,        Modified Mualem,,  0.637,
rlm,       Modified Mualem,,  0.637,
h3_sat,    Modified Mualem,,  0.637,
re_sat,    Modified Mualem,,  0.637,
# vadose zone material types (active) low anisotropy case (P=1 x & y,
P=1/3 z)
# using fit values for sand sequence and gravel sequence from MPR
h3_unsat,  Modified Mualem,,  0.637,
re_unsat,  Modified Mualem,,  0.637,
h2,        Modified Mualem,, -0.683,


~z-Aqueous Relative Permeability Card
# saturated zone curves not invoked since boundary conditions prescribe
head
# input same parameters as unsaturated gravels
basalt,    Modified Mualem,, -0.225,
ra,        Modified Mualem,, -0.225,
rlm,       Modified Mualem,, -0.225,
h3_sat,    Modified Mualem,, -0.225,
re_sat,    Modified Mualem,, -0.225,
# vadose zone material types (active) low anisotropy case (P=1 x & y,
P=1/3 z)
# using fit values for sand sequence and gravel sequence from MPR
h3_unsat,  Modified Mualem,, -0.225,
re_unsat,  Modified Mualem,, -0.225,
h2,        Modified Mualem,,  0.375,


#~Initial Conditions Card
```

```
# Initial conditions from historic simulation that were used to initialize
flow field in restart file.
# Run for 2000 years with equivalent boundary conditions.
#aqueous pressure,gas pressure,
#8,
#aqueous pressure,   180000,  Pa,  0.0,  1/m,  0.0,  1/m,  -9793.52,  1/m,
3,  60,   3,  69,  17,  25,
#gas pressure,     101325.0,  Pa,  0.0,  1/m,  0.0,  1/m,       0.0,  1/m,
3,  60,   3,  69,  17,  25,
#aqueous pressure,    95000,  Pa,  0.0,  1/m,  0.0,  1/m,       0.0,  1/m,
3,  60,  43,  69,  26,  71,
#gas pressure,     101325.0,  Pa,  0.0,  1/m,  0.0,  1/m,       0.0,  1/m,
3,  60,  43,  69,  26,  71,
#aqueous pressure,    95000,  Pa,  0.0,  1/m,  0.0,  1/m,       0.0,  1/m,
3,  60,  29,  42,  26,  72,
#gas pressure,     101325.0,  Pa,  0.0,  1/m,  0.0,  1/m,       0.0,  1/m,
3,  60,  29,  42,  26,  72,
#aqueous pressure,    95000,  Pa,  0.0,  1/m,  0.0,  1/m,       0.0,  1/m,
3,  60,   3,  28,  26,  73,
#gas pressure,     101325.0,  Pa,  0.0,  1/m,  0.0,  1/m,       0.0,  1/m,
3,  60,   3,  28,  26,  73,


~Solute/Fluid Interaction Card
1,
Tc-99 , Conventional, 2.50e-5, cm^2/s,, 2.130E+05,yr,
#I-129  ,Conventional, 2.50e-5, cm^2/s,, 1.570E+07,yr,
0,


~Solute/Porous Media Interaction Card
#
# lower saturated zone material types are not used (inactive)
#
basalt,  1.0,  m,  0.010,  m,
  Tc-99, 0.0, mL/g, 1.0,
#  I-129, 0.0, mL/g, 1.0,
ra,      1.0,  m,  0.010,  m,
  Tc-99, 0.0, mL/g, 1.0,
#  I-129, 0.0, mL/g, 1.0,
rlm,     1.0,  m,  0.010,  m,
  Tc-99, 0.0, mL/g, 1.0,
#  I-129, 0.0, mL/g, 1.0,
#
# upper saturated zone material types (active)
# “best” Kd values from PNNL-13037 (0.0 ml/g for Tc-99, 0.0 ml/g for I-129
in H3 and Ringold)
# In gwp15 case SZ longitudinal dispersivity = 1 m, transverse
dispersivity = 0.01 m.
#
re_sat,  1.0,  m,  0.010,  m,
  Tc-99, 0.0, mL/g, 1.0,
#  I-129, 0.0, mL/g, 1.0,
h3_sat,  1.0,  m,  0.010,  m,
```

```
  Tc-99, 0.0, mL/g, 1.0,
#  I-129, 0.0, mL/g, 1.0,
#
# vadose zone material types (active)
# In vzp00 case VZ dispersivities are lower values for gravelly sequence
and sandy sequence from MPR.
# “best” Kd values from PNNL-13037 (0.0 ml/g for Tc-99, 0.1 ml/g for I-129
in H2)
#
re_unsat,  20.0, cm, 2.00, cm,
  Tc-99, 0.0, mL/g, 1.0,
#  I-129, 0.0, mL/g, 1.0,
h3_unsat,  20.0, cm, 2.00, cm,
  Tc-99, 0.0, mL/g, 1.0,
#  I-129, 0.0, mL/g, 1.0,
h2,        25.0, cm, 2.50, cm,
  Tc-99, 0.0, mL/g, 1.0,
#  I-129, 0.1, mL/g, 1.0,


~Source Card
##############################################################################
##############################################
Solute, Tc-99, 22, 23, 43, 53, 71, 71, 2,
 0.0,yr, 0.000414620532271692,Ci/yr,
 10000.0,yr, 0.000414620532271692,Ci/yr,
#
Solute, Tc-99, 38, 39, 43, 53, 71, 71, 2,
 0.0,yr, 0.000414620532271692,Ci/yr,
 10000.0,yr, 0.000414620532271692,Ci/yr,
#
Solute, Tc-99, 22, 23, 40, 42, 72, 72, 2,
 0.0,yr, 0.000414620532271693,Ci/yr,
 10000.0,yr, 0.000414620532271693,Ci/yr,
#
Solute, Tc-99, 38, 39, 40, 42, 72, 72, 2,
 0.0,yr, 0.000414620532271693,Ci/yr,
 10000.0,yr, 0.000414620532271693,Ci/yr,
Solute, Tc-99, 22, 23, 39, 39, 72, 72, 2,
 0.0,yr, 0.00013414193691143,Ci/yr,
 10000.0,yr, 0.00013414193691143,Ci/yr,
#
Solute, Tc-99, 38, 39, 39, 39, 72, 72, 2,
 0.0,yr, 0.00013414193691143,Ci/yr,
 10000.0,yr, 0.00013414193691143,Ci/yr,


~Surface Flux Card
#
158,
#
# Surfaces for concentrations in 5-m interval below water table
# East and north edges of 100-m buffer zone are at i = 55 and j = 65
#
```

```
#File north2.srf writes fluxes for middle third of northern boundary cells
(180.00 m total) at 100-m buffer zone.
36,north2.srf,
Solute Flux, Tc-99,Ci/yr,,north,22,22,65,65,20,25,
Aqueous Volumetric,L/yr,L,north,22,22,65,65,20,25,
Solute Flux, Tc-99,Ci/yr,,north,23,23,65,65,20,25,
Aqueous Volumetric,L/yr,L,north,23,23,65,65,20,25,
Solute Flux, Tc-99,Ci/yr,,north,24,24,65,65,20,25,
Aqueous Volumetric,L/yr,L,north,24,24,65,65,20,25,
Solute Flux, Tc-99,Ci/yr,,north,25,25,65,65,20,25,
Aqueous Volumetric,L/yr,L,north,25,25,65,65,20,25,
Solute Flux, Tc-99,Ci/yr,,north,26,26,65,65,20,25,
Aqueous Volumetric,L/yr,L,north,26,26,65,65,20,25,
Solute Flux, Tc-99,Ci/yr,,north,27,27,65,65,20,25,
Aqueous Volumetric,L/yr,L,north,27,27,65,65,20,25,
Solute Flux, Tc-99,Ci/yr,,north,28,28,65,65,20,25,
Aqueous Volumetric,L/yr,L,north,28,28,65,65,20,25,
Solute Flux, Tc-99,Ci/yr,,north,29,29,65,65,20,25,
Aqueous Volumetric,L/yr,L,north,29,29,65,65,20,25,
Solute Flux, Tc-99,Ci/yr,,north,30,30,65,65,20,25,
Aqueous Volumetric,L/yr,L,north,30,30,65,65,20,25,
Solute Flux, Tc-99,Ci/yr,,north,31,31,65,65,20,25,
Aqueous Volumetric,L/yr,L,north,31,31,65,65,20,25,
Solute Flux, Tc-99,Ci/yr,,north,32,32,65,65,20,25,
Aqueous Volumetric,L/yr,L,north,32,32,65,65,20,25,
Solute Flux, Tc-99,Ci/yr,,north,33,33,65,65,20,25,
Aqueous Volumetric,L/yr,L,north,33,33,65,65,20,25,
Solute Flux, Tc-99,Ci/yr,,north,34,34,65,65,20,25,
Aqueous Volumetric,L/yr,L,north,34,34,65,65,20,25,
Solute Flux, Tc-99,Ci/yr,,north,35,35,65,65,20,25,
Aqueous Volumetric,L/yr,L,north,35,35,65,65,20,25,
Solute Flux, Tc-99,Ci/yr,,north,36,36,65,65,20,25,
Aqueous Volumetric,L/yr,L,north,36,36,65,65,20,25,
Solute Flux, Tc-99,Ci/yr,,north,37,37,65,65,20,25,
Aqueous Volumetric,L/yr,L,north,37,37,65,65,20,25,
Solute Flux, Tc-99,Ci/yr,,north,38,38,65,65,20,25,
Aqueous Volumetric,L/yr,L,north,38,38,65,65,20,25,
Solute Flux, Tc-99,Ci/yr,,north,39,39,65,65,20,25,
Aqueous Volumetric,L/yr,L,north,39,39,65,65,20,25,
#
#File north3.srf writes fluxes for eastern third of northern boundary
cells (218.559 m total) at 100-m buffer zone.
32,north3.srf,
Solute Flux, Tc-99,Ci/yr,,north,40,40,65,65,20,25,
Aqueous Volumetric,L/yr,L,north,40,40,65,65,20,25,
Solute Flux, Tc-99,Ci/yr,,north,41,41,65,65,20,25,
Aqueous Volumetric,L/yr,L,north,41,41,65,65,20,25,
Solute Flux, Tc-99,Ci/yr,,north,42,42,65,65,20,25,
Aqueous Volumetric,L/yr,L,north,42,42,65,65,20,25,
Solute Flux, Tc-99,Ci/yr,,north,43,43,65,65,20,25,
Aqueous Volumetric,L/yr,L,north,43,43,65,65,20,25,
Solute Flux, Tc-99,Ci/yr,,north,44,44,65,65,20,25,
Aqueous Volumetric,L/yr,L,north,44,44,65,65,20,25,
Solute Flux, Tc-99,Ci/yr,,north,45,45,65,65,20,25,
```

```
Aqueous Volumetric,L/yr,L,north,45,45,65,65,20,25,
Solute Flux, Tc-99,Ci/yr,,north,46,46,65,65,20,25,
Aqueous Volumetric,L/yr,L,north,46,46,65,65,20,25,
Solute Flux, Tc-99,Ci/yr,,north,47,47,65,65,20,25,
Aqueous Volumetric,L/yr,L,north,47,47,65,65,20,25,
Solute Flux, Tc-99,Ci/yr,,north,48,48,65,65,20,25,
Aqueous Volumetric,L/yr,L,north,48,48,65,65,20,25,
Solute Flux, Tc-99,Ci/yr,,north,49,49,65,65,20,25,
Aqueous Volumetric,L/yr,L,north,49,49,65,65,20,25,
Solute Flux, Tc-99,Ci/yr,,north,50,50,65,65,20,25,
Aqueous Volumetric,L/yr,L,north,50,50,65,65,20,25,
Solute Flux, Tc-99,Ci/yr,,north,51,51,65,65,20,25,
Aqueous Volumetric,L/yr,L,north,51,51,65,65,20,25,
Solute Flux, Tc-99,Ci/yr,,north,52,52,65,65,20,25,
Aqueous Volumetric,L/yr,L,north,52,52,65,65,20,25,
Solute Flux, Tc-99,Ci/yr,,north,53,53,65,65,20,25,
Aqueous Volumetric,L/yr,L,north,53,53,65,65,20,25,
Solute Flux, Tc-99,Ci/yr,,north,54,54,65,65,20,25,
Aqueous Volumetric,L/yr,L,north,54,54,65,65,20,25,
Solute Flux, Tc-99,Ci/yr,,north,55,55,65,65,20,25,
Aqueous Volumetric,L/yr,L,north,55,55,65,65,20,25,
#
#File east2.srf writes fluxes for middle third of eastern boundary cells
(200.00 m total) at 100-m buffer zone.
40,east2.srf,
Solute Flux, Tc-99,Ci/yr,,east,55,55,26,26,20,25,
Aqueous Volumetric,L/yr,L,east,55,55,26,26,20,25,
Solute Flux, Tc-99,Ci/yr,,east,55,55,27,27,20,25,
Aqueous Volumetric,L/yr,L,east,55,55,27,27,20,25,
Solute Flux, Tc-99,Ci/yr,,east,55,55,28,28,20,25,
Aqueous Volumetric,L/yr,L,east,55,55,28,28,20,25,
Solute Flux, Tc-99,Ci/yr,,east,55,55,29,29,20,25,
Aqueous Volumetric,L/yr,L,east,55,55,29,29,20,25,
Solute Flux, Tc-99,Ci/yr,,east,55,55,30,30,20,25,
Aqueous Volumetric,L/yr,L,east,55,55,30,30,20,25,
Solute Flux, Tc-99,Ci/yr,,east,55,55,31,31,20,25,
Aqueous Volumetric,L/yr,L,east,55,55,31,31,20,25,
Solute Flux, Tc-99,Ci/yr,,east,55,55,32,32,20,25,
Aqueous Volumetric,L/yr,L,east,55,55,32,32,20,25,
Solute Flux, Tc-99,Ci/yr,,east,55,55,33,33,20,25,
Aqueous Volumetric,L/yr,L,east,55,55,33,33,20,25,
Solute Flux, Tc-99,Ci/yr,,east,55,55,34,34,20,25,
Aqueous Volumetric,L/yr,L,east,55,55,34,34,20,25,
Solute Flux, Tc-99,Ci/yr,,east,55,55,35,35,20,25,
Aqueous Volumetric,L/yr,L,east,55,55,35,35,20,25,
Solute Flux, Tc-99,Ci/yr,,east,55,55,36,36,20,25,
Aqueous Volumetric,L/yr,L,east,55,55,36,36,20,25,
Solute Flux, Tc-99,Ci/yr,,east,55,55,37,37,20,25,
Aqueous Volumetric,L/yr,L,east,55,55,37,37,20,25,
Solute Flux, Tc-99,Ci/yr,,east,55,55,38,38,20,25,
Aqueous Volumetric,L/yr,L,east,55,55,38,38,20,25,
Solute Flux, Tc-99,Ci/yr,,east,55,55,39,39,20,25,
Aqueous Volumetric,L/yr,L,east,55,55,39,39,20,25,
Solute Flux, Tc-99,Ci/yr,,east,55,55,40,40,20,25,
```

```
Aqueous Volumetric,L/yr,L,east,55,55,40,40,20,25,
Solute Flux, Tc-99,Ci/yr,,east,55,55,41,41,20,25,
Aqueous Volumetric,L/yr,L,east,55,55,41,41,20,25,
Solute Flux, Tc-99,Ci/yr,,east,55,55,42,42,20,25,
Aqueous Volumetric,L/yr,L,east,55,55,42,42,20,25,
Solute Flux, Tc-99,Ci/yr,,east,55,55,43,43,20,25,
Aqueous Volumetric,L/yr,L,east,55,55,43,43,20,25,
Solute Flux, Tc-99,Ci/yr,,east,55,55,44,44,20,25,
Aqueous Volumetric,L/yr,L,east,55,55,44,44,20,25,
Solute Flux, Tc-99,Ci/yr,,east,55,55,45,45,20,25,
Aqueous Volumetric,L/yr,L,east,55,55,45,45,20,25,
#
#File east3.srf writes fluxes for northern third of eastern boundary cells
(253.655 m total) at 100-m buffer zone.
40,east3.srf,
Solute Flux, Tc-99,Ci/yr,,east,55,55,46,46,20,25,
Aqueous Volumetric,L/yr,L,east,55,55,46,46,20,25,
Solute Flux, Tc-99,Ci/yr,,east,55,55,47,47,20,25,
Aqueous Volumetric,L/yr,L,east,55,55,47,47,20,25,
Solute Flux, Tc-99,Ci/yr,,east,55,55,48,48,20,25,
Aqueous Volumetric,L/yr,L,east,55,55,48,48,20,25,
Solute Flux, Tc-99,Ci/yr,,east,55,55,49,49,20,25,
Aqueous Volumetric,L/yr,L,east,55,55,49,49,20,25,
Solute Flux, Tc-99,Ci/yr,,east,55,55,50,50,20,25,
Aqueous Volumetric,L/yr,L,east,55,55,50,50,20,25,
Solute Flux, Tc-99,Ci/yr,,east,55,55,51,51,20,25,
Aqueous Volumetric,L/yr,L,east,55,55,51,51,20,25,
Solute Flux, Tc-99,Ci/yr,,east,55,55,52,52,20,25,
Aqueous Volumetric,L/yr,L,east,55,55,52,52,20,25,
Solute Flux, Tc-99,Ci/yr,,east,55,55,53,53,20,25,
Aqueous Volumetric,L/yr,L,east,55,55,53,53,20,25,
Solute Flux, Tc-99,Ci/yr,,east,55,55,54,54,20,25,
Aqueous Volumetric,L/yr,L,east,55,55,54,54,20,25,
Solute Flux, Tc-99,Ci/yr,,east,55,55,55,55,20,25,
Aqueous Volumetric,L/yr,L,east,55,55,55,55,20,25,
Solute Flux, Tc-99,Ci/yr,,east,55,55,56,56,20,25,
Aqueous Volumetric,L/yr,L,east,55,55,56,56,20,25,
Solute Flux, Tc-99,Ci/yr,,east,55,55,57,57,20,25,
Aqueous Volumetric,L/yr,L,east,55,55,57,57,20,25,
Solute Flux, Tc-99,Ci/yr,,east,55,55,58,58,20,25,
Aqueous Volumetric,L/yr,L,east,55,55,58,58,20,25,
Solute Flux, Tc-99,Ci/yr,,east,55,55,59,59,20,25,
Aqueous Volumetric,L/yr,L,east,55,55,59,59,20,25,
Solute Flux, Tc-99,Ci/yr,,east,55,55,60,60,20,25,
Aqueous Volumetric,L/yr,L,east,55,55,60,60,20,25,
Solute Flux, Tc-99,Ci/yr,,east,55,55,61,61,20,25,
Aqueous Volumetric,L/yr,L,east,55,55,61,61,20,25,
Solute Flux, Tc-99,Ci/yr,,east,55,55,62,62,20,25,
Aqueous Volumetric,L/yr,L,east,55,55,62,62,20,25,
Solute Flux, Tc-99,Ci/yr,,east,55,55,63,63,20,25,
Aqueous Volumetric,L/yr,L,east,55,55,63,63,20,25,
Solute Flux, Tc-99,Ci/yr,,east,55,55,64,64,20,25,
Aqueous Volumetric,L/yr,L,east,55,55,64,64,20,25,
Solute Flux, Tc-99,Ci/yr,,east,55,55,65,65,20,25,
```

```
Aqueous Volumetric,L/yr,L,east,55,55,65,65,20,25,
#
# Surfaces for checking solute and water mass balance
#
10,mass_balance.srf,
# horizontal plane across domain near top of vadose zone
Solute Flux, Tc-99,Ci/yr,, bottom,  3, 60,  4, 69,  71,  71,
# horizontal plane across domain deep in H2 sand and fully above H3 gravel
Solute Flux, Tc-99,Ci/yr,, bottom,  3, 60,  4, 69,  48,  48,
# horizontal plane across domain at bottom of vadose zone
Solute Flux, Tc-99,Ci/yr,, bottom,  3, 60,  4, 69,  26,  26,
# horizontal area below west sump release area footprint at bottom of
vadose zone
Solute Flux, Tc-99, Ci/yr,, bottom, 22, 23, 30, 53,  26,  26,
# horizontal area below east sump release area footprint at bottom of
vadose zone
Solute Flux, Tc-99, Ci/yr,, bottom, 38, 39, 30, 53,  26,  26,
# horizontal area of domain up to north and east sides of 100-m buffer
zone at bottom of 5-m well screen interval
Solute Flux, Tc-99,Ci/yr,, bottom,  3, 55,  4, 65,  20,  20,
# vertical area across 5-m well screen interval along east side of 100-m
buffer zone
Solute Flux, Tc-99,Ci/yr,, east,   55, 55,  4, 65,  20,  25,
# vertical area below 5-m well screen interval along east side of 100-m
buffer zone
Solute Flux, Tc-99,Ci/yr,, east,   55, 55,  4, 65,  17,  19,
# vertical area across 5-m well screen interval along north side of 100-m
buffer zone
Solute Flux, Tc-99,Ci/yr,, north,   3, 55, 65, 65,  20,  25,
# vertical area below 5-m well screen interval along north side of 100-m
buffer zone
Solute Flux, Tc-99,Ci/yr,, north,   3, 55, 65, 65,  17,  19,
# horizontal plane across domain near top of vadose zone
#Aqueous Volumetric Flux, L/yr, L, top,     3, 60,  4, 69, 71, 71,
# horizontal area of IDF Phases I through III near top of vadose zone
#Aqueous Volumetric Flux, L/yr, L, top,     8, 53,  9, 62, 71, 71,
# horizontal plane across domain at bottom of vadose zone
#Aqueous Volumetric Flux, L/yr, L, bottom,     3, 60,  4, 69, 26, 26,
# vertical plane on west boundary of active saturated domain
#Aqueous Volumetric Flux, L/yr, L, west,    3,  3,  4, 69, 17, 25,
# vertical plane on east boundary of active saturated domain
#Aqueous Volumetric Flux, L/yr, L, east,   60, 60,  4, 69, 17, 25,
# vertical plane on north boundary of active saturated domain
#Aqueous Volumetric Flux, L/yr, L, north,   3, 60, 69, 69, 17, 25,
# vertical plane on south boundary of active saturated domain
#Aqueous Volumetric Flux, L/yr, L, south,   3, 60,  4,  4, 17, 25,


~Output Control Card
3,
# Monitor selected output at cell at 100-m buffer near expected overall
peak impact location at water table
  51, 55, 25,
```

```
# Monitor selected output at cell at 100-m buffer near expected overall
peak impact location at base of 5-m well screen
  51, 55, 20,
# Monitor selected output at cell at 100-m buffer near expected overall
peak impact location at base of active model
  51, 55, 17,
200,1,yr,m,8,8,8,
3,
solute aqueous conc, Tc-99,Ci/L,
#solute aqueous conc, I-129,Ci/L,
aqueous saturation,,
#matric potential,cm,
#xnc aqueous vol,m/yr,
#ync aqueous vol,m/yr,
znc aqueous vol,mm/yr,
#aqueous courant,,
9,
# Write plot files and restart files at selected times
  2052.0,yr,
  2152.0,yr,
  2552.0,yr,
  3051.0,yr,
  4051.0,yr,
  6051.0,yr,
  8051.0,yr,
  10051.0,yr,
  12051.0,yr,
9,
solute aqueous conc, Tc-99,Ci/L,
#solute aqueous conc, I-129,Ci/L,
#solute volumetric conc, I-129,Ci/L,
rock/soil type,,
aqueous moisture cont,,
aqueous saturation,,
matric potential,cm,
xnc aqueous vol,m/yr,
ync aqueous vol,m/yr,
znc aqueous vol,mm/yr,
aqueous courant,,


~Boundary Conditions Card
165,
#
# Infiltration case inf_d06 for distributed infiltration from background
rate of 3.5 mm/y
# Assumes IDF closed after Phases I and II construction
#
# north area outside IDF including cap north sideslope and corners
top,Neumann,zero flux,
3,60,61,69,71,71,1,
0,yr,-3.50,mm/yr,,,
# south area outside IDF including cap south sideslope and corners
top,Neumann,zero flux,
```

```
3,60,4,24,73,73,1,
0,yr,-3.50,mm/yr,,,
# west area outside IDF Phase I
top,Neumann,zero flux,
3,7,43,60,71,71,1,
0,yr,-3.50,mm/yr,,,
# IDF Phase I western outer cap recharge area
top,Neumann,zero flux,
8,8,43,60,71,71,1,
0,yr,-3.50,mm/yr,,,
# IDF Phase I western inner cap recharge area
top,Neumann,zero flux,
9,9,43,60,71,71,1,
0,yr,-3.50,mm/yr,,,
# IDF Phase I below liner west excavation sideslope area
top,Neumann,zero flux,
10,13,43,60,71,71,1,
0,yr,-3.5,mm/yr,,,
# IDF Phase I below liner west excavation sideslope base area
top,Neumann,zero flux,
14,14,43,60,71,71,1,
0,yr,-3.5,mm/yr,,,
# IDF Phase I below liner west area
top,Neumann,zero flux,
15,21,43,60,71,71,1,
0,yr,-3.5,mm/yr,,,
# IDF Phase I enhanced recharge zone below liner along west sump line
top,Neumann,zero flux,
22,23,43,60,71,71,1,
0,yr,-3.5,mm/yr,,,
# IDF Phase I below liner middle area
top,Neumann,zero flux,
24,37,43,60,71,71,1,
0,yr,-3.5,mm/yr,,,
# IDF Phase I enhanced recharge zone below liner along east sump line
top,Neumann,zero flux,
38,39,43,60,71,71,1,
0,yr,-3.5,mm/yr,,,
# IDF Phase I below liner east area
top,Neumann,zero flux,
40,46,43,60,71,71,1,
0,yr,-3.5,mm/yr,,,
# IDF Phase I below liner east excavation sideslope base area
top,Neumann,zero flux,
47,47,43,60,71,71,1,
0,yr,-3.5,mm/yr,,,
# IDF Phase I below liner east excavation sideslope area
top,Neumann,zero flux,
48,51,43,60,71,71,1,
0,yr,-3.5,mm/yr,,,
# IDF Phase I eastern inner cap recharge area
top,Neumann,zero flux,
52,52,43,60,71,71,1,
0,yr,-3.50,mm/yr,,,
```

```
# IDF Phase I eastern outer cap recharge area
top,Neumann,zero flux,
53,53,43,60,71,71,1,
0,yr,-3.50,mm/yr,,,
# east area outside IDF Phase I
top,Neumann,zero flux,
54,60,43,60,71,71,1,
0,yr,-3.50,mm/yr,,,
# west area outside IDF Phase II
top,Neumann,zero flux,
3,7,29,42,72,72,1,
0,yr,-3.50,mm/yr,,,
# IDF Phase II western outer cap recharge area
top,Neumann,zero flux,
8,8,29,42,72,72,1,
0,yr,-3.50,mm/yr,,,
# IDF Phase II western inner cap recharge area
top,Neumann,zero flux,
9,9,29,42,72,72,1,
0,yr,-3.50,mm/yr,,,
# IDF Phase II below liner west excavation sideslope area
top,Neumann,zero flux,
10,13,29,42,72,72,1,
0,yr,-3.5,mm/yr,,,
# IDF Phase II below liner west excavation sideslope base area
top,Neumann,zero flux,
14,14,29,42,72,72,1,
0,yr,-3.5,mm/yr,,,
# IDF Phase II below liner west area
top,Neumann,zero flux,
15,21,29,42,72,72,1,
0,yr,-3.5,mm/yr,,,
# IDF Phase II enhanced recharge zone below liner along west sump line
top,Neumann,zero flux,
22,23,29,42,72,72,1,
0,yr,-3.5,mm/yr,,,
# IDF Phase II below liner middle area
top,Neumann,zero flux,
24,37,29,42,72,72,1,
0,yr,-3.5,mm/yr,,,
# IDF Phase II enhanced recharge zone below liner along east sump line
top,Neumann,zero flux,
38,39,29,42,72,72,1,
0,yr,-3.5,mm/yr,,,
# IDF Phase II below liner east area
top,Neumann,zero flux,
40,46,29,42,72,72,1,
0,yr,-3.5,mm/yr,,,
# IDF Phase II below liner east excavation sideslope base area
top,Neumann,zero flux,
47,47,29,42,72,72,1,
0,yr,-3.5,mm/yr,,,
# IDF Phase II below liner east excavation sideslope area
top,Neumann,zero flux,
```

```
48,51,29,42,72,72,1,
0,yr,-3.5,mm/yr,,,
# IDF Phase II eastern inner cap recharge area
top,Neumann,zero flux,
52,52,29,42,72,72,1,
0,yr,-3.50,mm/yr,,,
# IDF Phase II eastern outer cap recharge area
top,Neumann,zero flux,
53,53,29,42,72,72,1,
0,yr,-3.50,mm/yr,,,
# east area outside IDF Phase II
top,Neumann,zero flux,
54,60,29,42,72,72,1,
0,yr,-3.50,mm/yr,,,
# west area outside IDF south end of Phase II
top,Neumann,zero flux,
3,7,25,28,73,73,1,
0,yr,-3.50,mm/yr,,,
# IDF south end of Phase II western outer cap recharge area
top,Neumann,zero flux,
8,8,25,28,73,73,1,
0,yr,-3.50,mm/yr,,,
# IDF south end of Phase II western inner cap recharge area
top,Neumann,zero flux,
9,9,25,28,73,73,1,
0,yr,-3.50,mm/yr,,,
# IDF south end of Phase II below liner west excavation sideslope area
top,Neumann,zero flux,
10,13,25,28,73,73,1,
0,yr,-3.5,mm/yr,,,
# IDF south end of Phase II below liner west excavation sideslope base
area
top,Neumann,zero flux,
14,14,25,28,73,73,1,
0,yr,-3.5,mm/yr,,,
# IDF south end of Phase II below liner west area
top,Neumann,zero flux,
15,21,25,28,73,73,1,
0,yr,-3.5,mm/yr,,,
# IDF south end of Phase II enhanced recharge zone below liner along west
sump line
top,Neumann,zero flux,
22,23,25,28,73,73,1,
0,yr,-3.5,mm/yr,,,
# IDF south end of Phase II below liner middle area
top,Neumann,zero flux,
24,37,25,28,73,73,1,
0,yr,-3.5,mm/yr,,,
# IDF south end of Phase II enhanced recharge zone below liner along east
sump line
top,Neumann,zero flux,
38,39,25,28,73,73,1,
0,yr,-3.5,mm/yr,,,
# IDF south end of Phase II below liner east area
```

```
top,Neumann,zero flux,
40,46,25,28,73,73,1,
0,yr,-3.5,mm/yr,,,
# IDF south end of Phase II below liner east excavation sideslope base
area
top,Neumann,zero flux,
47,47,25,28,73,73,1,
0,yr,-3.5,mm/yr,,,
# IDF south end of Phase II below liner east excavation sideslope area
top,Neumann,zero flux,
48,51,25,28,73,73,1,
0,yr,-3.5,mm/yr,,,
# IDF south end of Phase II eastern inner cap recharge area
top,Neumann,zero flux,
52,52,25,28,73,73,1,
0,yr,-3.50,mm/yr,,,
# IDF south end of Phase II eastern outer cap recharge area
top,Neumann,zero flux,
53,53,25,28,73,73,1,
0,yr,-3.50,mm/yr,,,
# east area outside IDF south end of Phase II
top,Neumann,zero flux,
54,60,25,28,73,73,1,
0,yr,-3.50,mm/yr,,,
#
# Saturated zone BCs for upper 9 m below steady-state water table at 119.5
m NAVD88
# w/ due east gradient of 2e-5 m/m
# Pressure specified at elevation of centroid of k = 17, i.e. 111.5 m
NAVD88
#
# Intermediate calculations retain more digits than significant
#
# dP/dz = dP/dh = -9793.52 1/m for a hydrostratic column per STOMP User's
Guide.
# dP/dy = 0
# dP/dx = (dh/dx)*(dP/dh) = (2e-5 m/m)*(-9793.52 Pa/m)
#
# P(east) = 101325 Pa + [(111.5 m NAVD88 - 119.5 m NAVD88) * (-9793.52
Pa/m)]
#         = 179673.160 Pa
#
# Length of domain in x from sum of spacings minus inactive nodes =
1597.109 m - 188.33 m - 125.56 m
#                                                                    =
1283.219 m
#
# P(west) = P(east) - (dh/dx)*(dP/dh)*dx
#         = (179673.160 Pa) - (2e-5 m/m)*(-9793.52 Pa/m)*(1283.219 m)
#         = 179924.505 Pa
#
# Similarly to specify pressure at node center x position for i = 3,
# dx(edge to node) = (83.71 m)/2 and P(node) = 179916.306 Pa
# etc.
```

```
#
west,seepage face,outflow,
3,3,4,69,17,71,1,
0,yr,179924.505,Pa,,,,,,,,
east,seepage face,outflow,
60,60,4,69,17,71,1,
0,yr,179673.16,Pa,,,,,,,,
south,seepage face,outflow,
3,3,4,4,17,71,1,
0,yr,179916.306,Pa,,,,,,,,
south,seepage face,outflow,
4,4,4,4,17,71,1,
0,yr,179902.643,Pa,,,,,,,,
south,seepage face,outflow,
5,5,4,4,17,71,1,
0,yr,179893.533,Pa,,,,,,,,
south,seepage face,outflow,
6,6,4,4,17,71,1,
0,yr,179887.459,Pa,,,,,,,,
south,seepage face,outflow,
7,7,4,4,17,71,1,
0,yr,179882.825,Pa,,,,,,,,
south,seepage face,outflow,
8,8,4,4,17,71,1,
0,yr,179878.418,Pa,,,,,,,,
south,seepage face,outflow,
9,9,4,4,17,71,1,
0,yr,179874.011,Pa,,,,,,,,
south,seepage face,outflow,
10,10,4,4,17,71,1,
0,yr,179870.339,Pa,,,,,,,,
south,seepage face,outflow,
11,11,4,4,17,71,1,
0,yr,179867.89,Pa,,,,,,,,
south,seepage face,outflow,
12,12,4,4,17,71,1,
0,yr,179865.932,Pa,,,,,,,,
south,seepage face,outflow,
13,13,4,4,17,71,1,
0,yr,179863.973,Pa,,,,,,,,
south,seepage face,outflow,
14,14,4,4,17,71,1,
0,yr,179862.014,Pa,,,,,,,,
south,seepage face,outflow,
15,15,4,4,17,71,1,
0,yr,179860.055,Pa,,,,,,,,
south,seepage face,outflow,
16,16,4,4,17,71,1,
0,yr,179858.097,Pa,,,,,,,,
south,seepage face,outflow,
17,17,4,4,17,71,1,
0,yr,179856.138,Pa,,,,,,,,
south,seepage face,outflow,
18,18,4,4,17,71,1,
```

```
0,yr,179854.179,Pa,,,,,,,,
south,seepage face,outflow,
19,19,4,4,17,71,1,
0,yr,179852.221,Pa,,,,,,,,
south,seepage face,outflow,
20,20,4,4,17,71,1,
0,yr,179850.262,Pa,,,,,,,,
south,seepage face,outflow,
21,21,4,4,17,71,1,
0,yr,179848.303,Pa,,,,,,,,
south,seepage face,outflow,
22,22,4,4,17,71,1,
0,yr,179846.344,Pa,,,,,,,,
south,seepage face,outflow,
23,23,4,4,17,71,1,
0,yr,179844.386,Pa,,,,,,,,
south,seepage face,outflow,
24,24,4,4,17,71,1,
0,yr,179842.427,Pa,,,,,,,,
south,seepage face,outflow,
25,25,4,4,17,71,1,
0,yr,179840.468,Pa,,,,,,,,
south,seepage face,outflow,
26,26,4,4,17,71,1,
0,yr,179838.51,Pa,,,,,,,,
south,seepage face,outflow,
27,27,4,4,17,71,1,
0,yr,179836.551,Pa,,,,,,,,
south,seepage face,outflow,
28,28,4,4,17,71,1,
0,yr,179834.592,Pa,,,,,,,,
south,seepage face,outflow,
29,29,4,4,17,71,1,
0,yr,179832.634,Pa,,,,,,,,
south,seepage face,outflow,
30,30,4,4,17,71,1,
0,yr,179830.675,Pa,,,,,,,,
south,seepage face,outflow,
31,31,4,4,17,71,1,
0,yr,179828.716,Pa,,,,,,,,
south,seepage face,outflow,
32,32,4,4,17,71,1,
0,yr,179826.757,Pa,,,,,,,,
south,seepage face,outflow,
33,33,4,4,17,71,1,
0,yr,179824.799,Pa,,,,,,,,
south,seepage face,outflow,
34,34,4,4,17,71,1,
0,yr,179822.84,Pa,,,,,,,,
south,seepage face,outflow,
35,35,4,4,17,71,1,
0,yr,179820.881,Pa,,,,,,,,
south,seepage face,outflow,
36,36,4,4,17,71,1,
```

```
0,yr,179818.923,Pa,,,,,,,,
south,seepage face,outflow,
37,37,4,4,17,71,1,
0,yr,179816.964,Pa,,,,,,,,
south,seepage face,outflow,
38,38,4,4,17,71,1,
0,yr,179815.005,Pa,,,,,,,,
south,seepage face,outflow,
39,39,4,4,17,71,1,
0,yr,179813.047,Pa,,,,,,,,
south,seepage face,outflow,
40,40,4,4,17,71,1,
0,yr,179811.088,Pa,,,,,,,,
south,seepage face,outflow,
41,41,4,4,17,71,1,
0,yr,179809.129,Pa,,,,,,,,
south,seepage face,outflow,
42,42,4,4,17,71,1,
0,yr,179807.17,Pa,,,,,,,,
south,seepage face,outflow,
43,43,4,4,17,71,1,
0,yr,179805.212,Pa,,,,,,,,
south,seepage face,outflow,
44,44,4,4,17,71,1,
0,yr,179803.253,Pa,,,,,,,,
south,seepage face,outflow,
45,45,4,4,17,71,1,
0,yr,179801.294,Pa,,,,,,,,
south,seepage face,outflow,
46,46,4,4,17,71,1,
0,yr,179799.336,Pa,,,,,,,,
south,seepage face,outflow,
47,47,4,4,17,71,1,
0,yr,179797.377,Pa,,,,,,,,
south,seepage face,outflow,
48,48,4,4,17,71,1,
0,yr,179795.418,Pa,,,,,,,,
south,seepage face,outflow,
49,49,4,4,17,71,1,
0,yr,179793.459,Pa,,,,,,,,
south,seepage face,outflow,
50,50,4,4,17,71,1,
0,yr,179791.501,Pa,,,,,,,,
south,seepage face,outflow,
51,51,4,4,17,71,1,
0,yr,179789.052,Pa,,,,,,,,
south,seepage face,outflow,
52,52,4,4,17,71,1,
0,yr,179785.38,Pa,,,,,,,,
south,seepage face,outflow,
53,53,4,4,17,71,1,
0,yr,179780.973,Pa,,,,,,,,
south,seepage face,outflow,
54,54,4,4,17,71,1,
```

```
0,yr,179776.443,Pa,,,,,,,,
south,seepage face,outflow,
55,55,4,4,17,71,1,
0,yr,179771.688,Pa,,,,,,,,
south,seepage face,outflow,
56,56,4,4,17,71,1,
0,yr,179765.614,Pa,,,,,,,,
south,seepage face,outflow,
57,57,4,4,17,71,1,
0,yr,179756.504,Pa,,,,,,,,
south,seepage face,outflow,
58,58,4,4,17,71,1,
0,yr,179742.84,Pa,,,,,,,,
south,seepage face,outflow,
59,59,4,4,17,71,1,
0,yr,179722.345,Pa,,,,,,,,
south,seepage face,outflow,
60,60,4,4,17,71,1,
0,yr,179691.604,Pa,,,,,,,,
north,seepage face,outflow,
3,3,69,69,17,71,1,
0,yr,179916.306,Pa,,,,,,,,
north,seepage face,outflow,
4,4,69,69,17,71,1,
0,yr,179902.643,Pa,,,,,,,,
north,seepage face,outflow,
5,5,69,69,17,71,1,
0,yr,179893.533,Pa,,,,,,,,
north,seepage face,outflow,
6,6,69,69,17,71,1,
0,yr,179887.459,Pa,,,,,,,,
north,seepage face,outflow,
7,7,69,69,17,71,1,
0,yr,179882.825,Pa,,,,,,,,
north,seepage face,outflow,
8,8,69,69,17,71,1,
0,yr,179878.418,Pa,,,,,,,,
north,seepage face,outflow,
9,9,69,69,17,71,1,
0,yr,179874.011,Pa,,,,,,,,
north,seepage face,outflow,
10,10,69,69,17,71,1,
0,yr,179870.339,Pa,,,,,,,,
north,seepage face,outflow,
11,11,69,69,17,71,1,
0,yr,179867.89,Pa,,,,,,,,
north,seepage face,outflow,
12,12,69,69,17,71,1,
0,yr,179865.932,Pa,,,,,,,,
north,seepage face,outflow,
13,13,69,69,17,71,1,
0,yr,179863.973,Pa,,,,,,,,
north,seepage face,outflow,
14,14,69,69,17,71,1,
```

```
0,yr,179862.014,Pa,,,,,,,,
north,seepage face,outflow,
15,15,69,69,17,71,1,
0,yr,179860.055,Pa,,,,,,,,
north,seepage face,outflow,
16,16,69,69,17,71,1,
0,yr,179858.097,Pa,,,,,,,,
north,seepage face,outflow,
17,17,69,69,17,71,1,
0,yr,179856.138,Pa,,,,,,,,
north,seepage face,outflow,
18,18,69,69,17,71,1,
0,yr,179854.179,Pa,,,,,,,,
north,seepage face,outflow,
19,19,69,69,17,71,1,
0,yr,179852.221,Pa,,,,,,,,
north,seepage face,outflow,
20,20,69,69,17,71,1,
0,yr,179850.262,Pa,,,,,,,,
north,seepage face,outflow,
21,21,69,69,17,71,1,
0,yr,179848.303,Pa,,,,,,,,
north,seepage face,outflow,
22,22,69,69,17,71,1,
0,yr,179846.344,Pa,,,,,,,,
north,seepage face,outflow,
23,23,69,69,17,71,1,
0,yr,179844.386,Pa,,,,,,,,
north,seepage face,outflow,
24,24,69,69,17,71,1,
0,yr,179842.427,Pa,,,,,,,,
north,seepage face,outflow,
25,25,69,69,17,71,1,
0,yr,179840.468,Pa,,,,,,,,
north,seepage face,outflow,
26,26,69,69,17,71,1,
0,yr,179838.51,Pa,,,,,,,,
north,seepage face,outflow,
27,27,69,69,17,71,1,
0,yr,179836.551,Pa,,,,,,,,
north,seepage face,outflow,
28,28,69,69,17,71,1,
0,yr,179834.592,Pa,,,,,,,,
north,seepage face,outflow,
29,29,69,69,17,71,1,
0,yr,179832.634,Pa,,,,,,,,
north,seepage face,outflow,
30,30,69,69,17,71,1,
0,yr,179830.675,Pa,,,,,,,,
north,seepage face,outflow,
31,31,69,69,17,71,1,
0,yr,179828.716,Pa,,,,,,,,
north,seepage face,outflow,
32,32,69,69,17,71,1,
```

```
0,yr,179826.757,Pa,,,,,,,,
north,seepage face,outflow,
33,33,69,69,17,71,1,
0,yr,179824.799,Pa,,,,,,,,
north,seepage face,outflow,
34,34,69,69,17,71,1,
0,yr,179822.84,Pa,,,,,,,,
north,seepage face,outflow,
35,35,69,69,17,71,1,
0,yr,179820.881,Pa,,,,,,,,
north,seepage face,outflow,
36,36,69,69,17,71,1,
0,yr,179818.923,Pa,,,,,,,,
north,seepage face,outflow,
37,37,69,69,17,71,1,
0,yr,179816.964,Pa,,,,,,,,
north,seepage face,outflow,
38,38,69,69,17,71,1,
0,yr,179815.005,Pa,,,,,,,,
north,seepage face,outflow,
39,39,69,69,17,71,1,
0,yr,179813.047,Pa,,,,,,,,
north,seepage face,outflow,
40,40,69,69,17,71,1,
0,yr,179811.088,Pa,,,,,,,,
north,seepage face,outflow,
41,41,69,69,17,71,1,
0,yr,179809.129,Pa,,,,,,,,
north,seepage face,outflow,
42,42,69,69,17,71,1,
0,yr,179807.17,Pa,,,,,,,,
north,seepage face,outflow,
43,43,69,69,17,71,1,
0,yr,179805.212,Pa,,,,,,,,
north,seepage face,outflow,
44,44,69,69,17,71,1,
0,yr,179803.253,Pa,,,,,,,,
north,seepage face,outflow,
45,45,69,69,17,71,1,
0,yr,179801.294,Pa,,,,,,,,
north,seepage face,outflow,
46,46,69,69,17,71,1,
0,yr,179799.336,Pa,,,,,,,,
north,seepage face,outflow,
47,47,69,69,17,71,1,
0,yr,179797.377,Pa,,,,,,,,
north,seepage face,outflow,
48,48,69,69,17,71,1,
0,yr,179795.418,Pa,,,,,,,,
north,seepage face,outflow,
49,49,69,69,17,71,1,
0,yr,179793.459,Pa,,,,,,,,
north,seepage face,outflow,
50,50,69,69,17,71,1,
```

```
0,yr,179791.501,Pa,,,,,,,,
north,seepage face,outflow,
51,51,69,69,17,71,1,
0,yr,179789.052,Pa,,,,,,,,
north,seepage face,outflow,
52,52,69,69,17,71,1,
0,yr,179785.38,Pa,,,,,,,,
north,seepage face,outflow,
53,53,69,69,17,71,1,
0,yr,179780.973,Pa,,,,,,,,
north,seepage face,outflow,
54,54,69,69,17,71,1,
0,yr,179776.443,Pa,,,,,,,,
north,seepage face,outflow,
55,55,69,69,17,71,1,
0,yr,179771.688,Pa,,,,,,,,
north,seepage face,outflow,
56,56,69,69,17,71,1,
0,yr,179765.614,Pa,,,,,,,,
north,seepage face,outflow,
57,57,69,69,17,71,1,
0,yr,179756.504,Pa,,,,,,,,
north,seepage face,outflow,
58,58,69,69,17,71,1,
0,yr,179742.84,Pa,,,,,,,,
north,seepage face,outflow,
59,59,69,69,17,71,1,
0,yr,179722.345,Pa,,,,,,,,
north,seepage face,outflow,
60,60,69,69,17,71,1,
0,yr,179691.604,Pa,,,,,,,,
```

Appendix B – Simulation Summary

Technetium

Simulation Input Waste Form K_d (mL/g)	R (unitless)	D_{obs} (cm^2/s)	C_{max} (pCi/L)
0	1	2.6E-09	26957.4
1	3	7.4E-10	14004.4
2	6	4.3E-10	9879.5
4	11	2.4E-10	6407.1
10	26	1.0E-10	3256.9
30	76	3.4E-11	1296.0
40	101	2.6E-11	1004.0
43	108	2.4E-11	941.0
45	113	2.3E-11	903.2
45.1	113	2.3E-11	901.4
48	121	2.2E-11	852.1
50	126	2.1E-11	821.2
61.9	155	1.7E-11	676.0
70	175	1.5E-11	603.8
100	250	1.0E-11	433.6
500	1247	2.1E-12	92.8
515.5	1286	2.0E-12	90.1
5000	12461	2.1E-13	9.5
5253.9	13094	2.0E-13	9.1
10000	21596	1.2E-13	4.765

Iodine

Simulation Input Waste Form K_d (mL/g)	R (unitless)	D_{obs} (cm^2/s)	C_{max} (pCi/L)
0	1.0	2.6E-09	24.691
0.01	1.0	2.5E-09	24.435
0.08	1.2	2.2E-09	22.798
0.1	1.2	2.1E-09	22.377
0.16	1.4	1.9E-09	21.215
0.2	1.5	1.7E-09	20.516
0.3	1.7	1.5E-09	18.984
0.5	2.2	1.2E-09	16.599
0.62	2.5	1.0E-09	15.470
5	13.5	1.9E-10	5.025
10	25.9	1.0E-10	2.983
16.15	41.2	6.3E-11	2.020
20	50.8	5.1E-11	1.686
188.4	470.5	5.5E-12	0.218
250	624.0	4.2E-12	0.166
490	1222.1	2.1E-12	0.087
1000	2493.0	1.0E-12	0.043
4334	10801.5	2.4E-13	0.010
7000	17445.3	1.5E-13	0.006

Nitrate

Simulation Input Waste Form K_d (mL/g)	R (unitless)	D_{obs} (cm^2/s)	C_{max} (mg/L)
0	1	2.6E-09	59.020
1	3.5	7.45E-10	30.700
5	13.5	1.93E-10	12.020
10	25.9	1.00E-10	7.130
6.34	16.8	1.55E-10	10.112
9.32	24.2	1.07E-10	7.540
10	25.9	1.00E-10	7.130
75.67	189.6	1.37E-11	1.230
93.35	233.6	1.11E-11	1.012
1000	2493.0	1.04E-12	0.103

Chromium

Simulation Input Waste Form K_d (mL/g)	R (unitless)	D_{obs} (cm^2/s)	C_{max} (mg/L)
10	25.9	1E-10	0.224
20	50.8	5.11E-11	0.127
26	65.8	3.95E-11	0.101
35.92	90.5	2.87E-11	0.076
50	125.6	2.07E-11	0.057
100	250.2	1.04E-11	0.030
310	773.5	3.36E-12	0.010
500	1247.0	2.08E-12	0.006
5794	14439.9	1.8E-13	0.001

Appendix C – Historical Leach Data Summary

Year	Tc D_{obs} (cm^2/s)			Method Used to Measure (Dobs)	Composition	Source
	Experimental Values, Pore Water	Experimental Values, DIW	Value Used in Performance Assessment			
2016.2	3.02E-11	3.05E-10	---	EPA 1315 (28 to 63 d avg)	Cast Stone SST Blend/Cast Stone High SO4 High I	PNNL-24297 Table 4-4
2016.2	6.15E-13	5.96E-12	---	EPA 1315 (28 to 63 d avg)	Cast Stone High Al Simulant (both)	PNNL-24297 Table 4-4
2013	---	1.24E-09	---	EPA 1315 (63d value)	Cast Stone SST Blend	PNNL-22747 Table D-11
2013	---	6.75E-12	---	EPA 1315 (63d value)	Cast Stone SST Blend	PNNL-22747 Table D-11
2005	---	3.16E-10	---	ANS 16.1 47 d	Cast Stone LAW simulant	RPP_RPT-26743 Table 6-25
2005	---	3.98E-11	---	ANS 16.1 47 d	Cast Stone LAW simulant	RPP_RPT-26743 Table 6-25
2013	---	5.50E-11	---			RPP-RPT-59660
1992	1.05E-08	3.90E-09	---	ANS 16.1	OPC/FA/BFS DSSF	Waste Management 1992 Table 8
1992		4.00E-11	---	ANS 16.1	OPC/FA/Clay PSW	Waste Management 1992 Table 6 PSW
2016	4.60E-12	1.00E-11	---	EPA 1315 63d value	Cast Stone LAW simulant	PNNL-25577 Section 3
2016	5.40E-13	2.00E-11	---	EPA 1315 63d value	Cast Stone LAW simulant	PNNL-25577 Section 3
2015	1E-12	1.58489E-11	---	EPA 1315 (28 to 140 d avg)	Hydrated Lime/Cast Stone WTP off gas simulant	PNNL-25129 (Table 5-5)
2015	3.16228E-15	3.16228E-15	---	EPA 1315 (28 to 140 d avg)	Hydrated Lime with Getter and WTP off gas simulant/Hydrated lime with 242-A simulant	PNNL-25129 (Table 5-5)
2017	1.99526E-08	1.58489E-08	---	EPA 1315 (28 to 100 d avg)	Hydrated lime with I getter	PNNL-26443 Table 6.6 and 6.7
2017	3.16228E-12	1.58489E-12	---	EPA 1315 (28 to 100 d avg)	Hydrated Lime	PNNL-26443 Table 6.6 and 6.7
2016	---	5.01E-10	---	EPA 1315 (28 to 63 d)	Cast Stone Tank 50 Waste Adjusted	SRNL-STI-2016-00619 Table 11
2016	---	1.26E-11	---	EPA 1315 (28 to 63 d)	Cast Stone Tank 50 Waste Adjusted	SRNL-STI-2016-00619 Table 11
2012	---	1.58489E-11	---	ANS 16.1	OPC:BFS 2:1 + Fishbone getter, Basin 43 groundwater	RPP-RPT-39195 Figure 5
2012	---	1.99526E-13	---	ANS 16.1	OPC:BFS 2:1, Tin Apatite Getter Basin 43 groundwater	RPP-RPT-39195 Figure 5
1995	---	---	2.00E-07	N/A	N/A	WHC-SD-WM-EE-004-Rev.1 Table 3.3
2003	---	---	3.20E-10	N/A	N/A	RPP-17675 Table B-10
2005	---	---	5.00E-09	N/A	N/A	Section 4.3 Technical Guidance Document for EIS 2005
2005	---		5.00E-10		Guess for secondary waste	PNNL-14805 Table 13
2005	---	---	1.00E-08		Conservative for secondary waste	PNNL-14805 Table 13
2011	---	3.16228E-10	---	ANS 16.1 average	Ceramicrete secondary waste	PNNL-20632 Table 5.3
2011	---	3.16228E-11	---	ANS 16.1 average	Duralith secondary waste	PNNL-20632 Table 5.3
2011	---	0.000000001	---	ASTM C1308 11d	Cast Stone Secondary Waste	PNNL-20632 Table 5.7
2011	---	1.25893E-10	---	ASTM C1308 11d	Duralith secondary waste	PNNL-20632 Table 5.7
2011	---	3.16228E-10	---	EPA 1315 63 d	Ceramicrete secondary waste	PNNL-20632 Table 5.11
2011	---	6.30957E-12	---	EPA 1315 63 d	Cast Stone Secondary Waste	PNNL-20632 Table 5.11
2012	---	2.30E-11	---	EPA 1315 14 to 63 d	Cast Stone Secondary Waste	Chung JNM 2010 Fig 9
2012	---	6.50E-13	---	EPA 1315 14 to 63 d	Cast Stone Secondary Waste	Chung JNM 2010 Fig 9
2017	---	3.00E-10	---	EPA 1315	Saltstone	SREL R-17-0005 Table 7
2017	---	5.70E-12	---	EPA 1315	Saltstone	SREL R-17-0005 Table 7
2015	---	2.00E-10	---	EPA 1315	Saltsotne	SREL R-15-0003 Table 7
2015	---	3.70E-10	---	EPA 1315	Saltsotne	SREL R-15-0003 Table 7
2010	---	1.07E-15	---	EPA Method 1315 14 d	Fly Ash : OPC : A530E Resin	PNNL-19681 Table 3.3
1989	---	6.80E-11	---	ANS 16.1 223 d		PNL-7121
1989	---	1.40E-11	---	ANS 16.1 223 d		PNL-7121
2001	---	7.94328E-09	---	ANS 16.1 90 d	Concrete	PNNL-13639 Table 3.3
2001	---	2.51189E-09	---	ANS 16.1 90 d	Concrete	PNNL-13639 Table 3.3

Year	I D_{obs} (cm^2/s)			Method Used to Measure (Dobs)	Source	Note	Sample
	Experimental Values, Pore Water	Experimental Values, DIW	Value Used in Performance Assessment				
2016	1.11E-08	1.58E-08	---	EPA 1315 (28 to 63 d avg)	PNNL-24297, Table 4.4	--	T21L-2.8HIS/
2016	1.80E-09	2.48E-09	---	EPA 1315 (28 to 63 d avg)	PNNL-24297,Table 4.4	--	T10H-5HIS/
2013	---	9.08E-09	---	EPA 1315 63 d value	PNNL-22747 Table D-10	--	Sample 23
2013	---	6.00E-10	---	EPA 1315 63 d value	PNNL-22747 Table D-10	--	Sample 1
2005	---	1.26E-08	---	ANSI/ANS 16.1	RPP_RPT-26743 Table 6-25	47 d sample	Condition 8
2005	---	1.26E-10	---	ANSI/ANS 16.1	RPP_RPT-26743 Table 6-26	456 h sample	19 d sampling
2016	2.00E-09	4.00E-09	---	EPA 1315 63 d value	PNNL-25577 Section 3	--	PNNL-25577
2016	6.00E-09	8.00E-09	---	EPA 1315 63 d value	PNNL-25577 Section 3	--	PNNL-25577
2017	1.58489E-08	1.25893E-08	---	EPA 1315 28 to 63 d avg	PNNL-26443 Table 6.6 and 6.7	--	T1/T6
2017	6.30957E-13	6.30957E-13	---	EPA 1315 28 to 63 d avg	PNNL-26443 Table 6.6 and 6.7	--	T3
2016	---	6.00E-09	---	EPA 1315 63 d value	SRNL-STI-2016-00619 Table 10	--	BS
2016	---	5.89E-13	---	EPA 1315 63 d value	SRNL-STI-2016-00619 Table 10	--	AgZ
2005	---	7.94328E-09	---	ANS 16.1	RPP-RPT-26725	--	RPP-RPT-26725
2005	---	3.16E-13	---	ANS 16.1	RPP-RPT-26725	--	RPP-RPT-26725
2017	---	--	5.70E-09	Average from 1315	PNNL-25194	--	
2005	---	--	1.00E-09	Suggested	PNNL-14805 Table 13	--	Conservative
1995	---	--	3.00E-08	Suggested	Shade et al. (1995) WHC-SD-WM-EE-004, Rev 1, Appendix P, Table P.5	--	
1992	---	8.00E-08	--	ANSI/ANS 16.1	Serne et al Waste Management 1992 Table 6	--	T-106 AN
1992	---	1.00E-10	--	ANSI/ANS 16.1	Serne et al Waste Management 1992 Table 6	-	PSW Sample
1995	---	---	1.00E-06	Selected	WHC-SD-WM-EE Rev 1, Table P.6	Selected	Degraded
1995	---	---	1.00E-08	Selected	WHC-SD-WM-EE Rev 1, Table P.6	Selected	Selected
1989	---	1.20E-10	--	ANS 16.1 223 d value	PNL-7121 Table 6.2		small sample
1989	---	1.30E-11	--	ANS 16.1 223 day value	PNL-7121 Table 6.2		large sample
2003	---	---	2.50E-09	Selected	RPP-17675 Table B-11	2003 Risk Assessment	
2005	---	---	1.00E-10	Selected	Section 4.3 Technical Guidance Document for EIS 2005		
2001	---	1.25893E-10	--	ANS 16.1 90 d	PNNL-13639 Table 3.3	Concrete	specimen 1
2001	---	3.98107E-11	--	ANS 16.1 90 d	PNNL-13639 Table 3.3	Concrete	specimen 2
2011	---	3.16228E-08	--	ANS 16.1 Avg	PNNL-20632 Table 5.5	Cast Stone	
2011	---	3.98107E-09	--	ANS 16.1 Avg	PNNL-20632 Table 5.5	Ceramicrete	Non-detect, might be lower
2011	---	3.98107E-08	--	ASTM C1308 11d	PNNL-20632 Table 5.9	Cast Stone	
2011	---	1.58489E-08	--	ASTM C1308 11d	PNNL-20632 Table 5.9	Ceramicrete	Non-detect, might be lower
2011	---	1.99526E-08	--	EPA 1315 Avg	PNNL-20632 Table 5.13	Duralith	
2011	---	1.58489E-09	--	EPA 1315 Avg	PNNL-20632 Table 5.13	Ceramicrete	Non-detect, might be lower
2015	---	3.16E-08	--	EPA 1315	SREL R-15-0003 Table 7	Saltstone	3 month reducing
2015	---	2.00E-08	--	EPA 1315	SREL R-15-0003 Table 7	Saltstone	3 month anoxic
2019	---	6.00E-12	--	EPA 1315	RPT-SWCS-013	AP-105 Off Gas Cast Stone	
2019	---	1.00E-11	--	EPA 1315	RPT-SWCS-013	AP-105 Off Gas Cast Stone	

Year	NO_3 D_{obs} (cm^2/s)			Source	Note	Sample Name
	Experimental Values, Pore Water	Experimental Values, DIW	Value Used in Performance Assessment			
2016	---	1.61E-08	---	PNNL-24297 Table 4.4	EPA 1315 (28 to 63 d avg)	T21L-7.8HIS
2016	---	2.40E-08	---	PNNL-24297 Table 4.4	EPA 1315 (28 to 63 d avg)	T18L2-7.8RAS
2013	---	2.80E-08	---	PNNL-22747 Table D-9	EPA 1315 63 d value	Sample 23
2013	---	3.58E-08	---	PNNL-22747 Table D-9	EPA 1315 63 d value	Sample 1b
2005	---	3.16E-08	---	RPP_RPT-26743 Table 6-25	ANSI/ANS 16.1 47 d	Condition 1
2005	---	3.16E-09	---	RPP_RPT-26743 Table 6-25	ANSI/ANS 16.1 47 d	Condition 8
1993	---	1.00E-06	---	PNL-8665	AN-106 grout pilot scale test	PNL-8665
1993	---	2.51E-07	---	PNL-8665		PNL-8665
1992	---	1.68E-07	---	Waste Management 1992 Table 8	ANS 16.1	10.5 x 10
1992	2.84E-08	8.40E-08	---	Waste Management 1992 Table 9	ANS 16.1	Arithmetic Avg
2016	6.00E-09	8.00E-09	---	PNNL-25577	PNNL-25577 Section 3	PNNL-25577
2016	3.00E-09	4.00E-09	---	PNNL-25577	PNNL-25577 Section 3	PNNL-25577
2015	1.99526E-08	7.76247E-10	---	PNNL-25129 Table 5.5	LSW	T2/T11
2015	2.51189E-10	3.16228E-11	---	PNNL-25129 Table 5.5	LSW	T13/T14
2017	0.000000001	1.25893E-09	---	PNNL-26443 Table 6.6 and 6.7		T2/T2
2017	---	1.99526E-10	---	PNNL-26443 Table 6.6 and 6.7		T4
2016	---	2.51E-08	---	SRNL-STI-2016-00619 Table 10	EPA 1315 Avg	SnA/AgZ
2016	---	1.26E-08	---	SRNL-STI-2016-00619 Table 10	EPA 1315 Avg	BS
2017	---	---	6.10E-09	RPT-RPP-59958	2017 IDF PA	
2003	---	---	2.50E-08	RPP-17675 Table B-11	2003 Risk Assessment	
2004	---	---	3.00E-08	PNNL-14805 Table 13	2005 PA Secondary Waste	Conservative
2004	---	---	5.00E-09	PNNL-14805 Table 13	2005 PA Secondary Waste	Probable
2015	---	3.16E-08	---	SREL R-15-0003 Table 7	EPA 1315	Saltstone 3 month oxic
2015	---	1.26E-08	---	SREL R-15-0003 Table 7	EPA 1315	Saltstone 6 month oxic

Year	Cr D_{obs} (cm^2/s)			Source	Note	Label
	Experimental Values, Pore Water	Experimental Values, DIW	Value Used in Performance Assessment			
2016	1.48E-14	3.31E-12	---	PNNL-24297 Table 4.4	EPA 1315 (28 to 63 d avg)	T18L2-7.8RAS/T13L-5AVG-5
2016	2.70E-15	1.80E-14	---	PNNL-24297 Table 4.4	EPA 1315 (28 to 63 d avg)	T8L-5RAS/T14L-7.8HIS
2013	---	2.00E-13	---	PNNL-22747 Table D-12	EPA 1315 63 d value	Sample 23
2013	---	1.00E-14	---	PNNL-22747 Table D-12	EPA 1315 63 d value	Sample 14
2005	---	3.98E-13	---	RPP_RPT-26743 Table 6-25	ANSI/ANS 16.1 47 d	Condition 8
2005	---	5.01E-14	---	RPP_RPT-26743 Table 6-25	ANSI/ANS 16.1 47 d	Condition 2
1992	1.36E-11	2.85E-11	---	Waste Management 1992 Table 9	ANS 16.1	Arithimetic Avg
1992	---	1.52E-12	---	Waste Management 1992 Table 8	ANS 16.1	15.5 x 15.6
2016	1.20E-13	1.20E-13	---	PNNL-25577 Section 3	EPA 1315	PNNL-25577
2016	---	2.51E-11	---	SRNL-STI-2016-00619 Table 11	EPA 1315 Last four intervals	AgZ
2016	---	2.51E-13	---	SRNL-STI-2016-00619 Table 11	EPA 1315 Last four intervals	BS
2017	---	---	1.10E-13	PNNL-25194		
2003	---	---	1.60E-11	RPP-17675 Table B-11	2003 Risk Assessment	
2004	---	---	5.00E-10	PNNL-14805 Table 13	2005 PA for Secondary Waste	Conservative
2004	---	---	1.00E-12	PNNL-14805 Table 13	2005 PA for Secondary Waste	Probable for Cr III

Distribution page

OFFSITE

Washington River Protection Solutions

EE Brown
KP Lee (ORANO)
RB Mabrouki
DJ Reid
RS Skeen
DJ Swanberg
JR Vitali

ONSITE

Pacific Northwest National Laboratory

RM Asmussen
CA Burns
JF Bonnett
EA Cordova
SN Kerisit
JJ Neeway
BP Parruzot
DK Peeler
JT Reiser
JV Ryan
LM Seymour
GL Smith
BA Stanfill

PNNL-28992 Rev. 0.0
RPT-SLAW-004 Rev. 0.0

Pacific Northwest National Laboratory

902 Battelle Boulevard
P.O. Box 999
Richland, WA 99354
1-888-375-PNNL (7665)

www.pnnl.gov